Diese Dissertation haben begutachtet

Prof. Dr. Robert LISKA

Prof. Dr. Jürgen STAMPFL

PhD Thesis

Dissertation

Fabrication of Flexible Optical Waveguides by Means of Two-photon-Induced Thiol-ene Polymerization

ausgeführt zum Zwecke der Erlangung des akademischen Grades eines Doktors der technischen Wissenschaften

unter der Leitung von

Ao. Univ. Prof. Dr. Robert Liska

E163

Institut für Angewandte Synthesechemie

eingereicht an der Technischen Universität Wien

Fakultät für Technische Chemie

von

Dipl.-Ing. Josef Theodor Kumpfmüller

e0727473

Schenkendorfgasse 3-5/1/1, 1210 WIEN

Wien, 25.02.2013 Dipl.-Ing. Josef Theodor Kumpfmüller

Ao. Prof. Dr. Robert Liska und Ao. Prof. Dr. Jürgen Stampfl sei an dieser Stelle für die attraktive Themenstellung gedankt, sowie dem ISOTEC Cluster und PHOCAM für die finanzielle Unterstützung.

Herrn Dr. Robert Liska bin ich für die ausgezeichnete Betreuung während meiner Arbeit, wie auch für wertvolle Anregungen und interessante fachliche Diskussionen zu besonderem Dank verpflichtet.

Mein Dank gilt auch allen Kolleginnen, Kollegen und Mitarbeitern des Instituts, die mich in meiner Arbeit unterstützt und zu einem positiven und angenehmen Arbeitsklima beigetragen haben. Wie schon zu Zeiten meiner Diplomarbeit war insbesondere sehr angenehm mit Klaus Stadlmann interdisziplinär zusammenzuarbeiten. Gleiches gilt auch für Valentin Satzinger von JOANNEUM Research, den ich sehr gerne in Weiz besucht habe, wo wir auf Hochdruck Wellenleiter strukturiert haben. Ihnen möchte ich danken sowie meinen einmaligen Laborkollegen Paul Potzmann und Christian Gorsche, die neben wertvollen fachlichen Ratschlägen und Hilfestellungen viele lustige Meldungen und Aktionen geliefert haben. Auch die Kollegen Clark Ligon, Andreas Mautner, Konstanze Seidler, Branislav Husar, Harald Wutzel, Xiaohua Qin, Zhiquan Li, Martin Schwentenwein, Stefan Benedikt, Parichehr Esfandiari, Niklas Pucher, Claudia Dworak, Maria Schachner, Michael Kellner, Dzanana Dautefendic, Kerstin Wallisch, Rosa Demeisinova, Patrick Knaack, Walter Dazinger, Patrick Murth, Isolde Hisch, und Katrin Fohringer werden mir immer in bester Erinnerung bleiben, da es einfach einen riesigen Spaß und eine große Freude bereitet hat, mit Ihnen zusammenzuarbeiten, zu feiern etc.

Mein ganz spezieller Dank richtet sich schließlich an meinen Vater, der mir das Studium ermöglicht und mich immer vorbehaltlos unterstützt hat, sowie an meine Gattin Ediana, die nach unserer Tochter Sarah Monika während der Diplomarbeitszeit nun während meines Doktoratstudiums unseren Sohn Frederico Josef zur Welt brachte, für den liebevollen Rückhalt. Selbstverständlich darf hier auch eine herzliche Danksagung an meine verstorbene Mutter und Großeltern, die mich fürs Leben mitgeprägt haben, nicht fehlen.

Introduction

I) Motivation

The telecommunication industry is becoming interested in optical data transfer on printed circuit boards as the classical copper-based electrical signaling is approaching its limits: The ever increasing demand with respect to miniaturization causes the problem of “cross-talk”, where signals interfere with each other, when neighboring copper wires are located too close to each other.[1] This problem does not exist for optical waveguides. Further advantages would be that no short-circuits can occur and light weight materials may be used. Disadvantages compared to copper wires are the more difficult handling of waveguides compared to copper wires, especially the necessity for an efficient coupling-process, which is everything but trivial. On the other hand, cheap standard polymer processing offers great potential for cost reduction of the platines. The challenge here is to implement these into processing of integrated optics.

II) Basics of Waveguide Technology

Due to optical damping minima certain ranges within the electromagnetic spectrum are of importance for optical signaling. In case of SiO_2 fibers it is the near infrared region and for optical polymer fibers the visible region. A fundamental property of optical materials is the refractive index, which can be expressed by the ratio of the speed of light in vacuum and the medium of question. A light beam that passes from an optically thin medium into a dense one is refracted towards the axis of incidence (Figure 1).

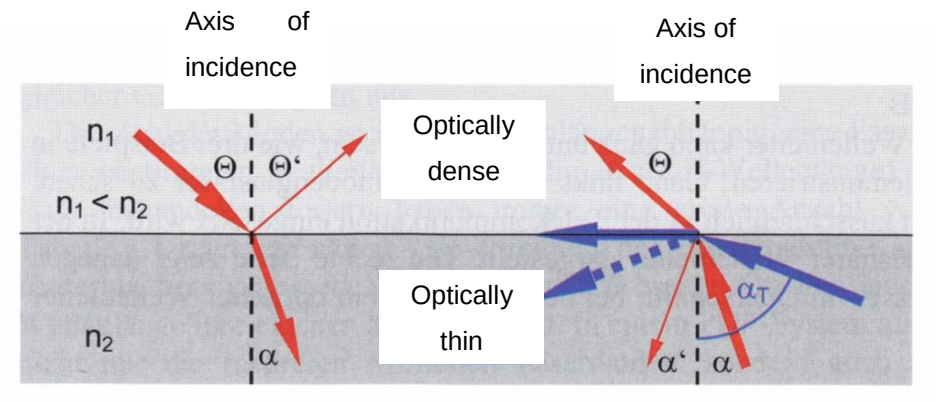

Figure 1: Refraction and total reflection[2]

Beyond the critical angle α_T no more light passes the boundary due total reflection. This angle is dependent on the ratio of n of the media in question (Equation 1).

$$\sin \alpha_T = \frac{n_1}{n_2}$$ **Equation 1**

The dependence of the refractive index on the temperature is much larger in polymers than in glass. The thermoptic effect is thus strong for polymers. Generally, the thermooptic coefficient in polymers is negative, in inorganic glasses, however positive. Considering the low thermal conductivity, interesting applications are thermooptic switches with low energy consumption. Also optical switches and modulators with low switching voltages are a topic here due to the special electro- and thermo-optical properties.

The dependence of the refractive index on the wavelength is named material dispersion. For polymeric materials it fortunately lies in the range of 10^{-6}/nm and plays an unimportant role in waveguide technology.

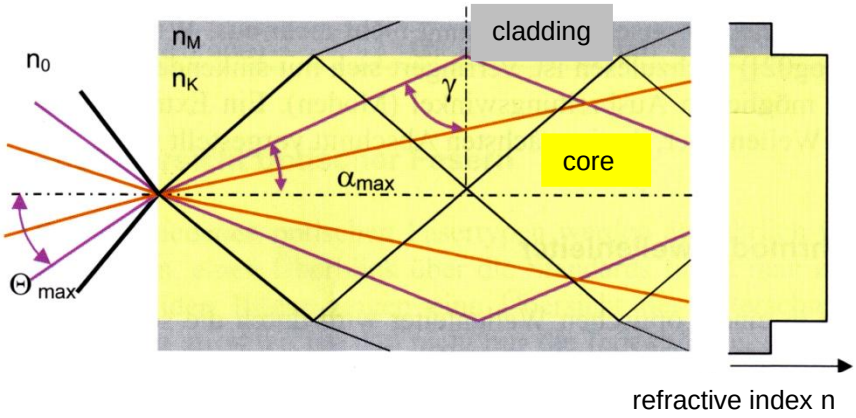

Figure 2: Waveguiding in the optical fibre[2]

A waveguide consists of a core and a surrounding cladding (Figure 2), where the refractive index of core must be larger than in case of the cladding to enable total reflection within the core. The angle of tolerance (Θ_{max}, Equation 2) represents the angle, below which total reflection is possible. Its sinus is called numerical aperture (NA) and is a function of the relative refractive index change from core to cladding (Equation 3):

$$\Delta = \frac{n_K^2 - n_M^2}{2 \cdot n_K^2} \approx \frac{n_K - n_M}{n_K}$$ **Equation 2**

$$NA = \sin \Theta_{max} = n_K \cdot \sqrt{2 \cdot \Delta}$$ **Equation 3**

The broadening of a light pulse is being influenced by a number of effects, which are summarized by the term dispersion. It is a relevant property for the quality of a polymeric waveguide with chromatic and mode dispersion having the greatest importance. In the following figure, mode dispersion will be discussed by the example of a step index profile fibre. In this case, the refractive index is uniform over the whole core and equal over the whole cladding. Light waves run exclusively on certain paths according to the condition of constructive interference at certain phase difference and are called modes.

The number of modes present in a waveguide depends on the wavelength, the radius of the core and the numerical aperture. For short distance signaling many modes are required.

Waveguides featuring a step profile exhibit between a hundred and a few million modes. As shown in Figure 3, different modes pass the waveguide at different times as they proceed at equal velocity along paths of different length, which broadens the net pulse.

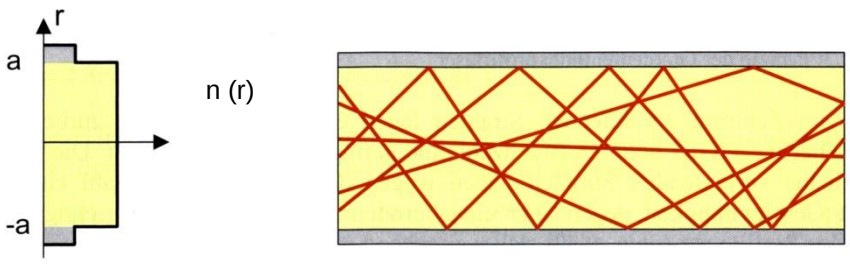

Figure 3: Refractive index distribution in a step index profile fiber[2]

This kind of dispersion is greatly reduced, if the refractive index decreases in a parabolic manner with increasing core radius (Figure 4). Modes running on the outer paths are accelerated due the lower refractive index in this region compensating for the longer distance.

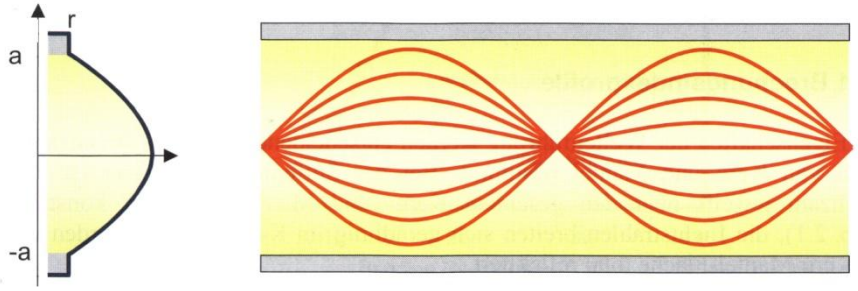

Figure 4: Principle of the gradient profile fiber[2]

The effect of the spectral broadness of a signal on the broadening of the entering pulse in terms of time is called chromatic dispersion. For multimode waveguides the dependence of n on the wavelength has large impact. The phenomenon is named material dispersion. Polychromic light thus features a large pulse broadening.

The optical damping is the crucial value for the performance of waveguides and the materials that they consist of. It is defined as the decadic logarithm of the ratio of coupled-in power and power as a function of the waveguide length. For clarity, an increase of the optical damping by 3 dB corresponds to a signal power loss by 50% as visualized in Figure 5 .

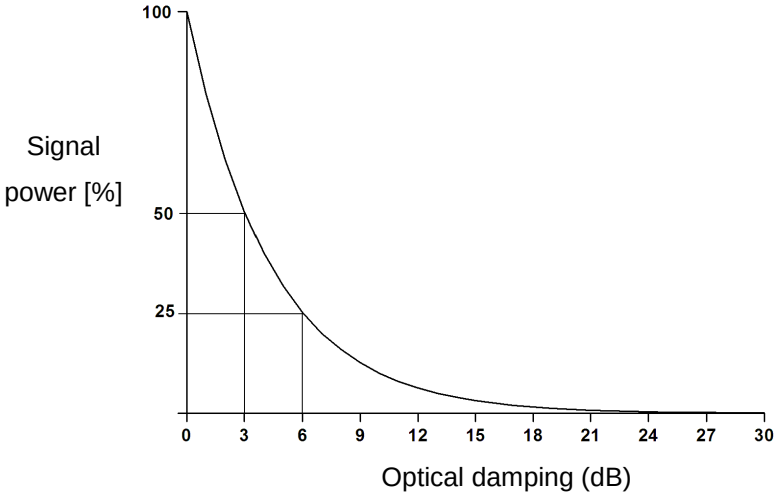

Figure 5: Visualization of the unit dB by means of the signal power

In many cases, the optical damping is applied to the waveguide length yielding the damping coefficient with the unit dB/cm. Compared to glass-based optical fiber the damping coefficient of polymeric waveguides is higher by three orders of magnitude, which is mainly due to absorption of C-H moieties as well as Rayleigh scattering. Another drawback is birefringence, which is the ability of a material to split a light bundle in two perpendicularly polarized bundles. It is caused by anisotropy of a material and results in an increase in the bit error rate in digital systems and pulse distortion. Hence, it is necessary to keep birefringence low. Polymeric materials can be produced relatively isotropically as far as the polymer chains do not get oriented too strongly, which can be achieved via 3D crosslinking. Polymers with a pronounced tendency towards orientation are polyimides and deuterated polysiloxanes.

Another very important issue in terms of power loss is the coupling of the light emitted by the laser into the waveguide. Rough interfaces and the difference in refractive index between air and the waveguide material cause partial reflection. Moreover, there are photons with a trajectory outside the angle of tolerance and

others which do not even hit the interface between air and waveguide. For this reason a very smooth interface and a precise alignment of the waveguide is crucial.
The most important tools for polymer chemistry to tailor the refractive index of materials towards certain values for n are the variation of packing closeness, the polarizability and the difference of the wavelength in use from the wavelengths of maximum absorption. Polarization caused by dipole orientation has an inferior role in solid polymers. The main factor is the electronic polarization resulting from facile displacement of electrons from their equilibrium distribution. Compared to purely aliphatic polymers, sulfur atoms and aromatic groups feature higher refractive indices due to high polarizability and packaging closeness. If agglomerated at high temperatures, a further increase of refractive index is possible. Also highly conjugated dyes exhibit an analogous effect due to their elevated polarizability. Fluorine atoms decrease the refractive index due to their greater steric demand compared to hydrogen atoms and the elevated polarizability of the C-F compared to the C-H bond.

III) Waveguide materials

Conventional waveguide materials are polymethylmethacrylate (PMMA), polystyrol (PS) and polycarbonate (PC). In the past decades, mainly four optical polymer classes have been established for optical waveguides: Fluorinated polyimides, halogenated or deuterated polyacrylates, perfluoro cyclobutyl arylethers and non-linear optical polymers. These are highly transparent with low absorption losses below 0.1 dB/cm at all wavelengths that are relevant for optical signalling (850, 1300 und 1550 nm).[3]
Polysiloxanes are able to form 3D amorphous networks, which are homogenous and without inner orientation. Excellent mechanical properties and high optical transparency make these materials interesting as well as the remarkable temperature stability. By means of the sol-gel process polysiloxane-based inorganic-organic hybrid materials can be formed by hydrolysis of halogenated or alkoxy silanes. Optical damping values of waveguides on the basis of polysiloxane are situated around 0.3 dB/cm.
Polydimethylsiloxane (PDMS) is highly transparent (Figure 6) and the damping at 850 nm is between 0.02 and 0.05 dB/cm. Its thermal stability lies around 290°C and

furthermore the material is mechanically flexible and not prone to shrinkage. All these advantages are being complemented by its resistance towards chemicals and good commercial availability.

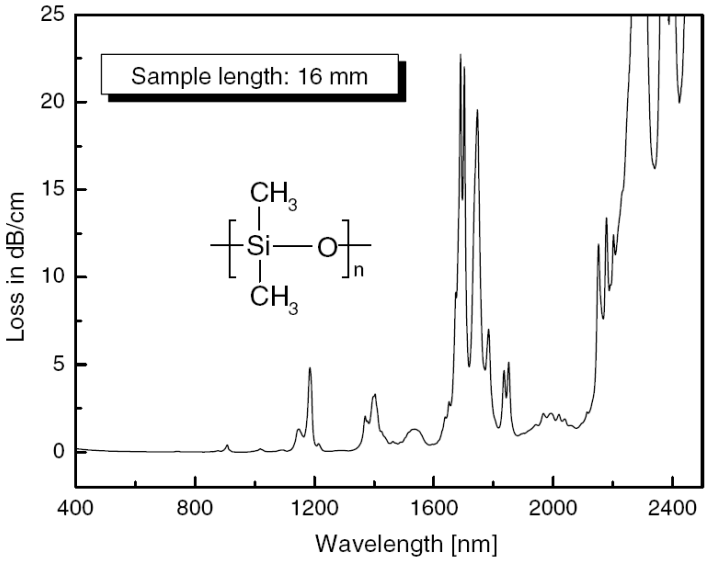

Figure 6: Optical loss in PDMS as a function of the wavelength of light[4]

After lamination of platines containing PDMS at 180°C for two hours and subsequent heating to 230°C for 5 minutes the optical losses were between 0.05 and 0.1 dB/cm (at 850 nm).

IV) Methods for Waveguide Structuring

The following paragraphs shall give an overview on interesting concepts for the photostructuring of optical waveguides. Generally, it is meaningful to differentiate between direct and indirect photostructuring.

An example for indirect photostructuring is reactive ion etching (Figure 7), where photoresists are being illuminated. The photoresist layer covers a core layer during the photolithography step, which again covers the cladding material. Depending on whether a negative (epoxy resin) or positive (novolak) photoresist finds application, photons cause a decrease or increase in solubility, respectively. The well-soluble part is removed subsequently by reactive ion etching to give planar waveguide structures, which are then covered with cladding material.

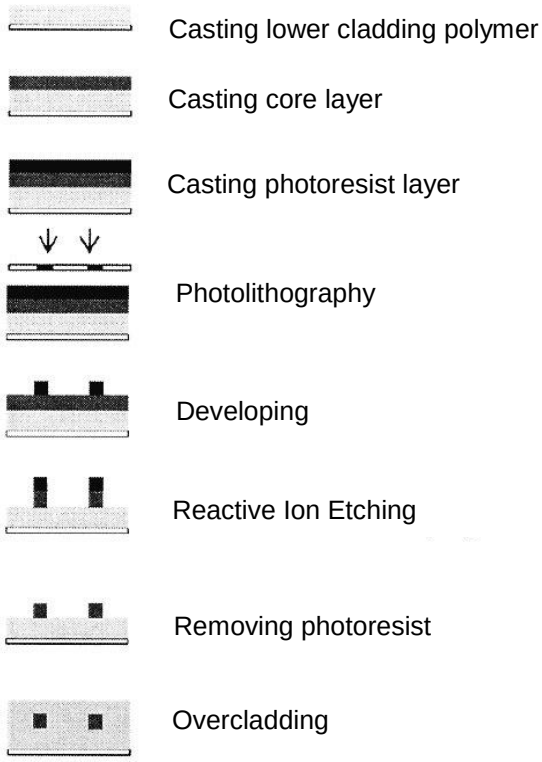

Figure 7: Waveguide structuring via reactive ion etching

Direct photostructuring of waveguides is performed by selectively curing planar monomer layers by means of a laser (laser structuring) or a photo mask (photolithography). The development comprises removal of excess monomer with solvent. Finally, the waveguides are coated with an appropriate material. As monomers, e. g. 1,2,3-propanetriol triacrylate and urethane diacrylate are used for curing. Corresponding waveguides exhibit a damping of 0.56 dB/cm at 1300 nm. Ormocers (Organic Modified Ceramics) have proven to be materials with potential regarding direct photostructuring of waveguides also. These are hybrid polymers, which are synthesized by means of the sol-gel process from diphenylsilandiol and trialkoxy silanes featuring methacryl and/or epoxy moieties.

An alternative concept to refractive index increase is the refractive index decrease. Irradiating hybrimeres of Si-O-Si with methacryl moieties lowered the refractive index. This was by illumination of azo benzene doped polymers due to the cis-trans isomerization of azo benzene. Analogous effects are achieved by photoisomerization and photoinduced dimerization reactions of photoreactive groups on polysilesquioxanes and photoinduced cycloaddition of polyvinyl cinnamate. Splitting-

off nitrogen and the lowering of the density by irradiation of azido compounds is worth mentioning in this context.

Another optical means for structuring is photolocking (Figure 8). A substance is photochemically fixed in a low refractive polymer and finally the non-reacted rest monomer is evaporated in vacuum or elevated temperature.

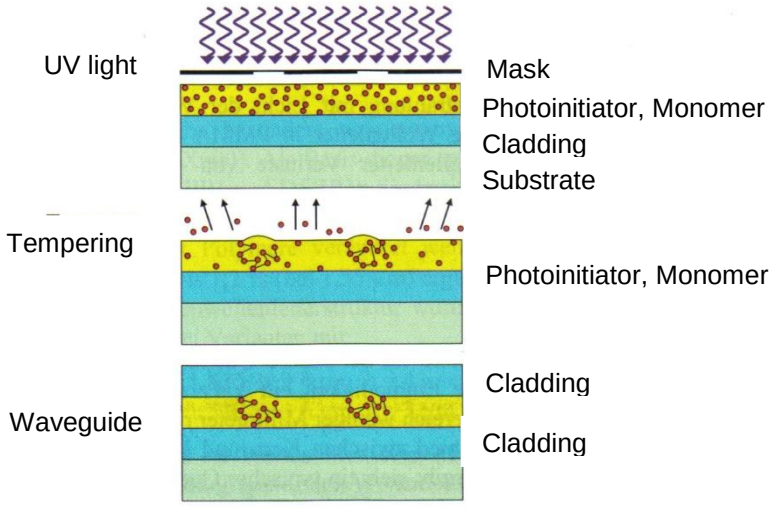

Figure 8: Schematic description of the photolocking process[5]

Thus it was possible to increase the value of n of modified PMMA via UV-irradiation by 0.015 with 16% ethyl-2-(1-naphtyl)acrylate as dopant. With this method waveguides with an optical damping value of 0.2 dB/cm at 633 nm could be fabricated by means of laser structuring. Resolution was improved using naphthalene thiol avoiding an undesired formation of dimers from ethyl-2-(1-naphtyl)acrylate. These dimers could not be evaporated but would diffuse and thus worsen the resolution. After development an increase of $\Delta n = 0{,}020$ (at 633 nm) was observed.

The polyguide-process, which was developed by DuPont, is a modified way of photolocking, where acylic monomers are inside a polycarbonate matrix. This is followed by diffusion of more acrylic monomer into the illuminated regions. After flood-curing and lamination, waveguides with refractive index changes between 0.002 and 0.05 at damping values of 0.08 – 0.12 dB/cm are formed.

The most elegant way of waveguide structuring, however, is the two-photon-induced polymerization (2PP). The phenomenon of two-photon absorption was postulated by the nobel laureate Maria Göppert-Mayer but experimentally observed only three decades after by Kaiser and Garret. It forms the basis for 2PP, where two photons

elevate a molecule from the electronic ground state via a virtual energy level to an excited state, where the energetic difference equals the sum of the energies of the photons (Figure 9). The probability for this process depends on the square of the light intensity. The photoinitiation is explained the following way: After two-photon absorption inter-system-crossing takes place from the short-lived singlet state to a triplet state. From both states electron transfer reaction can form radicals, which finally start polymerization.

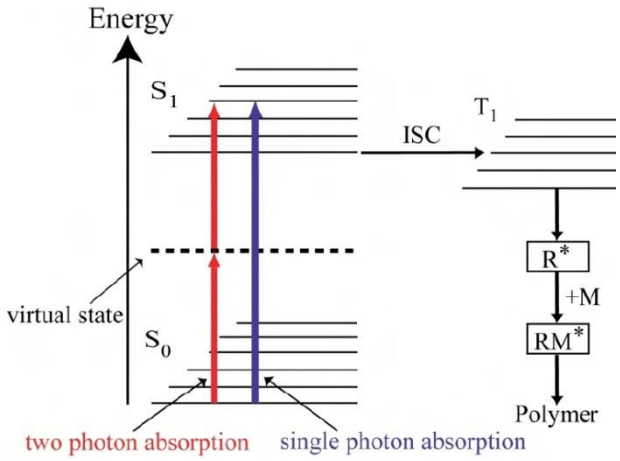

Figure 9: Comparison of one-photon and two-photon-excitation (left) and initiation (right)

The cause for high resolutions down to a few tens of nanometers is the dependency of two-photon absorption on the square of the light intensity. Figure 10 shows the difference between one and two-photon excitation by the example of rhodamin B solution. In this case of the one-photon-absorption, the UV-light is already absorbed at the surface of a resin, leading to excitation (and in a later stage polymerization) along the trajectory of the incident light. In case of the two-photon excitation, however, excitation takes only place in region with sufficiently large photon density, namely in the focal region of the microscope lens (Figure 11). By guiding the laser beam according to a given shape, 3D-structures can now be fabricated.

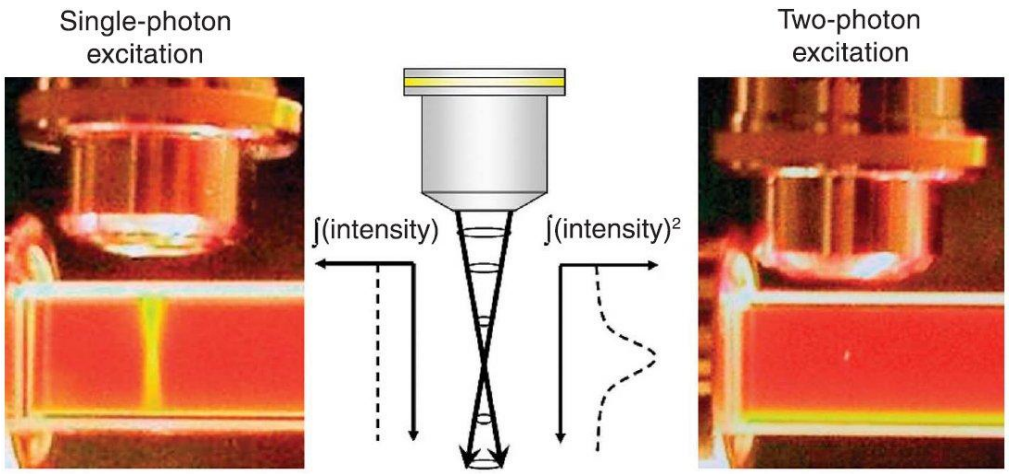

Figure 10: Comparison between one-photon excitation (right) und two-photon excitation (left)[6]

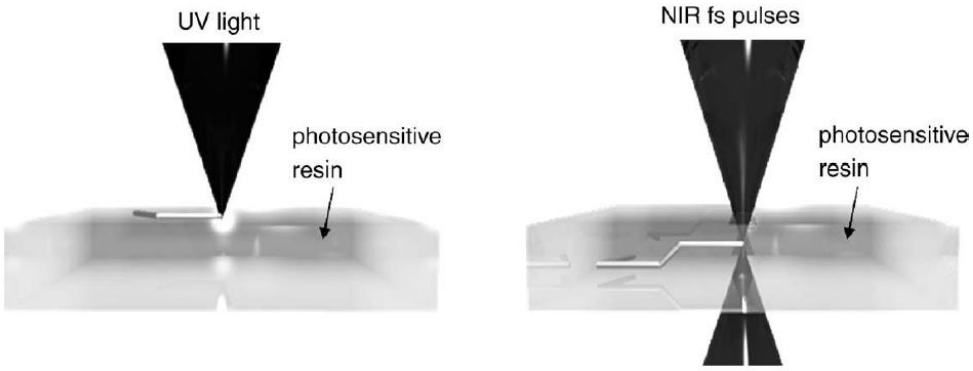

Figure 11: Comparison between one-photon (left) and two-photon-polymerization (right)[7]

V) Photopolymerization

Photopolymerization is a well-known technique for rapid curing, which is broadly used in industry for coatings, lithography, dental restorations, photoimaging etc. Important advantages are solvent-free processes, low energy consumption, high productivity, low spatial demand and good mechanical properties of the photopolymers. Compared to its thermal counterpart, photopolymerization allows for spatially directing the polymerization and for rapidly curing at ambient temperature, which is especially interesting for heat-sensitive substrates.

Photoreactive resins are smart formulations containing various additives such as fillers, plasticizers, stabilizers, inhibitors, surfactants etc. for an optimized set of properties.

A central role is played by the monomers. In most cases the polymerization is based on double bonds (e. g. methacrylates, thiol-ene monomers, vinyl esters, vinyl ethers, norbornenes etc.), but also the cationic photopolymerization (e. g. epoxides, cyclosiloxanes) and condensation reactions (e. g. alkoxysilanes) can be initiated photochemically. Clearly, the acrylate UV-curing is technologically most important due to the fast polymerization and the broad commercial availability. The most important shortcoming of this usually acrylate technology is probably the oxygen inhibition making oxygen scavenging additives, lamination, greatly elevated light intensities and/or nitrogen atmosphere necessary. A revolution in photopolymerization has been triggered by the concept onium ions by Crivello to liberate photoacids that are able to induce cationic polymerization lacking oxygen inhibition.[8] Also the thiol-ene polymerization (see end of this chapter) allows for avoiding this problem.

Beside the reactivity of the monomer, curing efficiency is also crucially influenced by the performance of the photoninitiator. The biggest role in large-scale industrial applications is played by UV-initiators, but there are also initiators for the VIS and IR range. The most frequently used initiators rely on the photochemical Norrish type 1 and type 2 reactions. Both types commence with the absorption of a photon by a molecule carrying a carbonyl moiety. In case of the type 1 reaction the photoinitiator molecule is excited to a singlet 1 (S_1) state from where it undergoes either fluorescence to the ground state or intersystem-crossing to a triplet 1 (T_1) state (Figure 12).

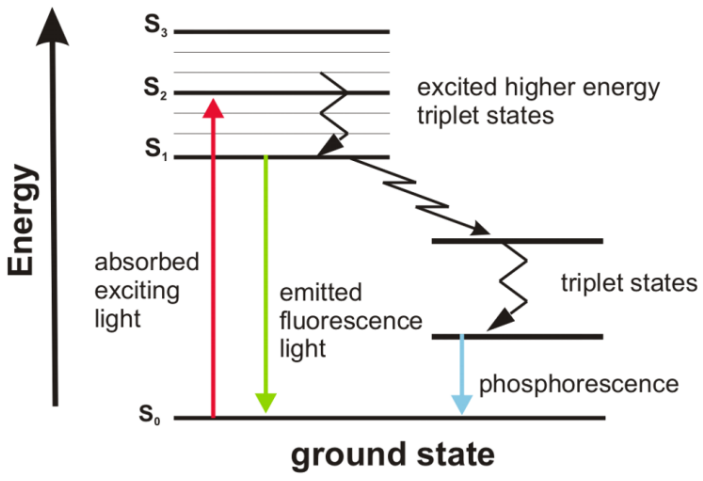

Figure 12: Simplified Jablonski Scheme about illustrating the photochemical mechanism of radical photoinitiation

The triplet state allows for α-cleavage, which means the homolytic cleavage of a bond adjacent to the carbonyl moiety. The resulting radicals are then able to initiate polymerization (Figure 13).

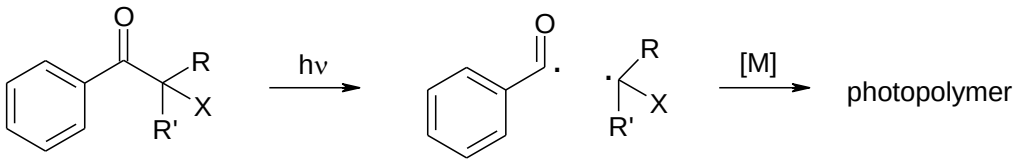

Figure 13: Norrish type 1 photoinitiation via α-cleavage

The type 2 reaction proceeds via bimolecular hydrogen abstraction (Figure 14). A biradical constellation resulting from the carbonyl excitation enables the intermolecular H-abstraction from ethers, amines, or thiols, the radical of which subsequently allows for polymerization.

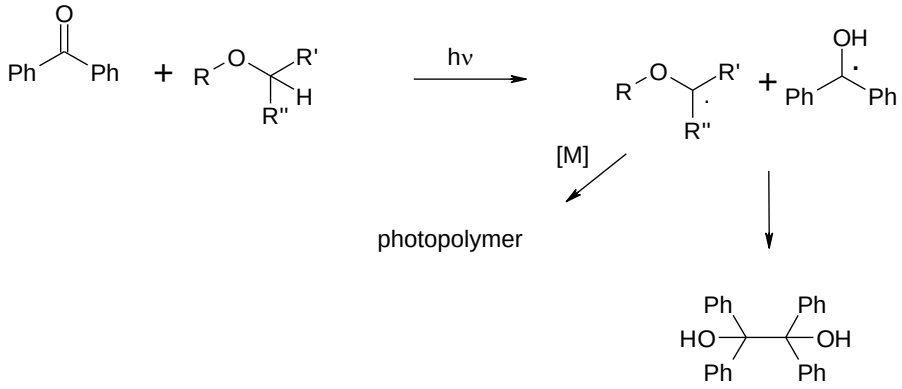

Figure 14: Norrish type 2 photoninitiation via H-abstraction

The radical formation in both cases is very efficient and initiation rates are dependent on the light intensity, temperature and the kind of PI.

Beside photo-induced initiation, photopolymerization features the following reactions: chain propagation, disproportionation, recombination, and intermolecular as well as intramolecular transfer reaction (see Figure 15).

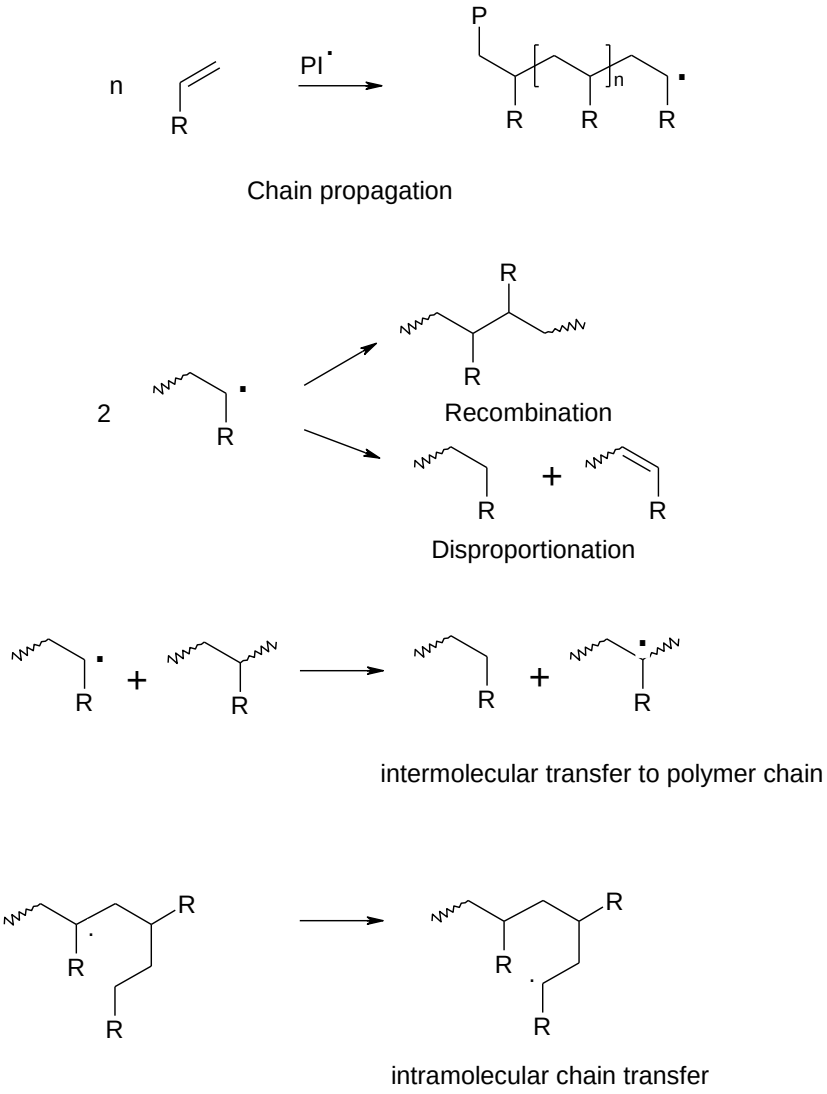

Figure 15: Reactions involved in photopolymerization

Although photopolymerization has been known and appreciated for a long time, researchers in this field have never stopped finding new interesting applications, where this technique can make a difference. A good example is the elegant two-photon-polymerization (see previous chapter), which has been a popular, emerging subject in lithography. There are classical one-photon-initiators, which can be used for two-photon-polymerization. Examples are Irgacure 369, Irgacure 819 and Irgacure OXE01 but they show a very narrow processing window with respect to laser feed rate and laser power.

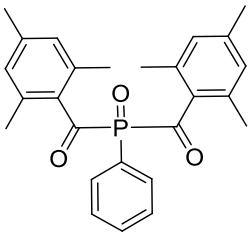

Irgacure 819

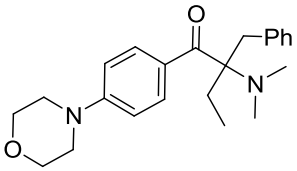

Irgacure 369

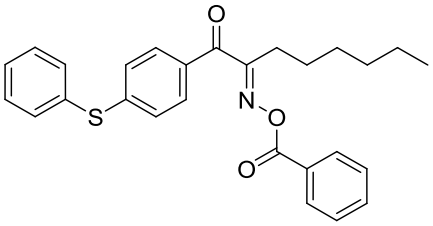

Irgacure OXE01

This is due to the rather low ability to absorb two photons at once, also called the two-photon cross-section (GM). To help this, many molecules featuring chromophores used in two-photon microscopy have been tested for their 2PP performance and published. It turned out, that extended conjugated π-systems with donor and acceptor moieties and planarity are salient to the two-photon-cross-section. In most cases, however, the yield of initiating radicals was rather not satisfactory as the fluorescence yield was too high. Cis-trans isomerization was also an unwanted side reaction. A TPI with excellent performance is R1 (E,E-1,4-bis[40-(N,N-di-nbutylamino)styryl]-2,5-dimethoxybenzene) from the Marder group.

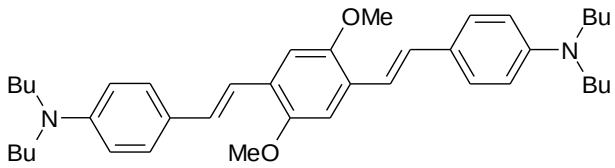

R1

It is based on a D-π-D-system with bis(styryl)benzene moieties and has also been used in this work. As shown in Figure 16, the wide structuring window is located at low laser intensities.

Due to the sparse offer of new TPIs in literature, successful efforts have been made to combine the large two-photon cross-section of TPIs from literature with the high radical formation quantum yield of classical radical initiators.

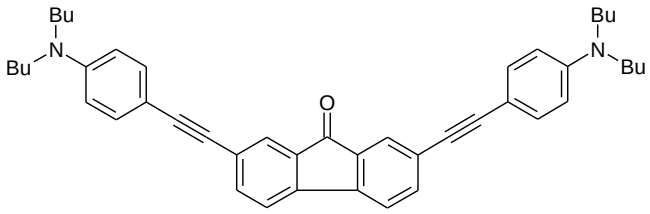

B3FL

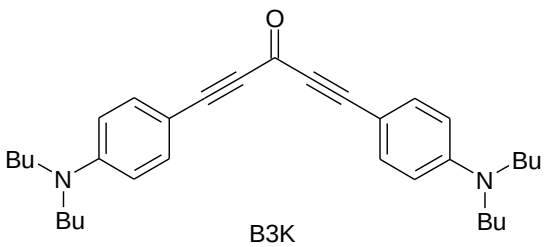

B3K

The resulting novel initiators B3FL and B3K feature:

- A donor-π-acceptor-π-donor system
- Planarity
- a carbonyl unit in conjugation with alkynyl moieties

The latter TPIs reach the S_1-state via excitation by two photons in the near infrared (NIR) region. From this state they undergo intramolecular charge transfer followed by intermolecular electron transfer enabling initiation.

The 2PP performance of classical PI Irgacure 369, R1, B3K and B3FL was qualitatively tested by fabricating grid structures over a range of laser power and feed rate in an acrylic resin. The quality was then classified with very good (green), good (yellow) and poor (orange) and very poor (red). As shown in Figure 16 the performance of B3K is similar to that of R1, where B3K features a slightly broader structuring window for very good quality. The minimum laser power is lowest for R1. B3FL exhibits a significantly broader structuring window, but the minimum laser intensity for very good quality is higher. With Irgacure 369 only very poor quality can be achieved at higher laser powers.

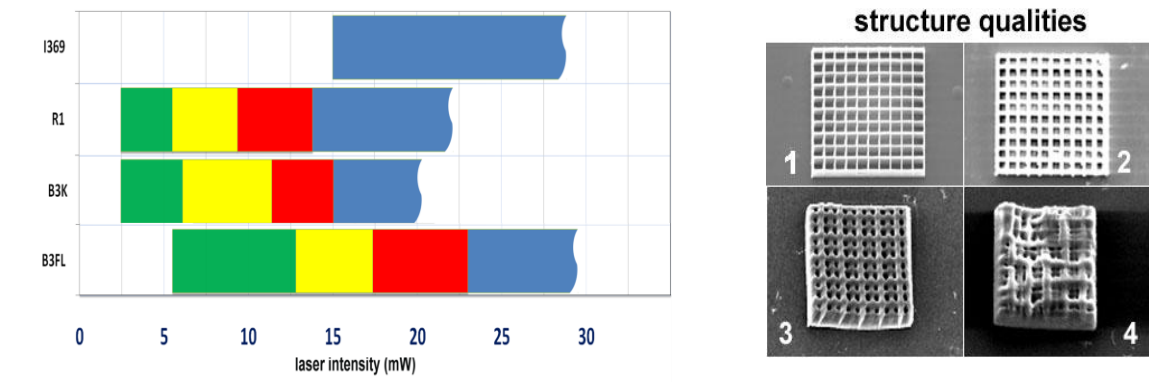

Figure 16: Structuring quality test of the Irgacure 369 (I369), R1, B3K and B3FL. Left: Structuring windows with respect to laser intensity and at constant feed rate. Green: very good (corresponding to grid structure 1 on the right), Yellow: good (corresponding to grid structure 2 on the right), Yellow: poor (corresponding to grid structure 3 on the right) Red: very poor (corresponding to grid structure 4 on the right).

As in case of UV-curing, also the discipline of 2PP is dominated by acrylate photopolymerization. As 2PP-materials are still a major bottleneck, this is the chance for other radical polymerization techniques to become established in this field:

The thiol-ene reaction has been known since the beginning of the last century and has experienced a revival in the last two decades. In contrast to acrylates, polymerization follows a step growth mechanism (Figure 17) bringing unique properties to this interesting class of materials. Late gelling greatly reduces shrinkage and the photonetworks become very uniform compared to the conventional, acrylate-based systems.

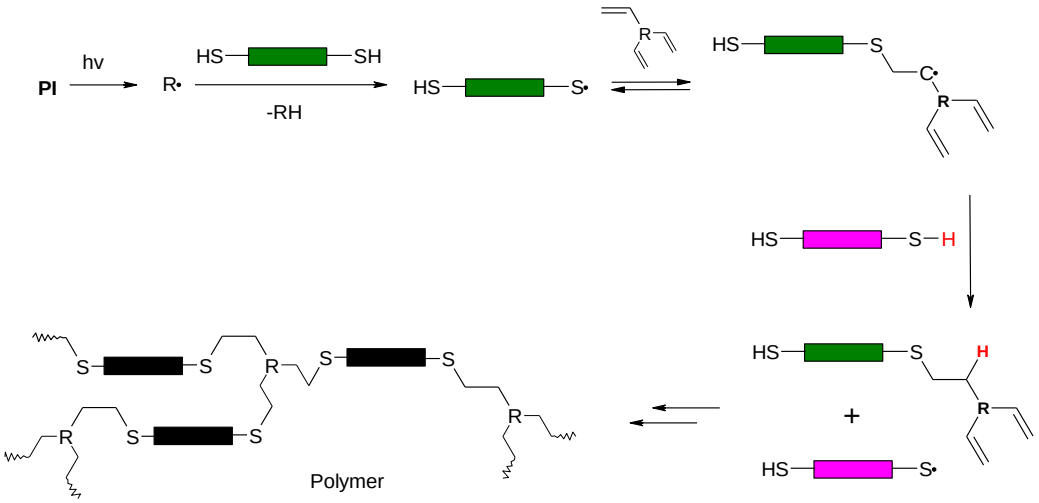

Figure 17: Mechanism of network formation in thiol-ene-based formulations

Excellent reviews have been written by C. Hoyle and C. Bowman.[9-11] The thiol-ene reaction fulfills many of the criteria of the class of “click-reactions” established by Sharpless: Very high conversions and reaction rates can be achieved under mild conditions in the presence of oxygen or water. Thiol-ene reaction products are formed regioselectively and need no essential clean-up. Furthermore, the thiol-ene reaction can be carried out using a wide variety of educts. Amongst them are silicone systems, which employ the UV-initiated thiol-ene reaction to give silicone rubber films with a high tensile strength and elongations up to 500%.[12] The applications of these materials range from fiber optics to immobilization of ceramics. Several ene functionalities attached to silicone fluids such as, allyl, alkenyl as well as vinyl, allyl, hexenyl, norbornenyl and others have been presented.[13] Amongst these, vinyl functionalities have been reported as the most reactive due to the high electron density.[10] In case of the effect of the corresponding thiol on reaction rates, the substituent neighboring the mercapto moiety is important.[14]

Objective & Targets

The task of this thesis was to develop new materials and methods to fabricate flexible optical waveguides via two-photon polymerization with polysiloxanes serving as the basic cladding material.
This should in principle be carried out by curing a high refractive, photoreactive monomer formulation inside the polysiloxane-based matrix material and thus locally increasing the refractive index (n). Drawbacks in former works such as scattering of guided photons due to phase separation in the waveguide materials or elaborate processing should be significantly improved. An ideal process should involve a post-processing as straightforward and as less time consuming as possible. In earlier concepts, cured silicone rubbers had been swollen with photoreactive monomer formulations exhibiting high values for n. This impractical swelling procedure should be avoided by

i) postponing the curing of the matrix material to the stage of post-processing or
ii) via a selective curing chemistry of the matrix, that leaves these monomer formulations untouched.

In other previous works the final step was to evaporate unreacted high refractive monomer from the 2PP-processed sample in order to fully develop the refractive index difference between waveguide core and cladding. The innovative approach of this thesis will be to exploit the local enrichment of high refractive material in the two-photon illuminated regions due to diffusion of monomers making a development step, where the unreacted monomer is removed, dispensable. From the material point of view, waveguide material should most importantly exhibit low optical damping, good thermal stability up to 250°C and high increase in refractive index upon 2PP.
These tasks should be approached from different directions with respect to crosslinking polymerization mechanism. In three different material concepts

i) a thixotropic liquid consisting of UV-curable silicone acrylate and a two-photon-reactive acrylate-based formulation

ii) a silicone rubber, which is orthogonally epoxy cured in the presence of a two-photon-reactive high refractive thiol-ene monomer formulation

iii) an acetoxy condensation cured silicone rubber, which is orthogonally cured in the presence of a high refractive thiol-ene monomer formulation

should be employed for waveguide inscription. Subsequently flood curing should be used in all cases as a post-processing step to stabilize the system avoiding an evaporating step.

State of the Art – Optical materials applied for two-photon-polymerization

A) Acrylic Resins

Acrylic monomers have been used extensively in 2PP research as they are well known from the coatings industry. A wide variety of (meth)acrylates with different size and numerous functionalities are commercially available. The most outstanding property is the high polymerization speed of acrylates allowing for rapid processing. As the processing viscosity, the overall reactivity and the final shrinkage are one of the critical formulation parameters, monomers have to be selected carefully. Some typical examples of commercially available monomers are shown in Figure 18.

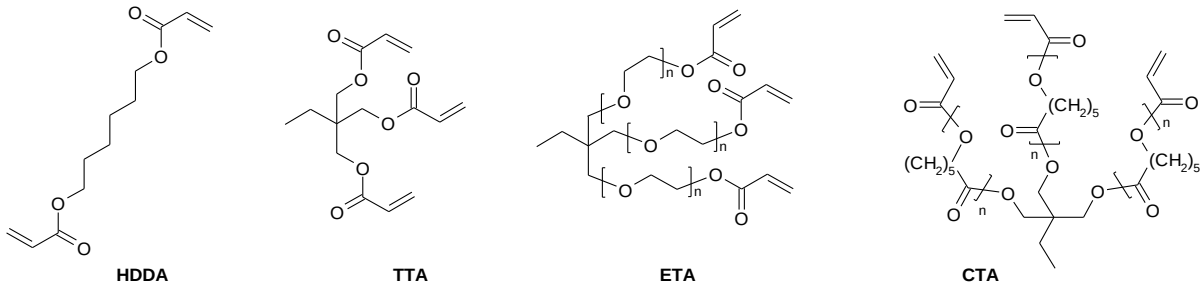

Figure 18: Typical monomers for radical photopolymerization.

Low molecular reactive diluents such as TTA or HDDA form tightly crosslinked networks with good resistance against swelling by various solvents. These monomers have generally low viscosity and high reactivity, but due to the higher number of reactive groups per gram, higher shrinkage has to be accepted. Therefore, higher molecular weight monomers such as ETA or CTA are frequently applied. Oligomeric building blocks increase the overall viscosity significantly, but due to the lower shrinkage advantageous optical behavior is described.[6] Beside the molecular weight of the monomers, the selection of functional groups in the backbone is also essential. Urethane groups giving hydrogen bridges lead to improved mechanical properties, but also have higher viscosity. Linear aliphatic chains like polyethylene glycol, polypropylene glycol or polycaprolactone between the acrylate functionalities lead to a decrease of the glass transition temperature while aromatic units as found

in epoxyacrylates form to hard and stiff materials. By choosing the right set of monomers and reactive diluents, the mechanical properties can be tuned over a broad range from elastomer-like polymers to hard and stiff materials.

SCR-500 is a frequently used acrylate-based formulation for 2PP in literature and consists of different urethane acrylate oligomers with molecular weights from 480 to 1200. The exact composition of the resin and the structure of the urethane acrylate oligomer are not disclosed. It is only known that low molecular weight urethane acrylate monomers act as diluting agents lowering the viscosity to about 850 mPas. The commercially available resin contains either Irgacure 369 or Irgacure 184 (Ciba SC, Basel) as PIs for radical single- and two-photon polymerization. In the cured material, a modulus of 160 MPa and a tensile strength of 6.0 MPa go along with a strain at failure of 10% and a glass transition temperature of 140°C.[15] The refractive index before and after polymerization is given as 1.52 and 1.53, respectively.[16]

For the formation of thin films that can be structured by 2PP, spin coating has been chosen in most cases. It has to be noted that the film is sometimes covered with glass slides to prevent oxygen inhibition and to control the film thickness.[17] Additionally, it is used to exclude moisture from air that is able to hydrolyse Ti^{4+} complexes that are sometimes added.[18]

Generally, as TPIs Irgacure 369, Irgacure 184 or 2,2-diethoxy-acetophenone[18] have been used. After 2PP fabrication, unreacted resin can be removed easily by immersing it in ethanol and subsequently drying the sample in air.[17] To get an impression of the applicability of SCR-500 for 2PP, a few examples shall be given: In 2004, Duan et. al. reported the 2PP fabrication of a diamond PhC (Figure 19) on the basis of SCR-500.[18] In order to increase the refractive index, TiO_2 nanoparticles were integrated in the photopolymer. Therefore, titanium ethoxide was reacted with methacrylic acid and mixed with SCR-500 and 2,2-diethoxy-acetophenone as PI. After 2PP processing of this novel resin, TiO_2 was formed via hydrolysis of the Ti^{4+} methacrylate complexes. Finally, development with ethanol and thermal post-treatment were carried out. The existence of a high quality photonic band gap was confirmed using transmission spectroscopy.

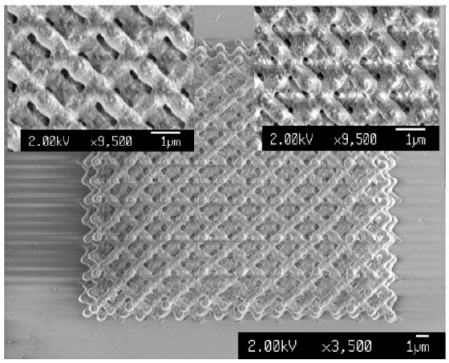

Figure 19: Scanning electronic microscopy (SEM) image of 3D diamond PhCs structure of inorganic nanoparticles-polymer composite materials produced by 2PP[18]

Deeper insight into the 2PP reactivity of radically polymerizable resins was provided by the group of Sun, who studied the temperature dependence of PhC writing in SCR-500:[19] It had been predicted that the structuring resolution could be greatly improved with decreasing temperature. This statement was based on the suppression of local photoinduced radicals and the reduction of Brownian motion. Contrary to this, however, the voxel size at -60°C, which is significantly below the freezing point of SCR-500, was found to be only little smaller than at ambient temperature. In addition, a phenomenon was discovered, in which the previously formed radicals in the frozen state did not polymerize until reaching a temperature of 10°C. This indicates the option of minimizing unwanted effects as floating or distortion during laser scanning. Conducting 2PP at elevated temperature gave less crosslinked voxels due to enhanced chain termination and thus lower polymerization rate. Finally, the photonic band gaps (PBG) of the PhCs were tailored via thermal processing. In some other studies, Xia and coworkers were able to manufacture 15μm scale micro spherical and Fresnel lenses with a SCR-500 as shown in Figure 20.[16]

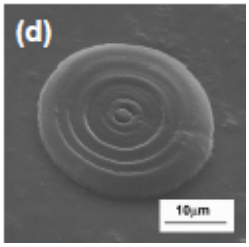

Figure 20: Micro Fresnel lens fabricated via 2PP of SCR-500[16]

Besides the highly important SCR 500, there are several other acrylic resins that have frequently been employed for 2PP of photonic elements. Sartomer 368, Tris (2-hydroxy ethyl) isocyanurate triacrylate (Figure 21), is a white, crystalline compound. It is used in UV-cured coatings, inks and adhesives.

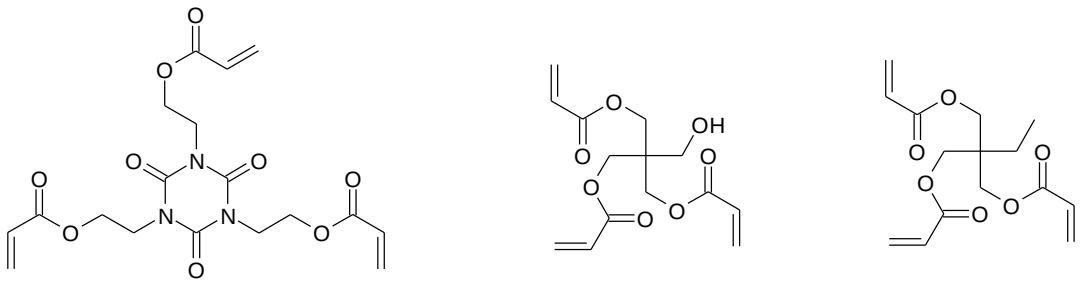

Figure 21: Tris (2-hydroxy ethyl) isocyanurate triacrylate (Sartomer 368, left), pentaerythritol triacrylate (Sartomer 444, center) and trimethylolpropane triacrylate (Sartomer 351, right)

Above its melting temperature of 52-54°C, Sartomer 368 exhibits rather low viscosity. The polar isocyanurate ring moiety is responsible for the excellent adhesion of Sartomer 368 containing films and their lack of brittleness in spite of high strength. Good weathering properties are caused by the saturation of Sartomer 368. This triacrylate furnishes photoreative resins with high reactivity and scratch-resistance, which are accompanied by chemical resistance and heat resistance.[20] Creating a film is possible by casting and evaporation of solvent[21] or by using calibrated spacers between two glass plates. Fourkas and coworkers modified a glass substrate employing (3-methacryloxypropyl) trimethoxysilane in order to obtain enhanced adhesion of a photopolymer formulation based on Sartomer 386.[22] The need for regulation of the refractive index contrast between the core of a waveguide and the cladding[21] can make it necessary to prepolymerize the matrix with white light. For the development of Sartomer 368 containing cured resins, N,N-dimethylformamide,[22] ethanol[23] or methanol[24] are solvents of choice. Rinsing durations are on a time scale of seconds and minutes. The trifunctional monomer Sartomer 368 has been used in various formulations, which were especially adapted for 2PP with the intention to fabricate optical structures: A possibility to integrate Sartomer 386 into a resin with other components such as binder and photoinitator is dissolution of all parts in chloroform and subsequent evaporation of the solvent after casting.[21] This method was applied by a French research group, which succeeded in connecting optical

fibers with waveguide structures. Furthermore, they were able to fabricate Y-splitters and a March-Zehnder structure. In this case, poly(styrene-co-acrylonitrile) served as a binder and (E, E, E, E, E, E)-1,13-bis-[4-(diethylamino)phenyl]-tri-deca-1,3,5,6,8,10,12-hexaen-7-one as TPI (Figure 21; L-Mich).[21,25]

In some other work it was combined with dipentaerythritol pentaacrylate as comonomer and Lucirin-TPO-L for the initiation of 2PP in order to create a high performance microring resonator (Figure 22), as done by Fourkas and coworkers. [23]

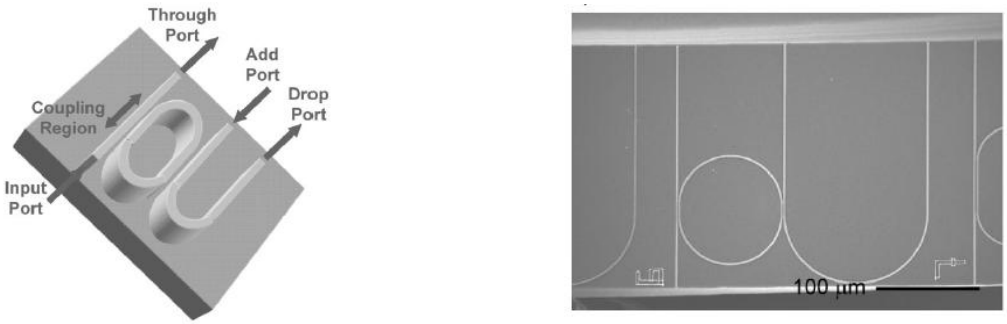

Figure 22: Principle of a microring resonator (left) based on 2PP fabricated waveguide structures (right)[23]

Moreover Sartomer 368 was used in a 50:50 wt% blend with the alkoxylated difunctional acrylate Sartomer 9008 along with 4,4'-bis(di-n-butylamino)biphenyl (12a) or E,E-1,4-bis[4-(di-n-butylamino) styryl]-2,5-dimethoxybenzene (14a) as TPI (Figure 16). Using this mixture, Perry et al. achieved intriguing 65 nm line widths in woodpile photonic crystal structures (Figure 31), which showed stop band gaps in the near infrared spectral region.[24]

Another monomer that is applied for the introduction of defects in PhC structures is trimethylpropane triacrylate (Sartomer 351, Figure 21: Tris (2-hydroxy ethyl) isocyanurate triacrylate (Sartomer 368, left), pentaerythritol triacrylate (Sartomer 444, center) and trimethylolpropane triacrylate (Sartomer 351, right)). Due to the trifunctionality this clear liquid contributes resistance against water and chemicals, abrasion and heat as well as weathering to a resin formulation in the crosslinked state. Its volatility is low and curing proceeds rapidly. A low viscosity of 106 cps at 25°C is accompanied by a glass transition temperature of 62°C and a relatively low refractive index of 1.4723, when it comes to optical elements.

In some remarkable works of Braun et al.[26-30] PhC replica structures were equipped with 3D defects (Figure 23).

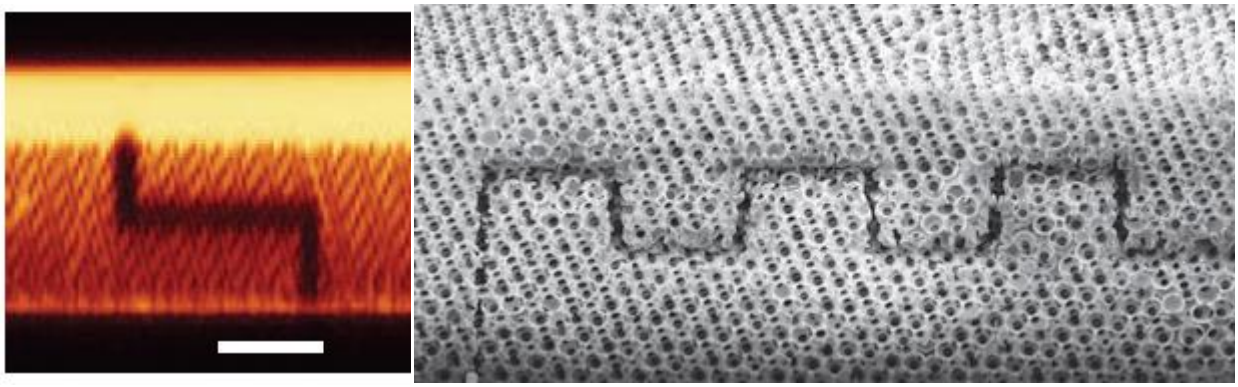

Figure 23: Double-bend waveguides embedded in a 3D PBG material (left, scale bar 10 µm) Vertical cross-section of air features embedded within silicon air inverse opals after removing polymer (right, scale bar 3 µm) [26]

First they created a silicon-air PhC from a SU-8 template, which had been formed via interference lithography. The strength of this method is the ability to form periodic structures in a high-throughput manner. Secondly, the PhC structures were infiltrated with two-photon-sensitive Sartomer 351-based resin. They used 0.1 wt% of AF-350 (tris[4-(7-benzothiazol-2-yl-9,9-diethylfluoren-2-yl)phenyl]amine) as PI (Figure 32) and a boron dipyromethene fluorescence dye for imaging purposes. After inserting defined defects via 2PP, which exhibits an excellent possibility to create non-periodic structures, ethanol was applied to remove unreacted Sartomer 351-based resin.[27]

In a different work of Braun and coworkers, they formed 3D-defects within a silica colloidal crystal by means of 2PP. The following high-index replication step and the removal of the opal template gave embedded defects in 3D silicon photonic crystals. The first waveguiding of NIR radiation around sharp bends in a complete photonic band gap material was reported also.[26]

Besides the above mentioned most popular monomers, a broad range of other acrylates have found an application in photonics-related 2PP as the following examples underline. Our group recently came up with an innovative concept for flexible waveguides structures:[31] Krivec et al. prepared low refractive, organically modified silica monoliths, which were flexible and served as a host for the polymeric, acrylate-based waveguides. The porous monoliths were prepared by using a surfactant-based template (Figure 24: Suggested pathway to fabricate waveguides by 2PP

in a porous silica host material. The porosity is generated by employing a liquid L3 ‘sponge’ phase and addition of appropriate silica precursors.[31]

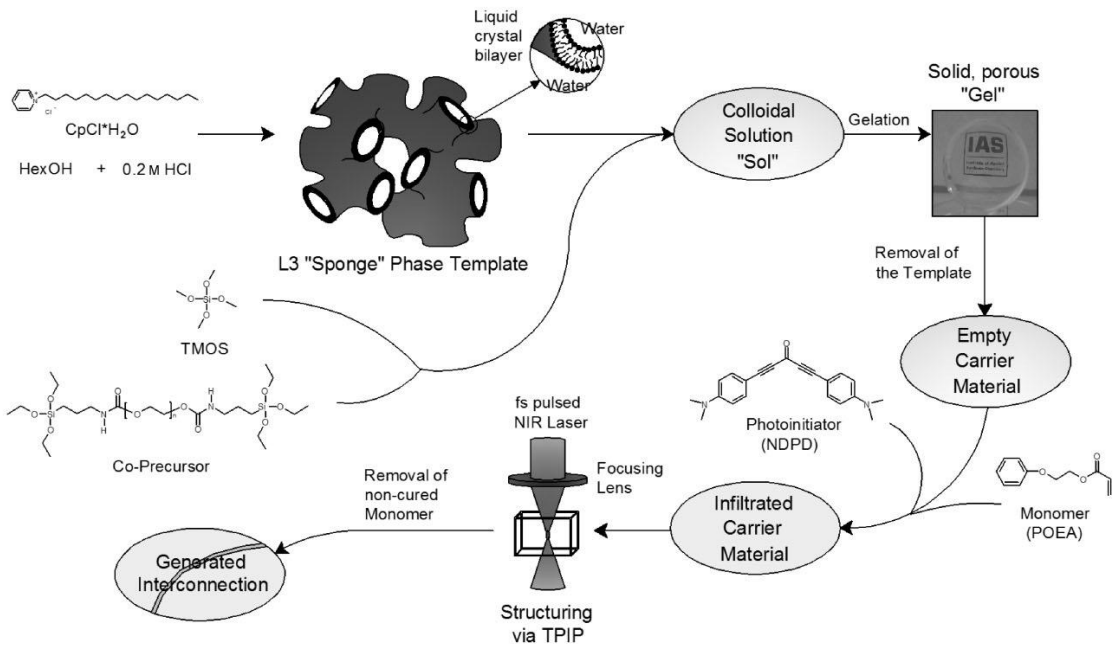

Figure 24: Suggested pathway to fabricate waveguides by 2PP in a porous silica host material. The porosity is generated by employing a liquid L3 ‘sponge’ phase and addition of appropriate silica precursors.[31]

After removal of the template, the host material was infiltrated with high refractive 2-phenoxyethyl acrylate and the TPI B3K.[32] 2PP yielded waveguide structures and a proof for waveguiding was accomplished (Figure 25)

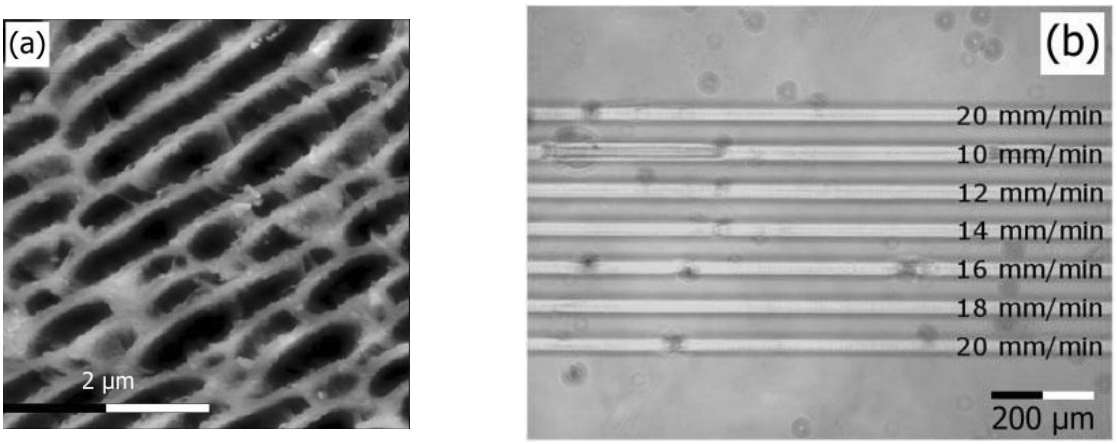

Figure 25: Atomic force microscopy (AFM) image of a porous monolith (left) and light microscopy image (right) showing waveguide bundles with a spacing of 75 mm structured in a monolithic sample at writing speeds from 10 mm/min to 20 mm/min.[31]

Another concept is derived from photolocking:[33,34] A low refractive polydimethylsiloxane film (PDMS) was swollen with an acrylic mixture containing the TPI B3K.[32] The extent of swelling was controlled via the ratio of acrylic acid isobornyl ester, which is well compatible with the PDMS and 1,4-butanediol diacrylate as crosslinker with worse compatibility. 2PP structuring of waveguides was followed by removal of unreacted monomers at reduced pressure. In Figure 26, a qualitative proof for optical waveguiding is depicted. Our current research is focused on avoiding the swelling procedure by mixing of the monomer formulation and the liquid polysiloxane matrix material with orthogonal reactivity prior to selective matrix curing in the presence of high refractive monomers as for example 2-phenylthioethyl acrylate.

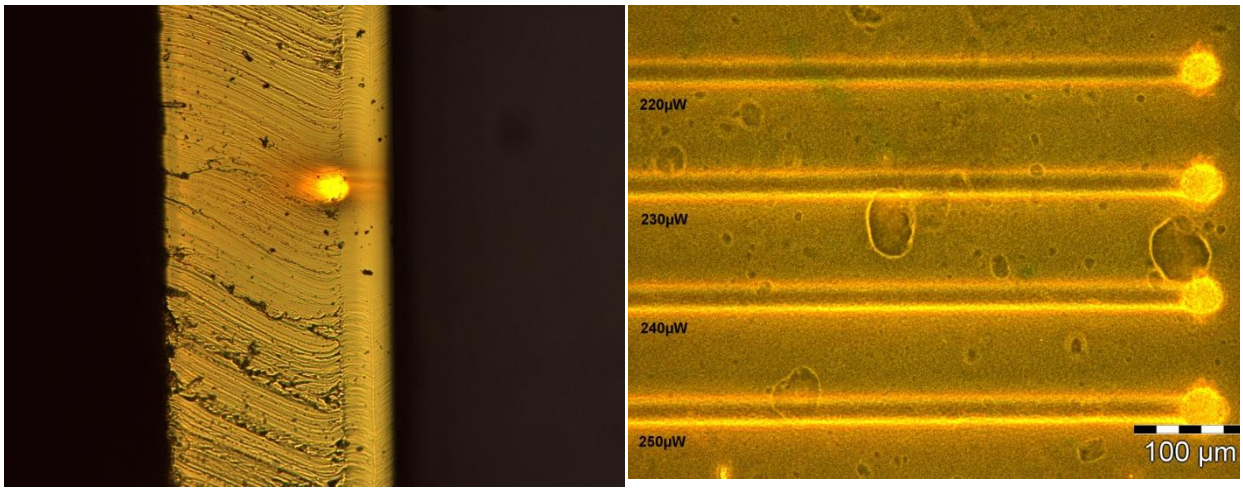

Figure 26: Left: Cross-section of a light-guiding optical waveguide bundle fabricated in PDMS, which was swollen with a 2PP reactive acrylic formulation. Right: Phase contrast image of waveguide structures based on a polysiloxane formulation, which was cured selectively in the presence of a 2PP reactive acrylic mixture

An analogue process of optical waveguides has been applied by the group of Kern.[35] They used phenyl and benzyl methacrylate as high refractive monomers, which do not interfere with hydrosilylation and thus allow for a process, where a Si-H addition cure of a phenyl containing silicone rubber is carried out in mixture with the two-photon-reactive monomer formulation. Promising efforts on the TPA-fabrication of optical interconnects for printed circuit boards have been presented. A refractive index difference of 0.02 between the illuminated core material and the non-illuminated cladding material was achieved. Kern et al. suggested that the current

optical damping value of 1.69 dB/cm obtained from cut-back measurements can be improved by changing the shape of the waveguides. Cross-sections of the latter are shown in Figure 27.

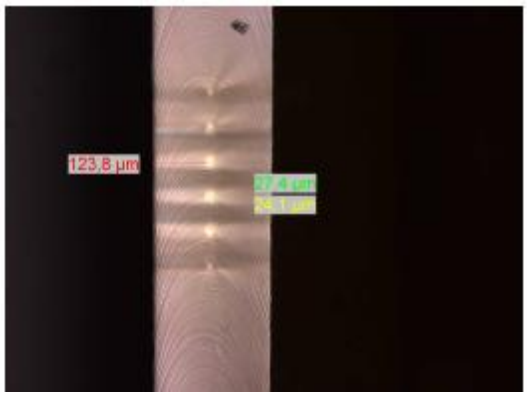

Figure 27: Illuminated cross-sections of inscribed polysiloxane-methacrylate based waveguides[35]

B) Thiol-ene resins

A considerable material class used for 2PP in optics is formed by thiol-ene-based resins. Commercially available are the product numbers 61, 63, 72 and 81 from the NOA (Norland Optical Adhesives) series, which were initially developed for UV-curing. Detailed chemical information has only been published for the NOA 61 formulation (Figure 41),[36] although a precondensation of the hydroxyfunctional vinylether with the isocyanate seems to be more realistic. Trimethylolpropane tris(2-mercaptoacetate) reacts with the double bonds of trimethylolpropane diallyl ether (Figure 28) via the UV, or TPA induced thiol-ene reaction (320-380 nm) with benzophenone as the PI. The curing process of the resins is carried out in two steps: Precure in the time range of seconds is followed by a final cure of a few minutes. NOA 63, 72 and 81 contain mercapto esters too and are also based on polyurethanes. With tetrahydrofurfuryl methacrylate another ene-compound in case of NOA 72 is given by the manufacturer.[37]

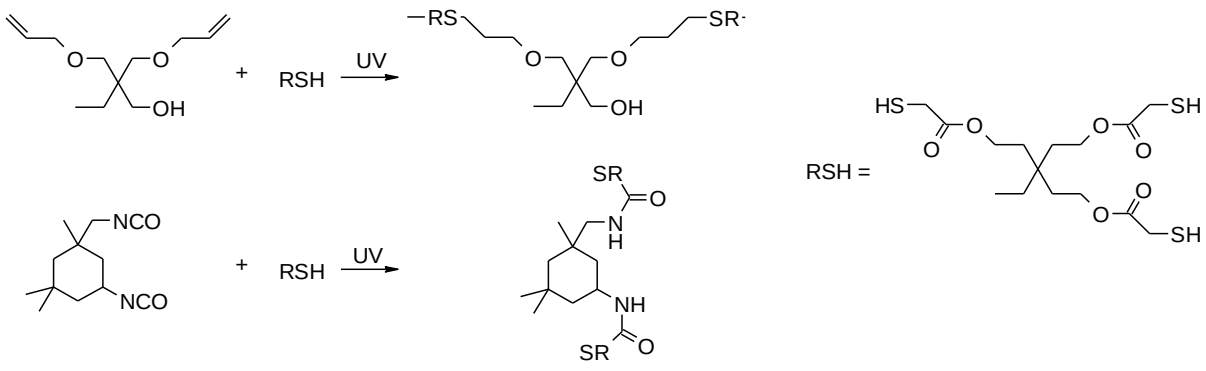

Figure 28: Crosslinking reactions of NOA 61 resin

In most optical applications, curing is conducted in two steps. A short, uniform exposure, or pre-cure, is carried out first followed by a main cure, which brings about full crosslinking and solvent resistance. Surface adhesion is optimized during the time after the cure, when chemical bonds are formed with the substrate.

The thiol-ene polymerization causes lower shrinkage values (e.g. 1.5% for NOA 61) than other resin types. Moreover comparatively high refractive indices around 1.56 at 635 nm are achieved with these organic materials in the crosslinked state. The viscosities of the liquid resins range from155 cps to 2000 cps.

All NOA thiol-ene resins exhibit very good transparency in the visible and NIR region. The 2PP polymerization was generally initiated by unknown PI within the NOA formulations, which are apparently also 2PP sensitive despite of their original application in UV curing. In one case, the curing was started by means of the blue emission of 465 nm of the added NIR two-photon absorbing fluorophore AF183 (6-benzothiazol-2-yl-2-naphtyl diphenylamine) causing the radical PI of NOA 72 to form radicals.[38] After 2PP curing the development of the microstructures is carried out with standard solvents as ethanol,[39] ethyl acetate,[40] and methanol. Thiol-ene based resins have been used for several 2PP experiments regarding optical elements as the following examples shall underline: Already in 1999, Prasad and coworkers[38] used a mixture of NOA 72, the epoxy glue EPO-TEK 301 (Polytek PT) and the TPI AF 183 for structuring optical elements such as beam-splitters, a grating coupler and waveguides in bulk. The components were mixed via heating and stirring. EPO-TEK 301 herein acts as a hardener, which causes a rubber like consistency of the NOA 72 film prior to 2PP writing after thermal crosslinking. The refractive index difference of 0.0234 between the non-illuminated cladding material and the illuminated waveguide

core regions was sufficient for waveguiding without a developing procedure. NOA 72 was also used by Kirkpatrick et al. to construct periodic grid structures with a holographic 2PP technique using NOA 72.[41] In this case, the TPI AF 380 was dissolved in NOA 72 in a benzene solution and via spin coating a film for 2PP was generated.[41] Furthermore, a Fresnel zone plate as well as multistep diffractive phase lenses were fabricated by Sun et al. using NOA 61 (Figure 29).[39]

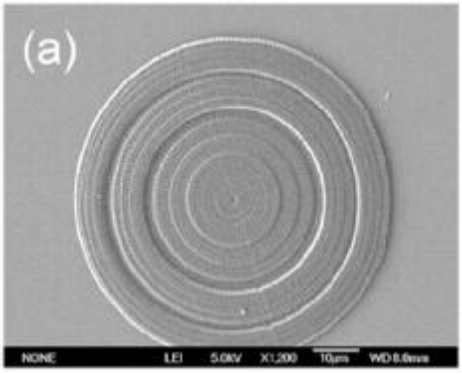

Figure 29: Multistep diffractive phase lenses fabricated via 2PP[39]

In another report, NOA 63 has been used to place line and point defects within Ormocer replica PhC structures applying the PI isopropyl thioxanthone (ITX).[40] For this purpose, a PhC was infiltrated with NOA 63 after adding some acetone for lower viscosity and better solubility of the PI.[40] A crucial issue for introducing defects in a controlled manner is imaging. Hence, Coumarine 6 was added as a dye for fluorescence microscopy (Figure 30).

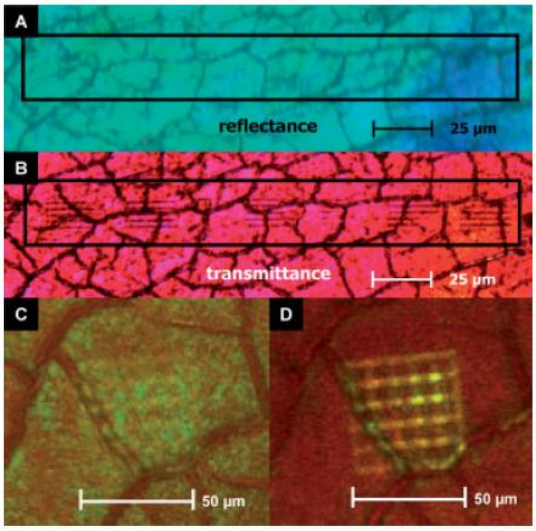

Figure 30: Images showing embedded defects in a replica structure. A: Reflected light microscopy does not make defect visible B: Transmitted light shows defects as thins dark lines C&D: Confocal microscopy: When focus is on the surface, defect is hardly visible (C); Focus inside replica shows defect clearly yellow (D) [40]

An interesting technology has been pioneered by the group of Cojoc.[42] For the first time axicon lenses, convergent lenses and ring-shaped phase masks were fabricated on top of an optical fiber (Figure 31) with NOA 63 as the resin of choice.

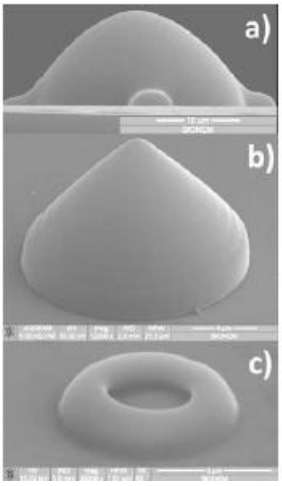

Figure 31: Different micro-optical elements fabricated on top of optical fiber by two-photon lithography: (a) convergent lens, (b) axicon lens, and (c) ring shaped phase mask.[42]

The simple processing prior to 2PP was to deposit a drop of NOA 63 on a glass substrate followed by UV pre-curing. They employed NOA 63 due to the good adhesion on glass, easy processing, the suitable refractive index of 1.56 of the

photopolymer and the low cost. In addition, NOA 63 - due to its glassy appearance after exposure - was reported to be a well-suited resin for the 2PP patterning of optical rotors (Figure 32), which are fueled by laser tweezer systems.[43] In a different paper, microscopic diffractive optical elements, which can create orbital angular momentum from Gaussian laser beams for optical trapping, were fabricated employing NOA 81.[44]

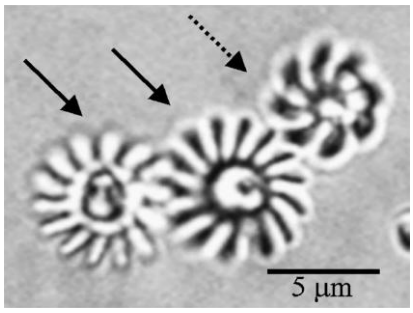

Figure 32: Complex micromachine built by the two-photon technique: two engaged cogwheels are rotated by a light driven rotor. The solid arrows point to the cogwheels rotating on axes fixed to the glass surface. The dashed arrow points to the rotor, which is rotated by a laser tweezer and drives the micromachine. [43]

C) Sol-gel derived resins

Due to the ever increasing demands in optics, composites are getting more and more indispensable because of their broad tunability of the material properties. For applications on the nanoscale, composites must be formed in situ. For this, the sol-gel technology provides a suitable tool. In the following chapter, the successful application of Ormocers will be discussed in detail followed by a few remarks on Zr-containing inorganic-organic hybrid materials.

Ormocers are an interesting class of nanocomposites, because they combine excellent material properties with the ease of conventional processing techniques.[45] An excellent overview is given by Sanchez.[45] They are popular materials in important research fields, such as integrated optics, coatings, dentistry etc. Ormocer photosensitive resins consist of sol-gel derived oligomers containing organic and inorganic groups, purely organic monomers and other additives such as a PI. Generally, they contain no solvent, which can, however, be added to control the viscosity and processability. Ormocers are so-called class II hybrid materials, which possess especially strong covalent or iono-covalent bonds between inorganic and

organic regions of the hybrid molecules. Beside metals such as Al, Zr or Ti, silicon is the most popular element for realizing organic-inorganic networks while alkoxide functionalities are usually employed for a sol-gel based assembly of them. Thus, most frequently organo-alkoxysilanes serve as precursors for Ormocers. Thanks to the stability towards hydrolysis of the Si-C bond it is possible to introduce various functional groups at different sol-gel environments bringing along novel properties such as flexibility, refractive index modification etc. Virtually any organofunctional group may be part of Ormocer. If the organic moiety is polymerizable, it plays the role of a network former. Other silanes as for example diphenylsilane diol are employed as network modifiers.[45]

According to literature, low absorption - a key property for photonic materials - can be achieved by a low content of C-H and silanol moieties. The latter is an outstanding feature of optical Ormocers, the synthesis for which is depicted in Figure 33.

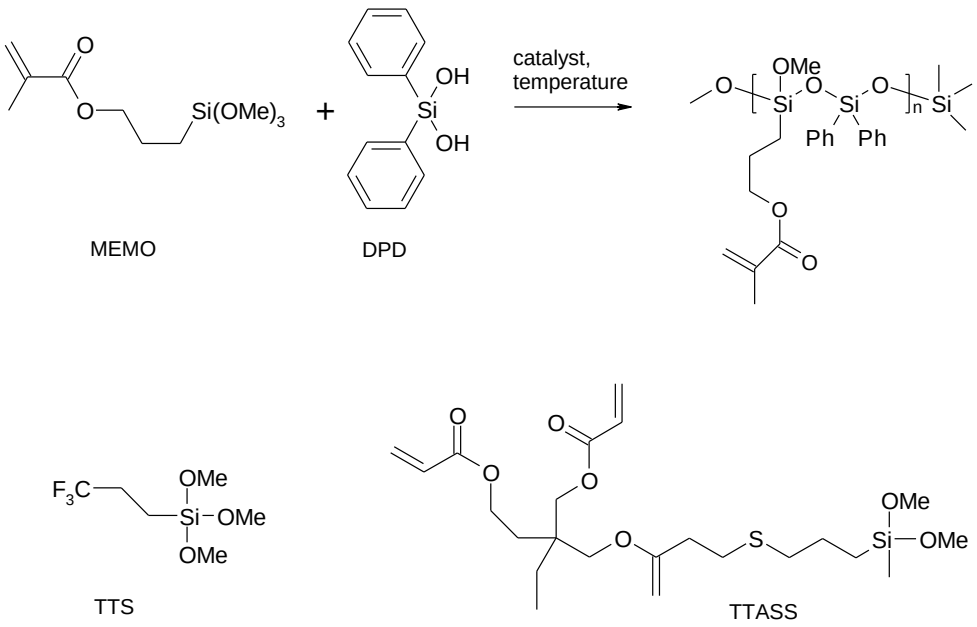

Figure 33: Example for an Ormocer sol gel process[46] and components (TTS and TTASS) for Ormocomp

Diphenylsilanediol (DPD) is reacted with methacryloxypropyltrimethoxysilane (MEMO) in a sol-gel reaction with a condensation catalyst at temperatures between 60°C to 100°C allowing for high reaction rates and kinetic control. This sol-gel process is carried out without adding water, which allows for focusing on the alkoxylation reaction of diphenylsilanediol (DPD).[47] Furthermore, the high sterical

demand of DPD caused by the phenyl groups kinetically favors alkoxylation reactions and prevents self-condensation of DPD. Thus silanol groups are hardly present in the final polysiloxane network. The by-product methanol or ethanol is usually evaporated.[48] Typical formulations for Ormocer resins for optical applications are Ormocore (DPD + MEMO), Ormoclad (DPD + MEMO + TTS) and Ormocomp (TTS and TTASS). [49]

As discussed later, it is desirable to integrate high refractive elements such as sulfur (Ormocomp) or titanium in Ormocer resins. Typical Ti-containing formulations consist of 17 mol% MEMO, 50 mol% DPD and 33 mol% $Ti(OEt)_4$. Processing viscosity is adjusted by application of different solvents such as THF or cyclopentanone.

Although Ormocer resins are as well cured via the classical radical photopolymerization in the UV-region, two striking benefits distinguish this technology from conventional UV-curable resins: Precursor oligomers of the siloxane part with a size of 1-5 nm provide a basis for very high resolution in UV-lithography, which is further completed by the fact that sterical hindrance of crosslinking causes the radical chain mechanism to break down quickly, which in turn suppresses unwanted polymerization in non-illuminated regions.[45]

Ormocers gain hardness, chemical resistency and transparency from their glassy component. Durability, ease of processing and functionalizability results from the partially organic character. Silicone-like elements ensure flexibility and adequate surface properties.[50]

By applying trialkoxysilanes and trifunctional metal alkoxides, Young's moduli greater than 10 GPa are obtained due to the tight crosslinkage. Glass transition is in some cases completely missing, in other cases it occurs in the range of ambient temperature. Difunctional equivalents form linear or cyclic oligomers with the behavior of elastomers. Low Young's moduli around 5-100 MPa and glass transition below room temperature are typical. Mixing different precursors such as tri- or difunctional alkoxysilanes, metaloxides and macromonomers enables controllability of mechanical properties from the range of soft and flexible polymers to rigid and sometimes brittle glasses.[45] A crucial optical property, optical attenuation, can be as low as 0.2 – 0.3 dB/cm at 1320 nm. In combination with this, refractive indices can be tuned from 1.47 to 1.58 (at 633 nm) enabling e. g. waveguiding applications. As photocurable Ormocer resins do not require any solvents, the shrinking behavior is

comparatively moderate. Their high thermal stability up to 270°C is necessary to meet the requirements for mass fabrication of e. g. printed circuit boards, which are laminated at similar temperature. The root mean squared (rms) roughness given in Table 1 stands for an almost perfect planarization behavior, which is important for substrates and makes the material interesting for highly sophisticated optical applications.[48]

Table 1: Properties of the three Ormocer resins for optical applications

Property[49,www.microresist.de]	Ormocore	Ormoclad	Ormocomp
Thermal stability (rate 5K min^{-1})	Weight loss <5% up to 270°C		
Young's modulus	860 +/- 120 MPa		925 +/- 100 MPa
Shrinkage	2-5 Vol.-%		
Rms roughness	2-4 nm		
Refractive index @ 635 nm	1.553	1.534	1.519
Optical attenuation @ 633 nm	<0.1 dB cm^{-1}	≤0.1 dB cm^{-1}	
Optical attenuation @ 1310 nm	0.23 dB cm^{-1}	0.26 dB cm^{-1}	
Optical attenuation @ 1550 nm	0.5 – 0.6 dB cm^{-1}	0.48 dB cm^{-1}	

Prior to 2PP microfabrication of optical elements, Ormocer (Ormocomp, Ormocore) resins may be prebaked for a few minutes at 80°C in order to increase the viscosity. It is also useful to carefully clean the (glass) substrate and thus exploit the good adhesion properties of the resin. In most cases films are prepared by spincoating but also by simply casting the resin into the cavity between two cover slips. [48,51,52,53]
As radical TPI Irgacure 369 is frequently used.[54-56] Ormocer is liquid prior to exposure but rapidly becomes solid within the illuminated regions. Thus the refractive index change upon polymerization has to be taken into account in the optical setup. On the other hand, main advantages result from this circumstance as online monitoring of the fabrication is easily possible. This is not the case for cationic systems as e.g. SU-8, where the polymerization only takes place during the postbake process. As

mentioned above, crosslinking is sterically hindered, so parasitic radical reactions in non-illuminated regions are eliminated. This is an important aspect in the case of 2PP contributing to the extremely high resolutions that are achieved with Ormocers.

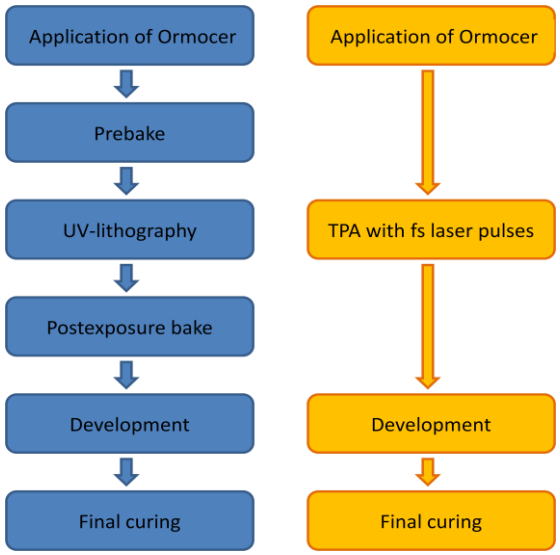

Figure 34: Processing techniques of Ormocers – UV (left) and TPP lithography (right)

Moreover the 2PP method provides for a double shortcut in case of processing: Pre- and post-exposure bake as well as dilution with solvent is not necessary as for conventional UV-curing, because the polymerization takes place within the resin volume (Figure 34).[48] Post-baking can, however, be useful because the adhesion of the microstructures to the substrate is improved.[52] As shown in a study on PhCs,[57] it is possible to enhance the resolution of PhC microstructures via post thermal treatment at temperatures between 150°C and 300°C after removing unreacted resin with 4-methyl-2-pentanone and isopropanol, a common solvent for the development of Ormocer.[54] Final curing assures that the maximum crosslinking degree is reached.
In literature, there are several different applications where Ormocers were successfully employed. A distributed-feedback-resonator, which might be used for optical lab-on-a-chip applications, was fabricated via 2PP by Woggon et al. using the Ormocomp resin.[52] The resonator is based on a 400 nm periodic grating with 40 nm height modulation. Partial 2PP structuring within the substrate, which is caused accidently by slight tilting of the cover slip, was circumvented by fabricating the resonator on a stage with a thickness of a voxel. For the active material layer the organic semiconductor tris-8-hydroxyquinoline aluminum doped with the laser dye 4-(dicyanomethylene)-2-methyl-6-(4-dimethylaminostyryl)-4H-pyrane was applied.

Finally the extensive work of the Fraunhofer institute, where Ormocer materials were actually developed, must be mentioned here: Especially Houbertz and coworkers have successfully implemented Ormocer technology into 2PP structuring of optical elements.[46, 48, 55, 58, 59]

In an interesting work, waveguides were fabricated to connect a photodiode and a laserdiode on a printed circuit board using only one material: The 2PP structured areas served as the core material while the surrounding material represented the cladding. During polymerization organic polymerizable moieties diffuse towards the polymerizing region and cause therefore the desired refractive index change. Importantly, it is therefore not necessary to use a solvent for developing processes. Only a post-curing step is required. PhC research has also been done by that group using Ormocers. Shrinkage problems have been tackled by taking them into account during the structuring process.[48] With the intention to tackle the problem of not being able to create a full PBG with resins such as Ormocer, SU-8, Acrylates etc., Houbertz et al. invented a Ti-containing Ormocer-based 2PP resin named Ormocer PD92. PhC with a PBG in the NIR region were fabricated. Shrinkage upon 2PP, however, remained a problem typical to Ti-containing resins.[59]

Although Ormocers undoubtly dominate the class of sol-gel derived materials in 2PP technology for photonics, a similar type of resin has attracted considerable interest: Zr-based sol-gel resins exhibit advantages like controlling the refractive index via the Zr-content, an improved mechanical stability and – most importantly – very low volume shrinking.[60] If the laser power is sufficient, even PhC structures with no measurable shrinkage are viable.[61] This fundamental benefit is thought to be owed to the inorganic and organic double polymerization feature of the resin: Condensation reactions are amended by radical polymerization of the methacrylic moieties. The first step of the synthesis[62] is carried out by chelating Zirconium n-propoxide with methylmethacrylic acid (MMA) and adding a hydrolysed product of MEMO. Afterwards water is added and an interconnected porous cluster structure is obtained. 4,4-Bis(diethylamino)benzophenone is used as TPI in this case. The gelation step involves the removal of solvents and is typically carried out at 100°C. The formation of Si-O-Zr is kinetically favored under these conditions. Thus condensation is accelerated compared to other sol-gel derived resins, which is another advantage of this technology. Films for 2PP are generated via drop casting

or spin coating. 1-propanol is a suitable solvent to remove unreacted resin after 2PP structuring. In literature the aforementioned resin is applied for PhC fabrication[61-63] with a clear bandgap in the NIR region (Figure 35).

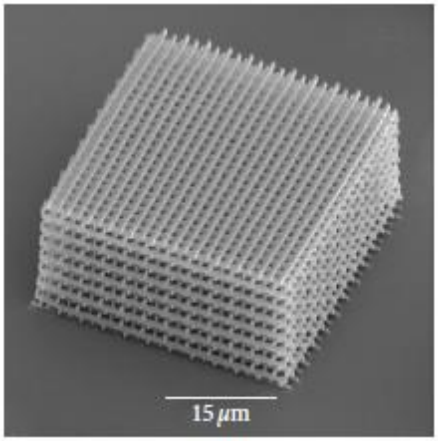

Figure 35: SEM image of Zr-containing photonic crystal structure (applied material MAPTMS:ZPO ratio is 8 : 2)[62]

D) Materials based on cationic polymerization

Besides radical polymerization, cationic photocuring is another important technique to get crosslinked polymers from a large set of commercially available monomers. For the cationic curing, mainly epoxy-monomers such as ECC or BDG (Figure 35) are used. To reduce the brittleness of this system, chain transfer agents based on multifunctional alcohols are added up to 10 wt%. For the photoinitiation process, photo acid generators such as iodonium or sulfonium salts are employed whereas the latter class is preferred when higher storage stability is required. As the absorption of these initiators generally tails out at ~ 300 nm, either heterosubstituted derivatives are used (Cyracure UVI-6976) or sensitizers are employed to extend the spectral range of sensitivity. While iodonium salts can be more easily sensitized by compounds like anthracenes, perylenes, phenothiazines, xanthones or thioxanthones, only a limited range of sensitizers (e.g. the former three) is available for sulfonium salts.

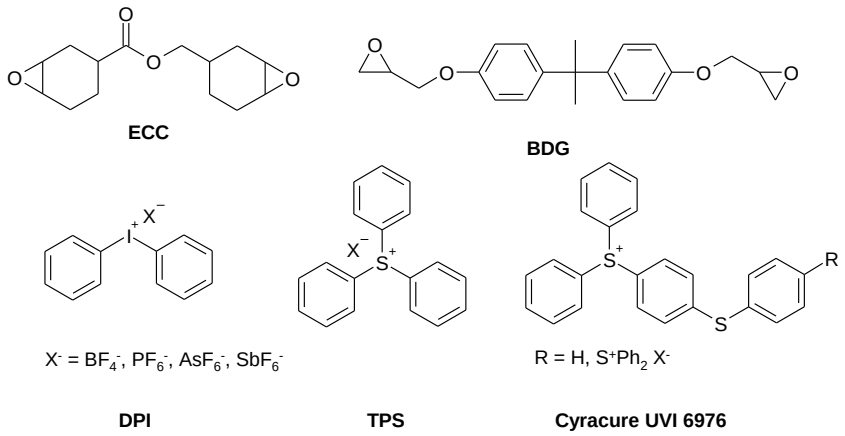

Figure 36: Typical epoxy monomers (top row) and PIs (bottom row) for cationic polymerization.

Advantages of cationic curing over radical polymerization are for sure the lower shrinkage and the absence of oxygen inhibition. Unfortunately, lower reactivity, sensitivity to moisture and high water uptake of the polymer are adverse effects.

The usage of resins, which have been TPA-cured via cationic polymerization, is nearly limited to EPON SU-8 (Figure 37), which in turn is one of the most popular products in 2PP related research.

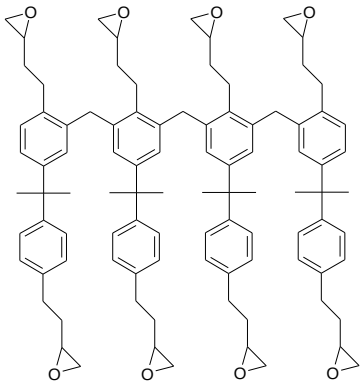

Figure 37: Chemical structure of SU-8

The epoxy-based SU-8 negative tone resist – originally developed for UV-curing in electronic applications by IBM[64] – is now established for the research on 2PP microfabrication, as it is readily available and inexpensive. The resin originates from bisphenol A, which is oligomerized using a Novolak condensation procedure, which is well known from the preparation of phenol formaldehyde resins. Subsequently the free hydroxyl groups are functionalized by means of epichlorhydrin. SU-8

formulations are typically composed of 10wt% of triphenylsulfonium hexafluoroantimonate as a UV- and two-photon-sensitive photoacid generator in a mixture with a variable ratio of SU-8 resin to organic solvents allowing for adjustment of the overall viscosity of the resist. Gamma butyrolactone was initially employed as solvent until Shaw and coworkers discovered technological benefits of cyclopentanone, such as improved wettability of low surface energy substrates and faster processing times.[65]

In case of single photon polymerization, a photoacid, which is generated by a photosensitive onium salt through protolysis, catalyses the crosslinking process via cationic ring opening polymerization of the epoxy functionalities at elevated temperature after exposure. This kind of polymerization has to such a degree amplification character that one protolysis event can cause several chains to grow, because the acid is not consumed. Furthermore, cationic polymerization does not exhibit oxygen exhibition, which is a central shortcoming of the radical 2PP of acrylates. In case of SU-8, each monomer gets crosslinked to seven others on average.[66]

Optical transparency as a fundamental material property for photonics and a high refractive index originates from the numerous aromatic ring structures[67] of the bisphenol A novolak oligomer. Thanks to eight epoxide functionalities per molecule, which provide for extensive crosslinking, SU-8 exhibits a high mechanical and thermal stability after light exposure as well as chemical resistance. Additionally, high aspect ratios as well and straight sidewall profiles are achieved. Another important advantage is the comparatively high glass transition temperature of the non-crosslinked resist of about 50°C: It turns out to be crucial to the high resolutions, which are achieved via UV- and two-photon lithography resulting from the very limited diffusibility of the photoacid prior to the post-exposure bake step.

In contrast to its numerous advantages, SU-8 processing comprises various processing steps: Substrate pre-treatment is followed by coating, soft baking and exposure. The post-processing involves postbaking, development, rinsing, drying and hardbaking. Another short-coming is shrinkage of approximately 7% depending on the thickness and area size of the structure.[68]

Via spin coating SU-8 allows for a uniquely broad range of film thicknesses from 2 to 300 µm in a single coating step. In order to remove the solvent and densify the film,

Microchem Corp. recommends a softbake process at 95°C. The spectral range for single photon exposure is given from 350 nm to 400 nm.

The exact mechanism of two-photon induced crosslinking of SU-8 has not been fully clarified yet: Due to pulse irradiances near the dielectric breakdown (around 1 T/cm2) and thus a highly ionized environment the cationic photopolymerization is likely to proceed in a different manner as in the single-photon case. It can be explained by absorption of spectrally broad emission of thermally non-equilibrated electrons when high irradiance femtosecond pulses are applied to the resist.[69]

In the event of 2PP, 800 nm Ti:Sapphir femtosecond lasers have proven to be suitable for effective structuring. Compared to other polymeric materials for 2PP microfabrication, SU-8 formulations do not undergo a liquid-solid phase transition under illumination, which turned out to be advantageous for the structuring resolution. In a conventional UV-lithographic process and the majority of 2PP patterning experiments reported up to now, the subsequent postbake process provides the activation energy for the cationic ring opening crosslinking reaction, which is inhibited at room temperature. Generally, the foregoing exposure exclusively causes the formation of photoacid. Recently, however, certain 2PP processing parameters were found, that allow to do without the postbake process and thus minimize diffusion of photoacid before postbaking. Here, the heat of exposure enables the crosslinking.[69] In the final step, the sample is developed with solvents like ethyl lactate.

The success of cationic 2PP strongly depends on the effective generation of a photoacid: As a consequence of limited success with 2PP using conventional photoacid generators, Marder et. al. synthesized the cationic PI BSB-S_2 based on a *bis*[(diarylamino)styryl]benzene core, which exhibits a D-π-D motif with covalently attached dialkyl aryl sulfonium moieties, known for their potential to generate H^+ in case of reduction by a one electron transfer process (Figure 38).[70]

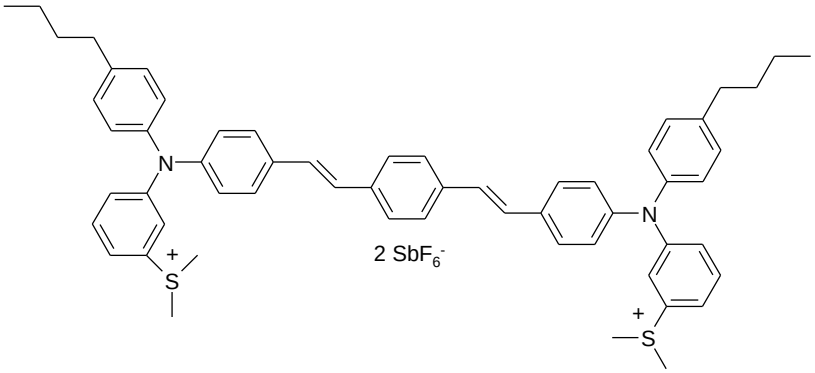

Figure 38: Structure of the TPI BSB-S2

This TPI allowed for the reliable fabrication of a “stack-of-logs” photonic bandgapstructure in SU-8 (Figure 39).

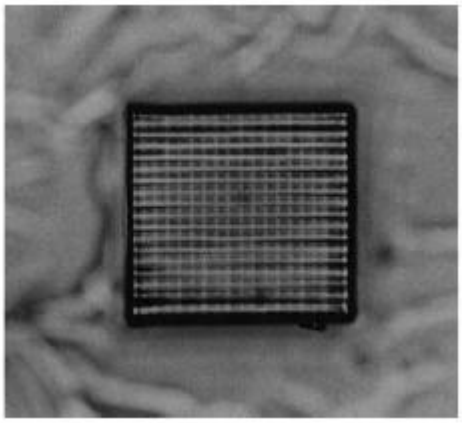

Figure 39: Optical transmission micrograph of a “stack-of-logs” photonic bandgap structure fabricated with an average power of 3.5mW[70] Reprinted from Journal of Photochemistry and Photobiology A

SU-8 - despite of its numerous advantages does not allow the manufacturing of PhCs with spectrally broad photonic band gaps due to its relatively low refractive index of 1.6 compared to inorganic materials. It is, however, well suited as a template material for PhCs. For Deubel et al.[71] an important reason to employ SU-8 as material to produce PhC templates via 2PP as well as the possibility to structure behind already polymerized regions due to the very small refractive index change upon polymerization. As further advantages they mention the fact that SU-8 is solid under

2PP conditions eliminating the need for interconnecting the written features immediately and the absence of oxygen inhibition. As shown by Serbin et al.,[67] SU-8 scaffold for PhCs can be removed via calcinations after infiltration and subsequent sol-gel crosslinking with titanium(IV)-isopropoxide. Very recently, Seet e. al. lately presented a SU-8 double inversion process.[72] The reason to use SU-8 was that the 100 nm resolution barrier has been passed with this material. Another interesting experiment was conducted by Sun et al.,[73] who succeeded in microfabricating a microlens with 100% filling factor using TPP in SU-8. In this case SU-8 was the material of choice due to its high transmission of light from the visible to the near-infrared wavelengths, the low volume shrinkage upon polymerization and its good mechanical properties. Transmission measurement revealed that the optical absorption by the microlens array was negligible: e.g. a 1.5-µm-thick polymerized SU-8 film yielded a transmittance of 99% in the wavelength range from 360 to 1100 nm. In 2008, the group of Chanda fabricated a three level optical diffractive element using SU-8 2002.[74] In some other work, Turberfield et al. were able to place a correctly aligned Mach-Zehnder interferometer structure consisting of linear waveguide motives via 2PP within a PhC that was created by means of holographic lithography (Figure 40).[75]

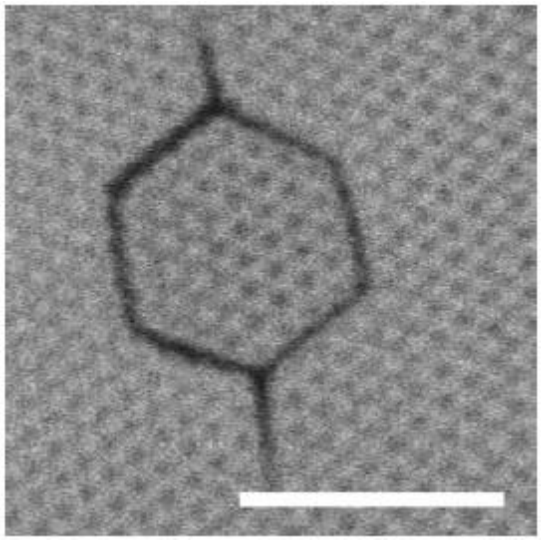

Figure 40: Photonic crystal pattern with inscribed Mach-Zehnder structure (confocal section through fluorescence of infiltrated dye, scale bar: 5µm[75]

Furthermore, Lee et al.[76] applied a two-photon laser-scanning microscope to produce 2-dimensional photonic crystal structures in SU-8 polymer films with circular, elliptical, rectangular, or diamond-shape unit cells in a hexagonal or square lattice. An aspect ratio of 6.9 with 250 nm line width was accomplished. Specific patterns, e.g. lines, dots, and Y-splitters were placed in the otherwise perfect photonic crystals.

General Part

1. General remarks on monomers and matrix materials

The crucial quantity of an optical interconnect is the optical attenuation describing the amount of light lost during waveguiding. Generally the guiding of photons is possible, when the core material exhibits a minimum relative change in refractive index (n) of 0.003, which is the increase in refractive index from cladding to core material divided by the n of the core material. Increasing relative change in refractive index widens the acceptance cone and simplifies the coupling-in of light to the waveguide. A second crucial property is the optical transparency of the material. In case of flexible optical interconnects manufacturing, however, further criteria have to be fulfilled by the material such as processing time and ease as well as thermal stability. A flexible material fulfilling all the criteria is polydimethylsiloxane (PDMS) and in the course of this work it is considered as the best choice for this application. Excellent optical, mechanical and thermal properties are accompanied by a well-established curing chemistry and good commercial availability of various polysiloxane copolymers with various functionalities (Table 2).

Table 2: Relevant properties of PDMS[1]

Properties	
Optical damping (850 nm)	0.02-0.05 dB cm^{-1}
Thermal stability	up to 290°C
Shrinkage	<0.1%
n	1.4

Its n of 1.4 allows for using a wide range of higher refractive monomers generating a local refractive index change. The thermal stability is more than sufficient for the industrial manufacturing process for printed circuit boards. Low shrinkage is an extremely important feature with respect to the precise alignment of the waveguide between the optical elements on the board. The absorption behavior of PDMS is illustrated in Figure 41.

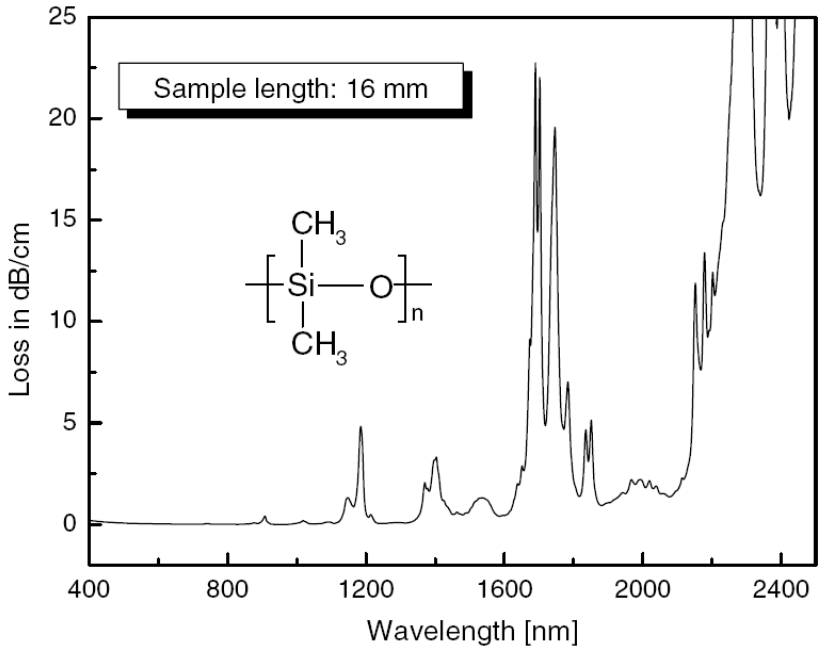

Figure 41: Optical absorption behavior of PDMS[4]

The spectrum exhibits no major absorbance at important telecommunication wavelengths as 850, 1300 and 1550 nm, which is another argument for its application in short distance data transfer.

While attempts in the past were based on the photopolymerization of (meth)acrylates forming hybrid materials with the cured polysiloxane matrix,[77-79] it was decided to apply thiol-ene networks because of their high n owing to the sulfur atoms, their high thermal stability and reduced shrinkage. The first criterion that monomers had to meet was a higher n of the corresponding photopolymer than the polysiloxane material as a local increase in refractive index was desired in the illuminated regions. Moreover, the monomer formulation should be able to form a crosslinked network upon 2PP and show an acceptable reactivity (2PP and UV) promoting fabrication speed. During the fabrication process the monomer should not evaporate significantly. The main bottle-neck prerequisite was the compatibility of the photopolymer with the matrix material to ensure transparency and minimum optical attenuation of the waveguides. To a certain extent, the curing chemistry of the polysiloxane rubber had to function in the presence of the thiol-ene formulation. Furthermore it should be selective so as not to react with either the thiol or the ene monomer. This obstacle could also be circumvented by postponing the matrix curing step after the 2PP structuring. 2PP fabrication of a liquid medium required some

means to hold the structured waveguides in place and prevent them from sinking due to their higher density compared to the uncured liquid. The most self-evident solution to this would probably be to work with a high molecular weight and very viscous polysiloxane matrix material and cure it after 2PP. But in this case the usage of rather non-futile solvents would be necessary to get monomer and matrix material mixed and to avoid bubbles. The removal of these solvents would make the process impractical. A more elegant way is to use a rheology additive, which in the course of a few hours turns the formulation into a thixotropic liquid leaving enough time for straightforward sample preparation. An additional benefit of 2PP in liquids compared to the situation in polysiloxane rubbers is the facilitated diffusion of monomer towards the illuminated volumes yielding a greater local enrichment of high refractive material and thus enhancing the local change in n.

2. 2PP Waveguide fabrication from a polysiloxane-based thixotropic liquid

2.1. Selection of Matrix Material

The development of a two-photon reactive thixotropic liquid, which allows the formation a transparent, flexible waveguide material started with a screening for a proper combination of crosslinkable polysiloxane and a rheology additive that is capable of turning into a thixotropic liquid in mixture: For conventional, hydrophobic PDMS no proper rheology additive was found to feature any thixotropic effect. Many rheology additives such as BYK 410 (Figure 42), BYK E 410 and BYK 420, however, are commercially available for more hydrophilic media. They are based on urea as the active ingredient featuring hydrogen atoms and short alkyl moieties attached to the nitrogen atoms.

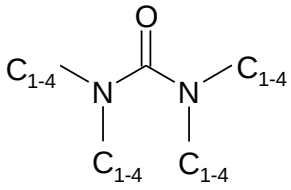

BYK 410

Figure 42: Chemical structure of BYK 410

The compatibilizing solvent is N-methyl-pyrrolidone (NMP) in the additives BYK 410 and BYK 420 or N-ethyl-pyrrolidone (NEP) in BYK E 410. After dissolution in the medium that should be provided with thixotropy, the urea derivative aggregates in a controlled manner, forming 3D networks of needle shaped tiny crystals yielding thixotropy (Figure 43). The latter can be reversibly destroyed upon shearing.

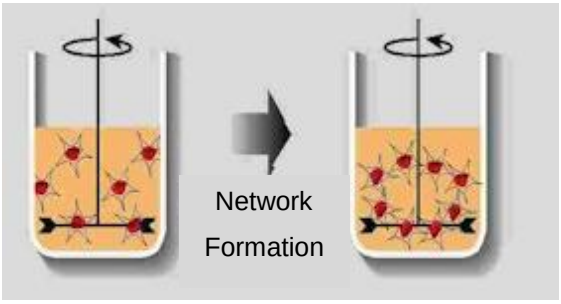

Figure 43: Formation of thixotropy in a resin after homogenization with BYK 410[80]

In contrast to plain silicones and phenylmethyl siloxane copolymers that are frequently used in optical applications, silicone polyether acrylate features polyether domains making it more hydrophilic and thus better applicable to the just mentioned rheology additives.

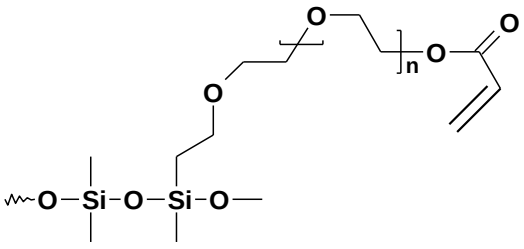

TEGO RAD 2200 N
Silicone polyether acrylate

The latter are commercially available under the trade name “TEGO RAD” with set of products for different specialized applications. Note that these resins exhibit a large range of small molecule acrylate impurities.[81] The silicone polyether acrylate based silicone additive TEGO RAD 2300 had turned out to be well-compatible with certain thiol-ene networks in former works.[82] As stated by the producer, TEGO RAD 2200N is the broadest compatible UV-curing silicone acrylate in the TEGO RAD series, which has been developed mainly for clear coatings, thus it was chosen for this work and tested for its applicability to BYK rheology additives. BYK 420, probably due to its higher polarity, caused strong clouding as a result of phase separation when added at a concentration of 2%. Apart from transparency being fundamental for waveguiding, thixotropy could not fully develop as the fine crystals could not be homogenously distributed in TEGO RAD 2200N. In contrast, adding BYK E 410 to TEGO RAD 2200 N at 2% yielded a rather clear medium. Foaming, however, was very pronounced. Thixotropy kicked in after a few hours due to interaction of the urea-based crystals with the hydrophilic polyethylene glycol units of silicone polyether acrylate. This could be preliminarily observed by means of the liquid remaining in place after turning the vessel upside down. After full development of the rheological effect a very limited cloudiness of the medium was observed, when looking through vessels with a diameter of a few centimeters containing the thixotropic liquid. This can clearly be explained by precipitation of the urea derivative due to evaporation of the compatibilizing solvent NEP over time. The size of the urea-based crystals must thus be larger than the wavelength range of visible light. This undesired phase separation bringing the thixotropic effect thus caused unwanted scattering of light at the phase boundaries making minimization of the content of rheology additive necessary: The relation of BYK E 410 concentration and thixotropy in TEGO RAD 2200N will be accounted for in section 2.7. The minimum concentration required for sufficient thixotropy to fabricate straight waveguides, which would remain in place during and after structuring until fixation by UV-curing, could only be determined by 2PP experiments in sections 2.2 and 2.8 .

Thus the waveguide manufacturing process (Figure 44) should be the following: Matrix material, rheology additive and a photoreactive monomer formulation should be mixed in the first step. After storing the sample until the thixotropic effect would kick in, 2PP waveguide inscription should be conducted and finally the material would be stabilized via UV-two-photon polymerization. Advantageously, the curing

chemistry for matrix material and monomer in this concept does not need to be orthogonal like in case of the former works.[83] Structuring waveguides inside a liquid should provide an advantage in terms of the efficiency of diffusion towards the two-photon-illuminated regions during 2PP compared to fabrication inside cured silicone rubbers. Another important advantage is the copolymerization of matrix material and monomer, which would avoid phase separation.

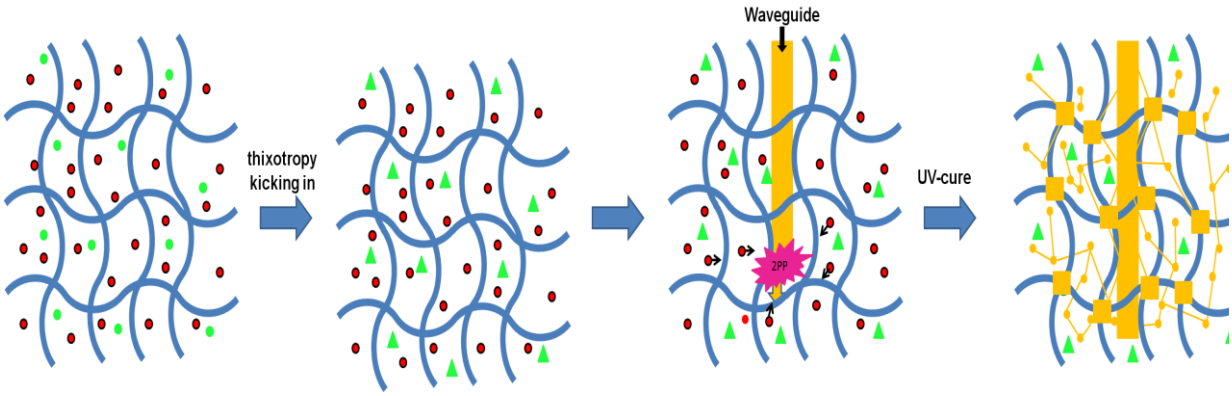

Figure 44: Manufacturing process of flexible waveguides (green dots: rheology additive prior to thixotropy, red dots: triacrylate TTA, blue wiggly lines: polysiloxane matrix material TEGO RAD 2200N, green triangles: rheology additive after thixotropy formation, black arrows: monomer diffusing towards 2PP focus, orange squares: TEGO RAD 2200N UV-crosslinks, interconnected orange dots: UV-cured monomer copolymerized with the matrix material)

Based on the proof principle that BYK E 410 is a rheology additive, which yields a feasible thixotropy in the polysiloxane-based matrix material TEGO RAD 2200N, extensive material development and optimization will be presented in the upcoming sections involving a number of formulations. For clarity, the compositions of the latter are summarized in Table 3

Table 3: Formulations for the development of the thixotropy-based waveguide fabrication (wt %).

Formulation	DPGDA	EGDMA	DOD	TTA	TT	B3FL	Darocur 1173	TEGO RAD 2200N	BYK E 410
2PP/1.1	11.0		8.2			0.8	2.0	75.0	3.0
2PP/1.1/2:3	12.8		6 .4			0.8	2.0	75.0	3.0
2PP/1.1/1:10	17.9		1.3			0.8	2.0	75.0	3.0
2PP/1.2		11.0	8.2			0.8	2.0	75.0	3.0
2PP/1.3			7.5	12.2		0.1	2.0	75.2	3.0
2PP/1.4/20				20		0.1	2.0	74.9	3.0
2PP/1.4/20a				20		0.1	2.0	75.9	2.0
2PP/1.4/20b				20		0.1	2.0	76.4	1.5
2PP/1.5/4:6				20	16.0	0.1	2.0	59.2	3.0
2PP/1.5/1:10				20	2.4	0.1	2.0	72.8	3.0
UV/1.4/0							2.0	98.0	
UV/1.4/10				10.0			2.0	88.0	
UV/1.4/20				20.0			2.0	78.0	
UV/1.4/20/BYK				20.0			2.0	76.0	2.0
UV 1.4/30				30.0			2.0	68.0	
UV/1.5/1:10				20	2.4		2.0	75.6	
UV/1.5/4:6				20	14.0		2.0	64.0	
Rheo1/1.4/10				10.0				89.0	1.0
Rheo1/1.4/30				30.0				69.0	1.0
Rheo2/1.4/20				20.0				78.0	2.0
Rheo3/1.4/10				10.0				87.0	3.0
Rheo3/1.4/30				30.0				67.0	3.0
DMTA/1.4/0							2.0	96.0	2.0
DMTA/1.4/20				20.0			2.0	76.0	2.0
DMTA/1.4/30				30.0			2.0	66.0	2.0
DMTA/1.5/4:6				20.0	14.0		2.0	62.0	2.0
DMTA/1.5/1:10				20.0	2.4		2.0	73.6	2.0
WG/1.4/20				19.9		0.1	2.0	76.0	2.5

Abbreviations: DPGDA (dipropyleneglycol diacrylate), EGDMA (ethylene glycol dimethacrylate, DOD (2,2′-(ethylenedioxy)diethane thiol), TTA (trimethylol propane triacrylate), TT (pentaerythritol tetrakis(3-mercaptopropionate)

The abbreviations of the formulations exhibit the structure *x/y/z*: They start with *x*, a description about the main purpose that the formulation was used for, such as 2PP or DMTA. Some formulations were used in more than one chapter, so *x* represents their function when used for the first time in this work. On the way to a formulation, which allows for the proof of principle for waveguiding, a screening for monomers was carried out, so *y* represents numbering of monomer combination of monomers used in the formulation. *Z* gives a hint on monomer content, ratio of thiol:acrylate or the presence of rheology additive.

2.2 Selection of monomer and preliminary 2PP experiments

In addition to the general monomer properties mentioned in section 1, highly reactive, compatible monomers with low viscosity and good diffusibility were required to build a stable photopolymeric network efficiently in the thixotropic liquid. As mentioned before, in former concepts, unreacted monomer had to be removed in the last step in vacuum.[77, 79] For the new strategy, where the enrichment effect of high refractive monomer diffusing into the VOXEL during 2PP writing should be exploited, also non-volatile, higher molecular weight monomers were among the candidates. Especially triacrylates due to their relatively low viscosity and rapid crosslinking behavior were of interest. These properties are well combined in trimethylol propane triacrylate (TTA).

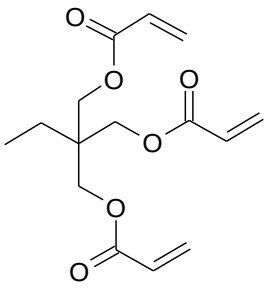

TTA

This commercially available monomer turned out to be compatible with the rheology additive containing silicone acrylate matrix material TEGO RAD 2200N and did not interfere greatly with the formation of thixotropy. An alternative trifunctional acrylate would be ethoxylated trimethylol propane triacrylate (ETA) contributing less brittleness to the hybrid material than TTA but on the other hand diffusion was

thought to be less efficient due to the size of the molecule. Hence, a formulation with the monomer content of 20% using exclusively the triacrylate TTA was tested (formulation **2PP/1.4/20**) successfully in 2PP waveguides structuring experiments: TTA is known to form a rather stiff photopolymer and thus enabled perfectly straight waveguides over a wide range of feed rates and laser power in the thixotropy liquid and using 3% BYK E 410. Exclusively acrylate-based systems, however, are known to feature disadvantages such as a low thermal stability, pronounced shrinkage and oxygen inhibition. For this reason it would be reasonable to introduce a thiol of at least a functionality of 2 into the system, which would tackle the latter drawbacks and generate an even higher local refractive index change. The following sections will address analytics on reactivity, thermal stability, rheological behavior and the effect of thiol on the material.

2.3 Photo-DSC investigations

Apart from needing a certain reactivity to be able to structure waveguides via 2PP at all, throughput is the major bottleneck that this technology is facing on its entry to industrial application. It is well known that triacrylates as TTA are comparatively photoreactive. Besides quantifying the photoreactivity of systems on the basis of the silicone polyether acrylate TEGO RAD 2200N containing TTA, the effect of the extremely high refractive tetrathiol pentaerythritol tetrakis(3-mercaptopropionate (TT) was of interest, which was thought to enhance the refractive index difference between waveguide core and cladding material and had been shown to lower shrinkage of acrylic photopolymers.[11]

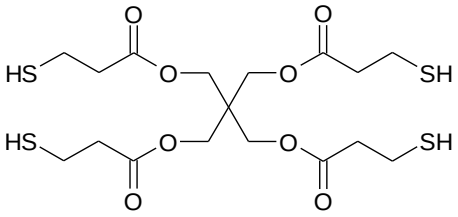

TT

Recently a means to determine the DBC in 2PP-borne, acrylate-based microstructures has been presented,[84] but to the best knowledge of the author there is no method available yet to determine the distribution of the double bond

conversion (DBC) of tiny waveguides embedded in a lower refractive polysiloxane. Although not ideally reflecting the 2PP-situation, one-photon photo-DSC measurements were carried out (Table 4, for calculation methods see section Materials and Methods). The latter is a fast and reliable method to quantify the reactivity of photoreactive resins and to determine the DBC, as far as the theoretical heat of polymerization $\Delta H_{0,P}$ is known. Based on the knowledge from last section a set of reasonable formulations for 2PP waveguide fabrication based on the acrylic matrix material TEGO RAD 2200N was selected for testing. The monomer (TTA) content was varied from 0% to 30%. The influence of the rheology additive BYK E 410 on the photo-DSC measurements turned out to be negligible: It was shown that 2% of BYK E 410 in formulation **UV/1.4/20/BYK** yielded practically the same results as formulation **UV/1.4/20** lacking the additive. $\Delta H_{0,P}$ for this acrylic system was assumed to be 78 kJ mol^{-1} with respect to acrylic moieties, which were to the largest extent provided by TTA.

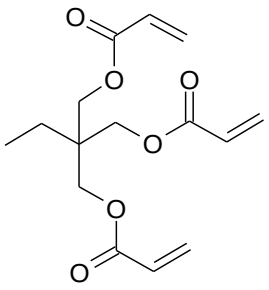

TTA

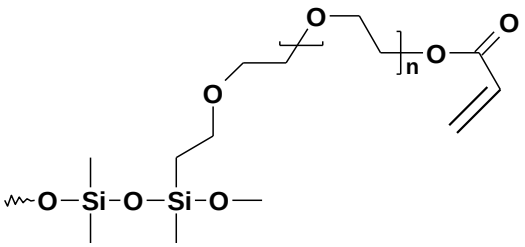

TEGO RAD 2200 N
Silicone polyether acrylate

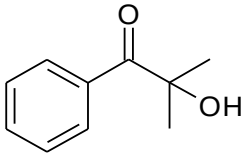

Darocur 1173

Table 4: Photo-DSC measurements of acrylate/polysiloxane based resins.

	T_{max} (s)	R_{pmax} (mol L^{-1} s^{-1})	DBC (%)
0% TTA (**UV/1.4/0**)	4.4	0.024	53.2
10% TTA (**UV /1.4/10**)	2.6	0.091	65.7
20% TTA (**UV 1.4/20**)	2.6	0.155	65.6
30% TTA (**UV /1.4/30**)	2.9	0.202	64.4

Unsurprisingly R_{pmax} strongly increased with rising TTA content, while between 10 and 30% TTA T_{max} underwent no relevant change. With respect to reaction speed the absence of monomer (formulation **UV/1.4/0**) caused a significant drop compared to formulations containing TTA. This is explained by the much lower mobility of acrylate moieties on the silicone acrylate of TEGO RAD 2200N compared to TTA. TTA content showed no significant influence on the overall DBC. Figure 45 shows the double bond conversion over time.

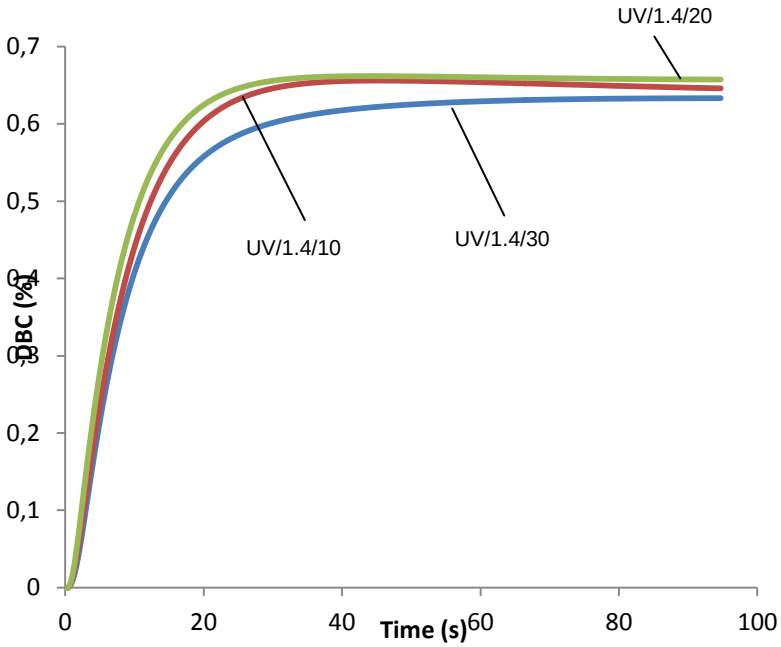

Figure 45: Photo-DSC plots for acrylate based waveguide fabrication formulations

To see the influence of thiol moieties on the photoreactivity, the tetrafunctional thiol TT was added to formulations containing 20% TTA (formulations **UV/1.5/4:6** and **UV/1.5/1:10,**

Table **5**). The ratio of acrylate moieties to thiol moieties contributed by TT to TTA was 6:4 in case of **UV/1.5/4:6** and 1:10 in case of **UV/1.5/1:10.** For the latter formulations containing 20% TTA, approximately 17% of acrylate moieties were additionally provided by the matrix material. For calculation of R_{pmax} and DBC, $\Delta H_{0,P}$ with respect to the acrylic moieties would have to be known. The latter, however, was not

accessible with the instrumentation used, because i) the heat of polymerization of the thiol-ene polymerization of TT with TTA and ii) the ratio of thiol-ene reaction to acrylic homopolymerization were not known. Thus, only T_{max}, the actual heat of polymerization ΔH_P (J g^{-1}) and the peak height *h* of the photo-DSC plot can be shown for the TT-containing formulations. In case of formulation **UV 1.4/21:10**, the small concentration of TT has almost no effect. Regarding formulation **UV/1.5/4:6**, TT clearly shows an increasing effect for ΔH_P (J g^{-1}) and *h* (W g^{-1}).

Table 5: Photo-DSC measurements of acrylate/polysiloxane based resins with tetrathiol

	T_{max} (s)	R_{pmax} (mol L^{-1} s^{-1})	DBC (%)	ΔH_P (J g^{-1})	*h* (W g^{-1})
20% TTA (**UV 1.4/20**)	2.6	0.151	66	124.7	12.1
20% TTA with TT (**UV/1.5/4:6**)	2.2			128.5	14.13
20% TTA with TT (**UV/1.5/1:10**)	2.5			124.6	12.33

Due to this lack of information on DBC, corresponding Real-Time-FTIR measurements will be discussed in the following chapter.

2.4 Real time FT-IR measurements

The DBC in 2PP is not uniform within the VOXEL as the photon density follows a certain distribution. Furthermore, the DBC is dependent on the laser power applied, the feed rate and the transparency of the resin to the femtosecond laser. For these reasons a monitoring of DBC over time is interesting supplementary information, especially for formulations **UV/1.5/4:6** and **UV/1.5/1:10**, where DBC was not accessible via photo-DSC as discussed in the previous section (for calculation methods see section Materials and Methods).

Also for the Real time FT-IR measurements, there was no means to measure during real 2PP fabrication. Thus the one-photon UV-curing of the formulations of the previous section was monitored by recording 14 FT-IR spectra per second. An accumulation of peaks representing the C=C bond of acrylate moieties on TTA was used for integration between 1604 and 1640 cm^{-1} to monitor DBC. The carbonyl peak from acrylate moieties at 1730 cm^{-1} served as a reference. Figure 46 shows the spectrum after and prior to UV-curing by the example of formulation **UV/1.4/30**.

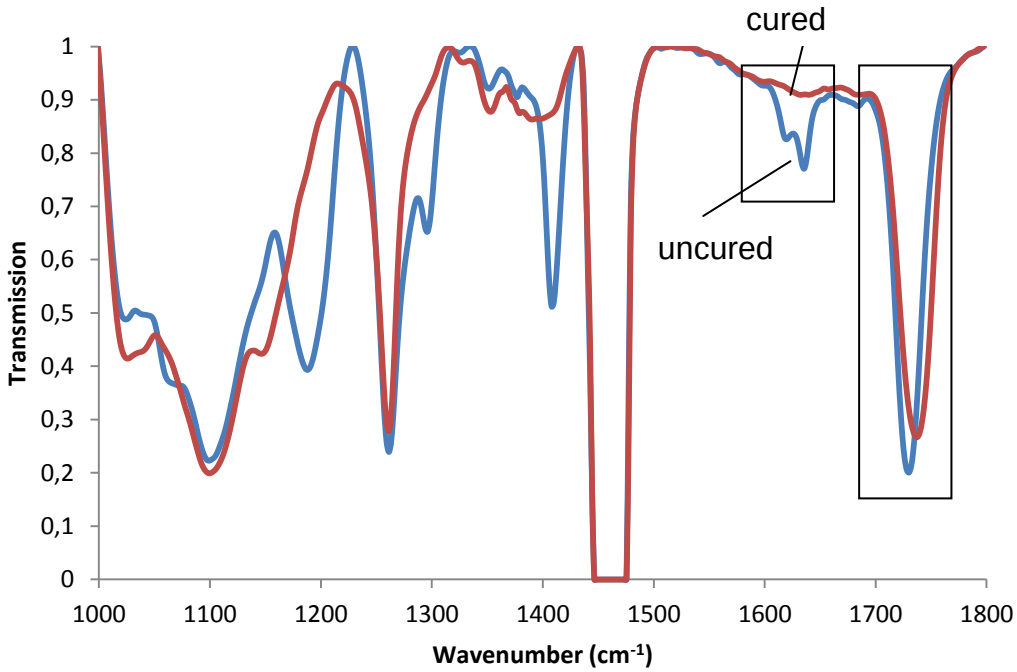

Figure 46: Real time FT-IR spectra from formulation UV/1.4/30 prior to and after curing. Accumulation of acrylic peaks (1604 to 1640 cm^{-1}) and the Si-CH_3 reference peak (1730 cm^{-1}) are marked with rectangles

To avoid oxygen inhibition, the formulations were sandwiched between two PE foils, as the waveguide fabrication also takes place below the inhibition depth.[1] Like above, the rheology additive was left out as it had shown only a negligible effect on the UV-curing (see last chapter 2.3). The light intensity at the surface of the sample was measured by means of an OCEAN OPTICS radiometer being 100 mW/cm^2 in a wavelength range between 300 and 500 nm (Figure 47).

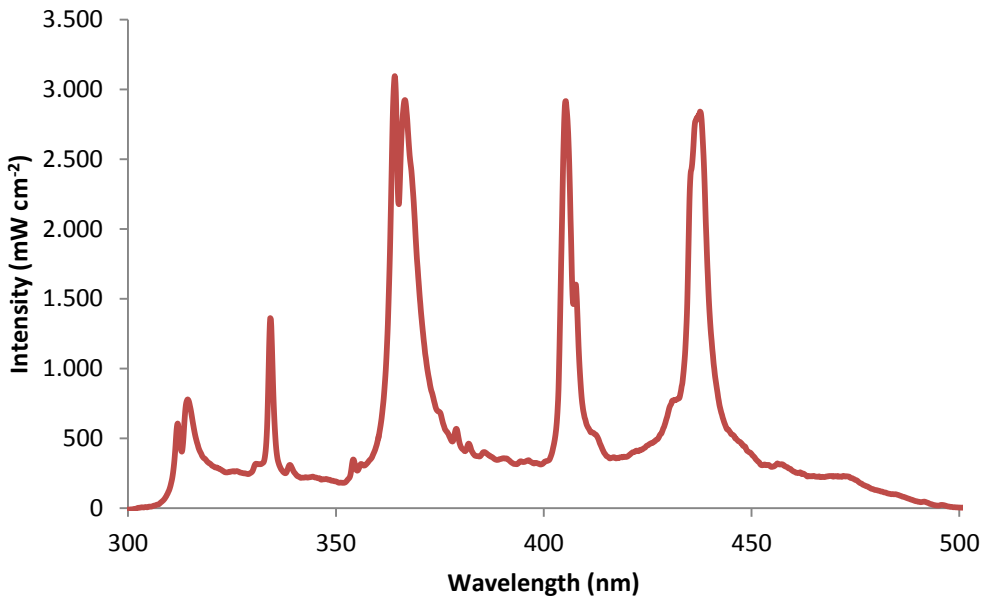

Figure 47: Emission spectrum of the Omnicure 2000 UV lamp at the sample surface inside FT-IR-spectrometer

The UV-irradiation could only be switched on approximately a second after the Real time FT-IR recording manually. Without exact knowledge about the onset of UV-irradiation, the inhibition period could not be determined. Thus the curves in Figure 48 and Figure 49 were modified to start at the onset of curing. As a supplementary information to the photo-DSC investigation, FT-IR was carried out with all formulations that were examined in the photo-DSC section except for formulation **UV/1.4/0** containing 0% TTA, because in this case the C=C peaks were too weak for evaluation.

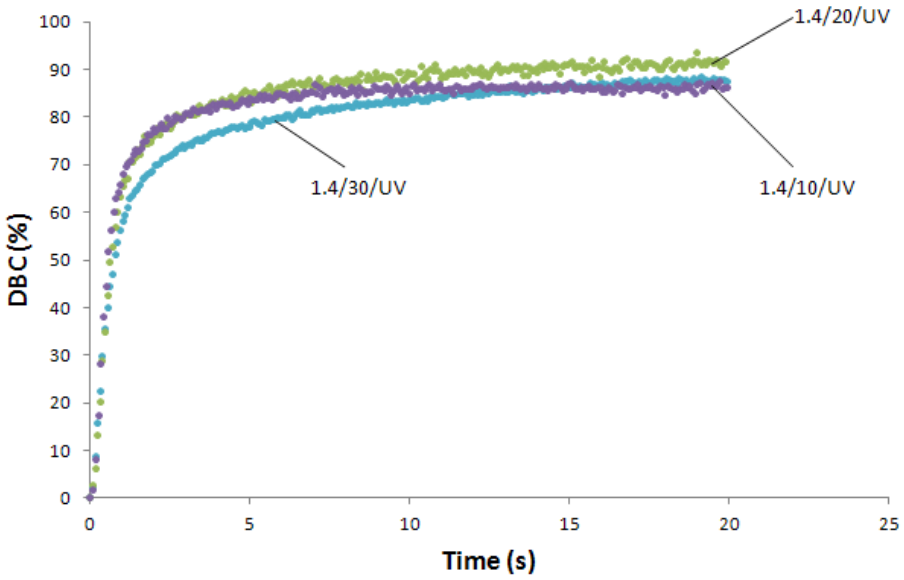

Figure 48: Real time FT-IR curve of acrylic based waveguide fabrication formulations

The DBCs achieved in the investigations of question (Figure 48) are slightly higher than those in the photo-DSC section (Table 4) due to the different setup for UV-curing. In all cases shown in Figure 48 DBC develops rapidly and linearly approximately during the first 0.5 s gradually reaching a plateau until around 12s the curing of each formulation is complete at DBCs between 85% and 91%. These are significantly higher values than achieved in case of the photo-DSC, although in the latter case inert gas was applied to tackle oxygen inhibition. This might be attributed to the lower sample thickness of approximately 20 µm compared to the one in the photo-DSC. In accordance with photo-DSC results (Figure 45), DBC develops more slowly in case of 1.4/30/UV than in case of the formulations with less monomer. The reaction speed, however, is highest for 30% monomer content simply because it features most acrylic moieties.

Subsequently, the influence of the tetrathiol TT on the UV-curing of formulations containing 20% of TTA was tested with the results illustrated in Figure 49 :

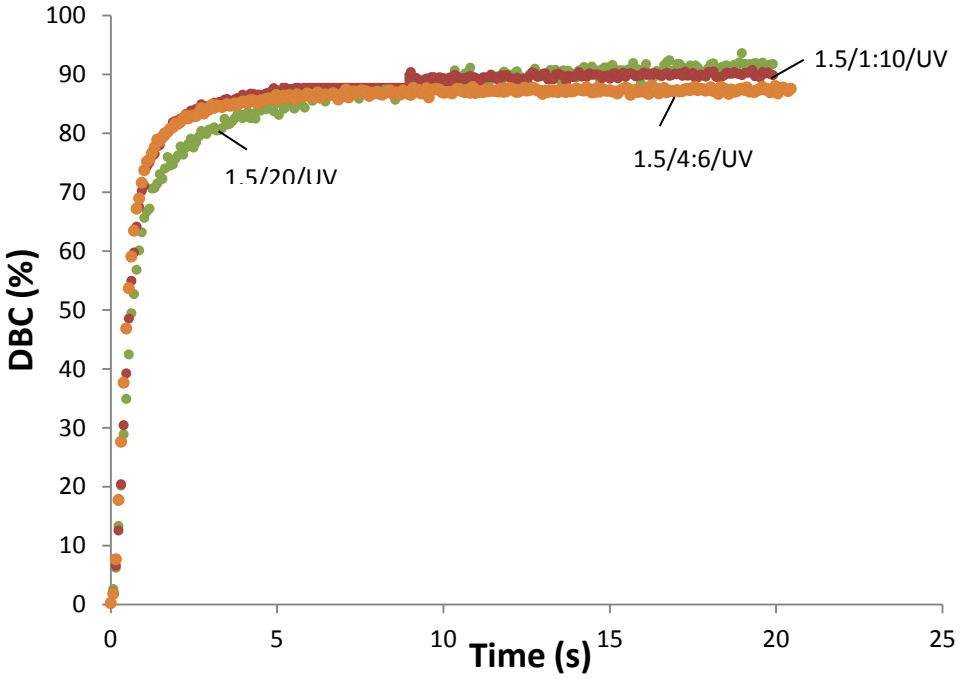

Figure 49: Real time FT-IR curve of acrylate-based waveguide fabrication formulations

The thiol-containing formulations **UV/1.5/1:10** and **UV/1.5/4:6** reach the plateau slightly faster than the pure acrylate-based sample **1.4/20/UV** due to partial thiol-ene polymerization. Also this investigation suggests the use of the tetrathiol TT as an additive due to reactivity enhancement of the purely acrylic formulations.

2.5 DMTA tests

During the lamination process of printed circuit boards the waveguide material undergoes a 2 h temperature ramp. The temperature is increased from approximately 50°C to 240°C and then held at 240°C for 20 min before being cooled down to 50°C, so the thermal stability was of interest. For this purpose, tests were carried out using dynamic mechanical thermal analysis (DMTA): The DMA 2980 device applied in this work (for details, see “Materials and Methods”) measures the time-delayed feedback force provoked by the sinusoidally applied oscillating bending force on the sample, which is required for a certain fixed bending amplitude. From this feedback force, viscoelastic properties such as the loss modulus and storage modulus can be calculated. Important applications of DMTA are the determination of glass transitions or the miscibility of polymers. For the task in question, DMTA was used to monitoring the storage modulus from -140°C to 300°C. Sudden changes at in this property at

certain temperature would indicate mechanical instability of the material at this temperature.

In the previous two sections, formulations containing 0, 10, 20 and 30% of the triacrylate TTA were investigated as well as formulations containing 20% TTA in combination with the tetrathiol TT. For the DMTA measurements it was reasonable to choose very similar formulations and investigate the influence of monomer content and partial thiol-ene reaction on the mechanical behavior on potential waveguide claddings. In contrast to section 2.3 and 2.4, rheology additive was added to the formulations to be closer to the cladding material developed in section 2.2.

As shown in Figure 50, the plain cured silicone polyether acrylate (formulation **DMTA/1.4/0**) underwent a broad glass transition. The storage modulus at -140°C was almost 4500 MPa. The material exhibited a very low storage modulus of a few MPa at temperatures higher than 70°C and was thermally stable up to 300°C as no sudden change in the curve could be detected.

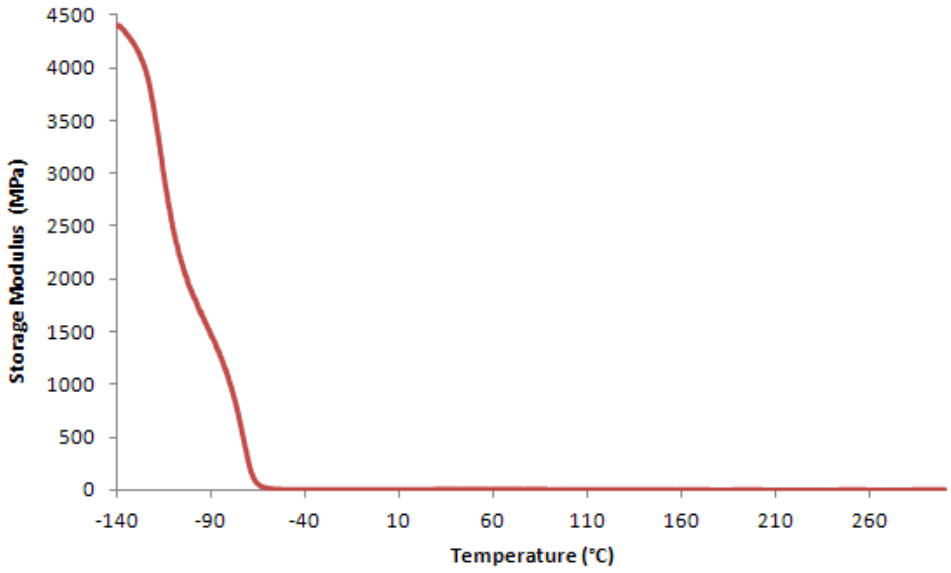

Figure 50: DMTA curve of the pure cured matrix material (formulation DMTA/1.4/0)

Subsequently DMTA tests were carried out with hybrid materials of TEGO RAD 2200N containing 20% and 30% of TTA (formulations **DMTA/1.4/20** and **DMTA/1.4/30**), which represent waveguide cladding materials (Figure 51). Moreover, a material containing 20% TTA and the tetrathiol TT in a ratio of thiol:acrylate moieties 4:6 were tested (formulation **DMTA/1.5/4:6**).

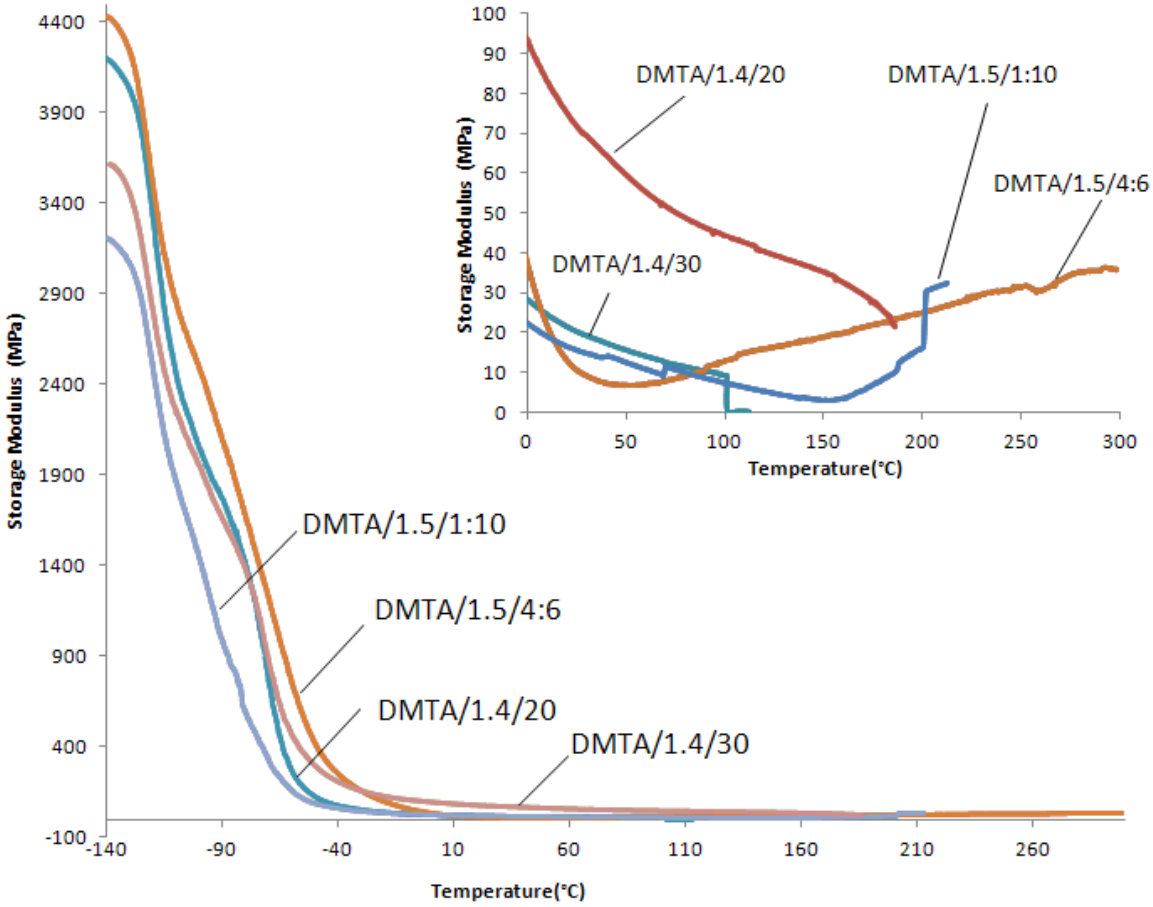

Figure 51: DMTA curve of acrylate- and thiol-acrylate based cured hybrid materials

Figure 51 shows similar behavior of all materials regarding glass transitions. The storage moduli at -140°C ranged from 3200 to more than 4400 MPa. The magnification shows that all materials except for DMTA/1.5/4:6 failed prior to reaching 300°C. **DMTA/1.4/30,** the material with the highest TTA content in this selection failed at 186°C. The less stiff **DMTA/1.4/20** also failed below 200°C. Adding some tetrathiol TT in case of formulation **DMTA/1.5/1:10** allowed for postponing to 210°C. Increasing the thiol content in case of **DMTA/1.5/4:6** led to mechanical stability in the desired temperature range without failing until 300°C. The latter thiol-containing materials showed an increase in storage modulus after reaching a minimum, which is probably attributed to additional thermal crosslinking reactions.

2.6 Refractive Index

The waveguiding principle relies on the refractive index properties of the material in question, so this work must not lack such investigations on n. The 2PP-induced change in refractive indexas the essence of waveguiding was not accessible as there was no experimental means on hand to determine the distribution of n in the tiny waveguides with diameters in the micron range. This would only be possible by methods involving very tricky sample preparation and high cost, which was not appropriate at that stage of waveguide development. The n of the cladding materials, however, was measurable by means of Abbé refractometry (Table 6).

Table 6: Values for n of the pure TEGO RAD 2200N matrix material and cladding materials

Material	n
UV/1.4/0 (matrix material)	1.442
UV/1.4/20	1.449
UV/1.5/1:10	1.449
UV/1.5/4:6	1.453

While the 20% TTA inside the matrix material yielded a change in refractive indexof 0.007, which is already enough for efficient waveguiding, the extremely high refractive TT causes n to undergo another increase of 0.004. It would be interesting to find out, if the raising of n in the cladding material by addition of high refractive monomer enhances the diffusion based enrichment process during 2PP yielding a higher change in refractive indexfrom waveguide core to cladding.
For the change of the distribution of n within the waveguide only limits can be given: As the 2PP-borne change in refractive indexis created upon diffusion into and enrichment of high refractive monomer in the VOXEL, the distribution of n lies between by the n of the cladding material (which is the UV-cured formulation) and that of pure, cured TTA or TTA/TT.

2.7 Rheological properties

As discussed in section 2.2, the proof of principle for the structuring of straight waveguide structures was achieved for 20% monomer and 3% of the rheology

additive BYK E410. Moreover, the waveguides were found to remain on the xy coordinates, where they had been fabricated. This behavior was attributed to the thixotropic effect of BYK E 410. However, there is also a negative aspect to the latter additive. Its partial incompatibility with the formulation causes scattering at the phase boundaries, which was fatal to the extent of waveguiding. Without controlled precipitation of the modified urea into needlelike crystals, which interact with the formulation and create thixotropy no rheology effect is obtained. Thus minimization of the additive concentration was self-evident. The minimum thixotropy for fabrication of straight waveguide structures that remain perfectly in place was also of interest in this context. The method of choice for investigating these aspects was rheometry of liquid samples with varying content of the rheology additive BYK E 340 and TTA as acrylic monomer in the silicone polyether acrylate-based waveguide formulations. Figure 52 shows quantitatively the building up of thixotropy in formulation **Rheo/1.4/20a**: During the weighing-in of the formulation the 3D network of crystals had already caused thixotropy to a certain extent. For this reason the formulation was sheared at a shear rate of $d\gamma/dt$ = 200 1 s^{-1} for 20 min to destroy these aggregates. Subsequently, marginal oscillations of the stamp at a gamma amplitude of 1% and an angular frequency of 10 rad/s allowed to follow the formation of the thixotropy over 70 h (Figure 52) by measuring the shear stress assuming that the slight oscillation would not greatly influence the aggregation process. The producer of BYK E 410 mentions that the building-up of the urea-based crystal 3D networks takes a few hours.[85] In fact, the effect of thixotropy that the medium does not flow any more when turned upside down is reached after a few hours. Concluding from the shear stress, thixotropy kept increasing much longer.

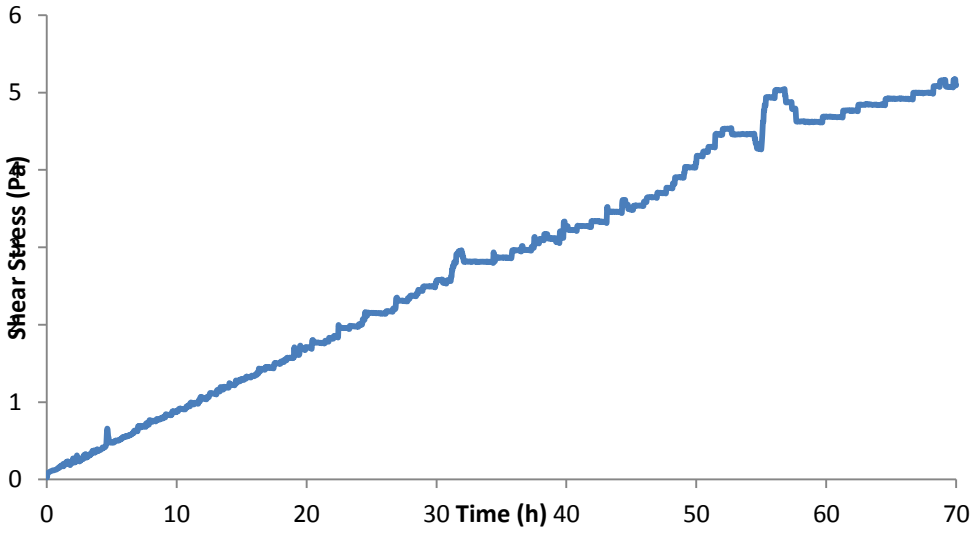

Figure 52: Monitoring of the formation of thixotropy of formulation **Rheo/1.4/20a** by means of its shear stress.

The formulation shows an almost linear increase of shear stress with time. Starting from 0.0794 Pa, the slope up to 60 h was determined to be 0.0802 Pa s^{-1}. After 60 h it decreased to 0.045 Pa s^{-1} indicating an approximation towards completeness of thixotropy formation. Extending the duration of the measurement until completeness of thixotropy was not reasonable as this is not interesting for industrial processes.

Still, a concentration of 3% BYK E 410 caused significant clouding of the material as discussed in section 2.2. For this reason a matrix of experiments investigating the effect of varying monomer content to 10% and 30% and rheology additive to 1% and to 3% in order to possibly find a way to lower the damping caused by the rheology additive (Figure 53).

Therefore, high rotational shear was applied to the samples at a rate of $d\gamma/dt$ = 200 1/s for 20 min to destroy all aggregates. Then the formulations were left for 5 hours in the rheometer for thixotropy to partially build up, which is a reasonable time for an industrial process. Finally, marginal oscillations of the stamp at a gamma amplitude of 1% and an angular frequency of 10 rad s^{-1} allowed for quantification of the formed thixotropy by means of the measured shear stress.

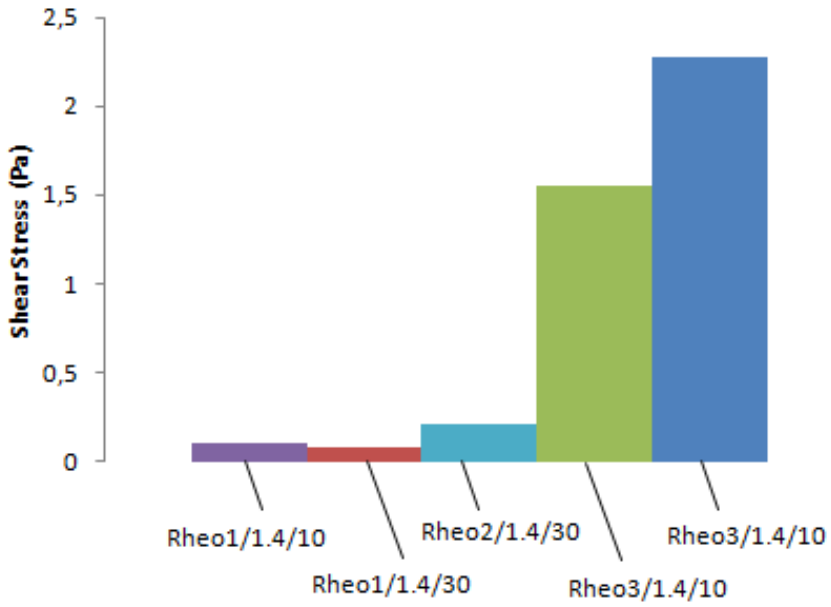

Figure 53: Comparison of shear stress after 5 h thixotropy formation for acrylic-based polysiloxane waveguide formulations varying concentration of rheology additive and monomer.

Each sample was measured three times with a maximum standard deviation of ±26% in case of formulation **Rheo3/1.4/30** containing 30% of the triacrylate TTA and 3% of the rheology additive BYK E 410. When comparing **Rheo3/1.4/30** with **Rheo3/1.4/10** it can be seen that at constant concentration of rheology additive, the increasing monomer content increases the thixotropy which can be achieved within 5 hours from a formulation. A quick test showed that pure TTA is a medium, where BYK E 410 can develop the thixotropic effect faster than in the pure matrix material TEGO RAD 2200N, which is probably due to its numerous ester units interacting with the urea-based additive crystals. The shear stress of the formulations containing only 1% of BYK E 410 lies below the detection limit and thus these formulations cannot be compared to each other. Unsurprisingly the shear stress building up within 5 hours depended very strongly on the amount of rheology additive.

Summing up, the investigations of this section showed that thixotropy could be enhanced by i) increasing the amount of BYK E 410 ii) storing the samples for longer periods and iii) increasing the amount of monomer TTA.

In case i) one had to put up with a serious decrease in transparency. Regarding ii), additional processing time is not desireable and in case of iii) increasing TTA content caused increasing stiffness in the hybrid material. Thus, **Rheo/1.4/20a** seemed as a good compromise for waveguide structuring.

2.8 2PP writing

In section 2.2, TTA was identified as a very well-suited monomer for 2PP-writing inside a thixotropic formulation with TEGO RAD 2200N. Despite of this discovery, it seemed reasonable to use some kind of thiol as an additive because of its salient qualities such as to elevate the change in n, to reduce shrinkage and oxygen exhibition and to enhance network uniformity.

In a former work dipropylene glycol diacrylate (DPGDA) and ethylene glycol dimethacrylate (EGDMA) had been applied in combination with 2,2′-(ethylenedioxy)diethane thiol (DOD) as monomer formulation for partial two-photon-induced thiol-ene polymerization and acrylate homopolymerization inside the aforementioned TEGO RAD 2300 matrix material.[82]

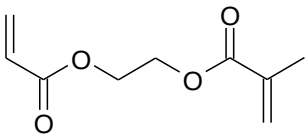

EGDMA

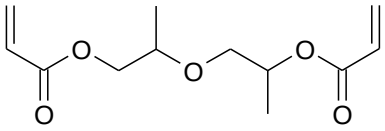

DPGDA

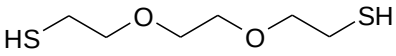

DOD

TEGO RAD 2300N had been UV-cured and the resulting silicone rubber had been swollen by a two-photon-reactive monomer formulation. After 2PP, unreacted monomer could be vastly removed in vacuum due to the proper volatility of DOD and DPGDA/EGDMA. Hence, these monomers were tested towards 2PP-processability of waveguide structures. Fortunately it turned out, that upon the addition of BYK 410 a medium consisting of 20% of an equimolar mixture (with respect to thiol and (meth)acrylate groups) of DOD/DPGDA or DOD/EGDMA (formulations **2PP/1.1** and **2PP/1.2**, respectively) and B3FL as TPI and the matrix material TEGO RAD 2200N attained thixotropy

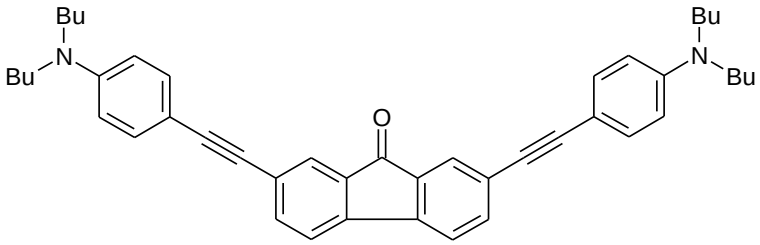

B3FL

Structuring screenings (carried out on the M3D-device in Vienna, see section Materials and Methods) over wide ranges in terms of laser power and feed rate yielded wiggly line structures instead of straight waveguides within these formulations (Figure 54).

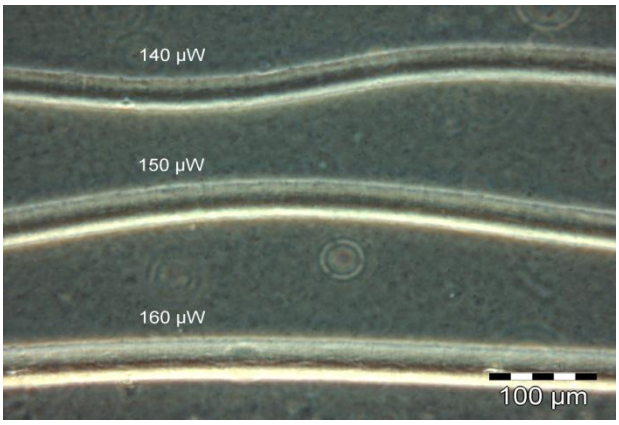

Figure 54: Wiggly lines resulting from 2PP in formulation 2PP/1.1.

Lowering the ratio of thiol:ene moieties from equimolar to 2:3 or 1:10 (formulations **2PP/1.1/2:3** and **2PP/1.1/1:10**, respectively) in order to enhance (meth)acrylate homopolymerization and thus increase crosslinking density did not improve the situation. Interestingly it could be observed in the camera attached to the 2PP device, that the structured lines were initially straight and formed wiggly lines only in the course of a few seconds. A possible explanation for this phenomenon is that waveguide structures become swollen with unreacted monomer and deform due to the low stiffness of the thiol-ene network.

A reasonable possibility to tackle the problems with waveguide straightness seemed to be enhancement of crosslinking density and thus stiffness of the material. To achieve this, it was most reasonable to enhance functionality using trifunctional TTA instead of the difunctional acrylate DPGDA and methacrylate EGDMA. A structuring

test with formulation **2PP/1.3** showed some improvement of the waveguide structures, which appeared straighter than if di(meth)acrylates were used, especially at elevated fabrication speed.

Consequently, the monomer screening was continued with the intention to further enhance crosslinking density using trifunctional TTA in combination with the tetrathiol pentaerythritol tetrakis(3-mercaptopropionate) (TT) as a substitute for difunctional DOD in formulations **2PP/1.5/4:6** and **2PP/1.5/1:10**.

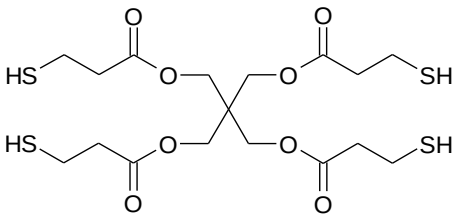

TT

But despite of the doubling of thiol functionality with respect to DOD no totally straight waveguide structures could be obtained.

In section 2.5 the influence of TT on the mechanical behavior of the acrylate-based cladding materials had elucidated (formulations **DMTA/1.5/4:6** and **DMTA/1.5/1:10**). At room temperature, **DMTA/1.5/4:6** containing more of the thiol TT showed half of the storage modulus of **DMTA/1.5/1:10**. Possibly this tendency regarding stiffness can be attributed to the wiggly lines. Because of latter drawbacks, the addition of thiol to the thixotropic waveguide fabrication system was abandoned and investigations were focused on TTA as the only monomer.

In section 2.2 a screening for monomers suitable for 2PP waveguide fabrication (using the M3D fabrication device, see section Materials and Methods) in a silicone polyether acrylate-based thixotropic medium was presented with the triacrylate TTA allowing to form straight waveguides that are not wiggly as it was the case upon the addition of thiols. The results from the previous section show, that the thixotropy is unsurprisingly dependent on the amount of the thixotropy additive BYK E 410, while the monomer content has a smaller, but also significant effect in this regard. Thus, for reasons of mechanical flexibility it was reasonable to continue investigation with 20% TTA content and find the minimum concentration of the rheology additive that would allow for avoiding wiggly structures. Thus fabrication screenings were carried out using M3D (see section Materials and Methods) with formulation **2PP/1.4/20a** and

2PP/1.4/20b containing 2 and 1.5% BYK E 410, respectively. The samples were stored over night for thixotropy to kick in. In case of formulation **2PP/1.4/20a** the lines were still straight, but when lowering the rheology additive content to 1.5% the structures became wiggly and it was impossible to structure 6+1 bundels of parallel waveguides, which would be frayed at the edges (Figure 55), so 2% BYK E 410 content (formulation **2PP/1.4/20**) was supposed to be close to the minimum BYK E 410 concentration allowing for straight waveguides.

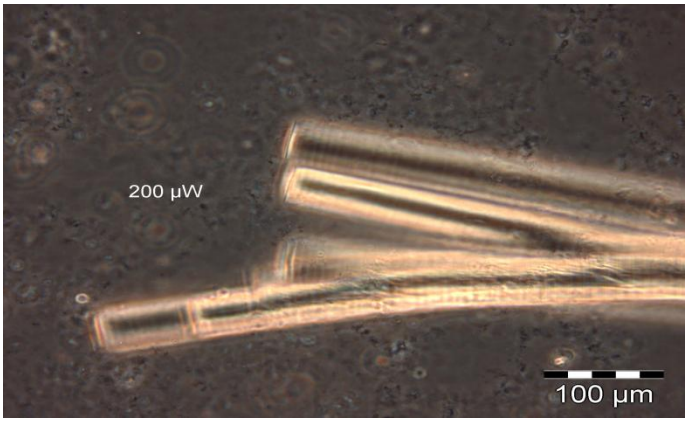

Figure 55: Snakeline waveguides structures as a result of insufficient thixotropy in case of a rheology additive concentration of 1.5%.

After the development of formulation **2PP/1.4/20a**, the next step was to get the cross-section into a round shape as the VOXEL up to that point had exhibited an elongate cross-section. This problem could be solved by using cylindrical lenses, which, however, seriously decreased the laser power arriving in the VOXEL, so it was reasonable to carry out further experiments on the 2PP device in Weiz, which was very well-suited to waveguide inscription. On this device, however, **2PP/1.4/20** yielded wiggly lines, which had not been the case on the M3D device (see Materials and Methods). The reason for this is unclear as the MTS device in Weiz differs in aspects such as VOXEL shape, repetition rate and many others. By raising the BYK E 410 concentration to 2.5% (formulation **WG 1.4/20**) this problem was successfully tackled, which meant of course accepting a lower transparency and thus higher optical damping. Straight waveguide structures could be obtained giving an excellent phase contrast. Structuring tests were very promising in the region of 110 to 160 µW as can be seen in Figure 56. Very strong phase contrasts were obtained, which should be due to the high diffusibility of monomer in the thixotropic liquid.

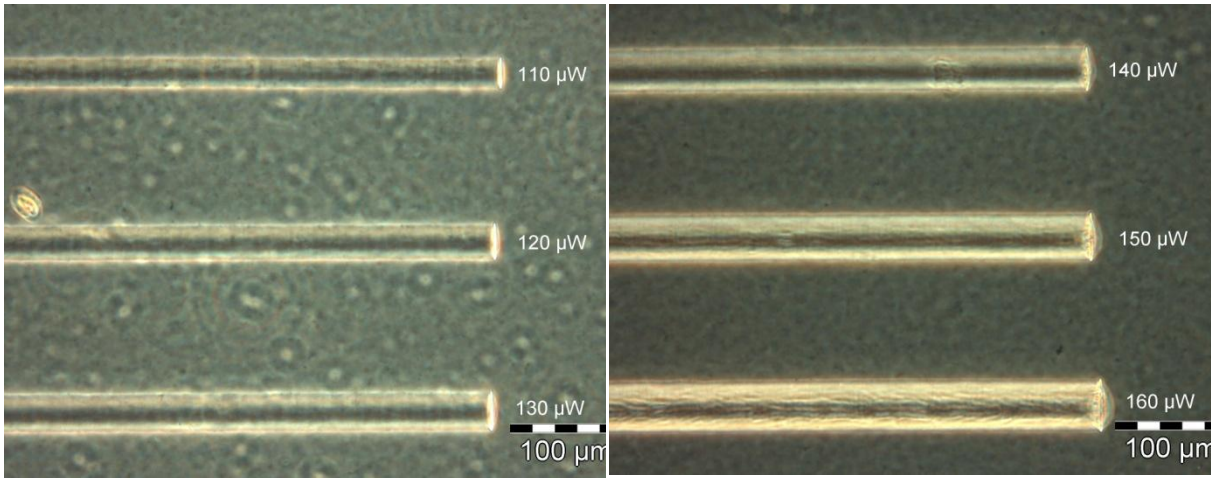

Figure 56: Phase contrast image of waveguide structures fabricated at writing speed of 4 mm/min and 110, 120 and 130 (top) 140, 150 and 160 µW laser power (bottom).

Waveguides were written in a depth of 120 µm as a consequence of oxygen-inhibition in the surface region. The higher the laser intensity was the better phase contrasts could be achieved, which was limited by burnt regions within the waveguide at high intensities. A shortcoming was clearly the low feedrate of 4mm/min, above which slight bending in the structures were observed.

2.9 Waveguiding

Having obtained an excellent local refractive index change via 2PP waveguide fabrication it was necessary to gain a proof principle for light guiding and subsequently assess, if the light guiding performance was high enough to carry out optical damping measurements.

A means to assess the light guiding performance of 2PP-borne waveguides for damping measurements is to make their cross-sections visible by cutting pieces out of the film containing the waveguides and bringing them into the white light of a microscope. (Figure 57)

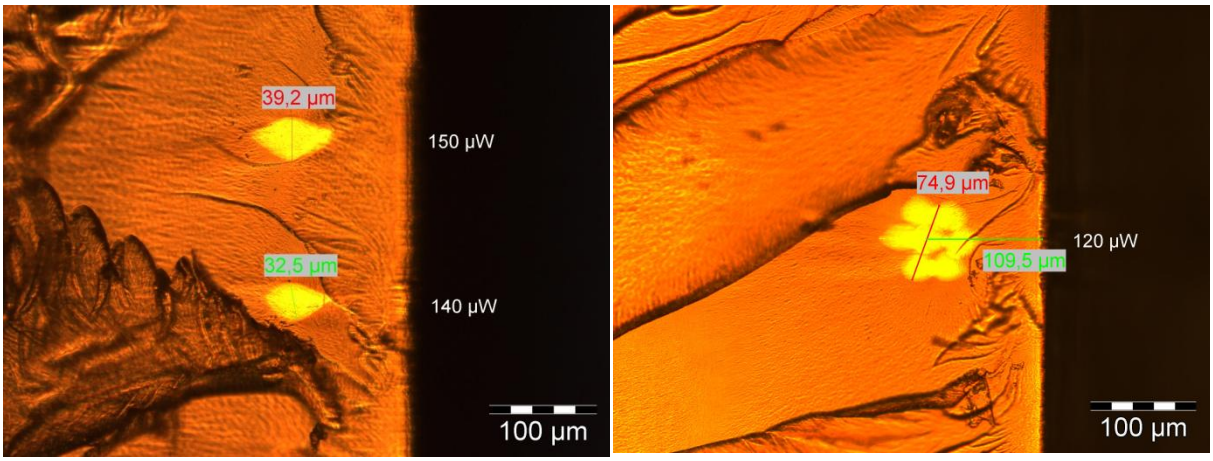

Figure 57: Left: Cross-sections of waveguides (yellow spots) written at 140 and 150 µW laser power and at 4 mm/min writing speed; dark regions represent unevenness of the cut. Right: Cross-section of a bundle of seven waveguides written at 120 µW laser power and at 4 mm/min writing speed; red line: bundle diameter, green line: depth of middle waveguide.

For waveguides between 120 and 150 µW laser power written at 4 mm/min feed rate (using formulation **WG 1.4/20**): the cross-sections could be strongly illuminated indicating that a high amount of light could be coupled in. The same was the case for 6+1 waveguide bundle, which increases the probability of an optical signal emitter on a printed circuit board to hit a waveguide with light and couple the latter in. Figure 56 also shows that the waveguide did not significantly sink towards the object slide after the structuring and UV-curing (from a structuring depth of approximately 100 µm to 120 µm), which is an important aspect for printed circuit board applications. In case of the 6+1 waveguide bundle the hexagon formed by the waveguide cross-sections is only distorted.

Thus the proof principle had been achieved and at the same time these good results suggested optical damping measurements as well as the implementation of the new technology on optical printed circuit board demonstrator:

Unfortunately, two preliminary experiments, where waveguides were written on printed circuit board demonstrators (Figure 58), were unsuccessful as the photo-current could not be increased compared to the value at their absence. A possible reason could be ineffective coupling-in due to misalignment of signal emitter and receiver either due to shrinking upon UV-curing of the thixotropic medium. Furthermore it is possible that the coupling-in did not function due to the non-perfect alignment of the waveguides to each other in the 6+1 waveguide bundle as observed with identic samples on object slides on the microscope (Figure 58).

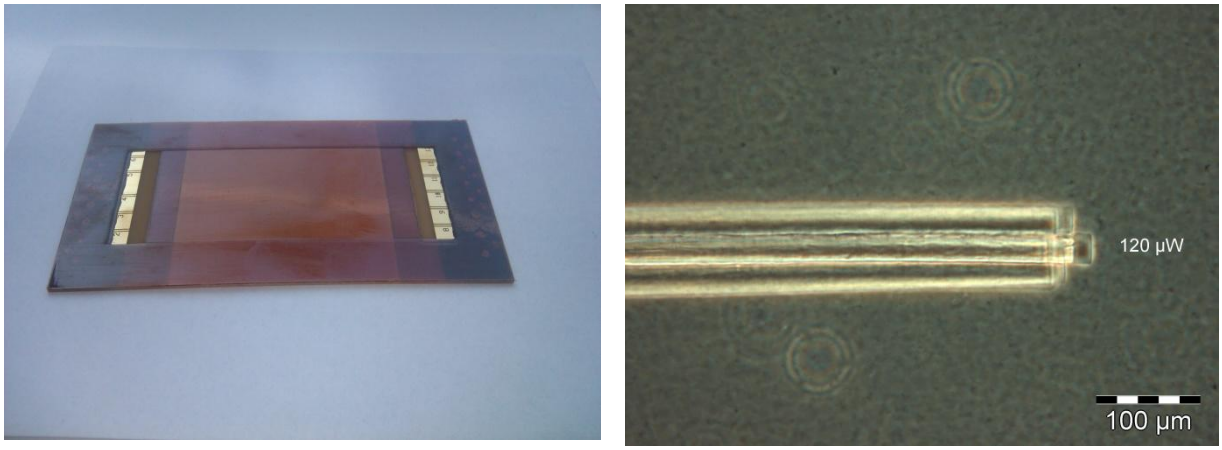

Figure 58: Left: Flexible printed circuit board demonstrator. Right: Phase contrast picture of "frayed" 6+1 waveguide bundle written at 4 mm min^{-1} and 120 µW laser power.

2.10 Optical damping & Absorption Behavior

Although the optical damping of the 2PP fabricated waveguides is the crucial property after all, knowing the damping behavior of the bulk material is also very useful for assessing the quality of the optical material in question. Therefore, test bars were produced (for details, see Section Materials and Methods) and brought into laser beams of wavelengths that are interesting in telecommunication. These measurements depend strongly on the coupling-in efficiency, which again is greatly influenced by the roughness of the end-plane of the test bar. By wetting the latter with immersion fluid and sticking glass plates to it, this roughness-related influence could be reduced. In section 2.8, formulation **WG 1.4/20** had turned out to most successful in terms of waveguide fabrication. Hence, investigations of the bulk material (for details see Section Materials and Methods) showed, that the main source of optical damping is the rheology additive BYK E 410, which was found to cause a damping value of 2.4 dB/cm at 633 nm and 1.5 dB/cm at 850 nm when added to the formulation at a concentration of 2.5% in contrast to the plain silicone polyether acrylate (**DMTA/1.4/0**) showing a damping of 0.2 dB/cm at 633 and 850 nm. This is due to the "necessary incompatibility" of BYK E 410 forming needle-shaped urea-based crystals that are responsible for the salient thixotropy, but are also greater than the wavelength of the coupled-in light. Thus, scattering of light at the phase boundaries is thought to be the reason for this rather high optical damping.

Due to the rather promising qualitative results from the last section with respect to coupling in white light, cut-back and transmission experiments were carried out by Nicole Galler (KFU Graz) to determine the optical damping of the 2PP fabricated waveguides. For this purpose waveguides were inscribed at a depth of approximately 125 µm with a laser feed rate of 4mm/min and laser powers of 100, 110, 120, 130, 140 and 150 µW into formulation **WG 1.4/20**. Cut-back measurements were conducted at 633 nm giving 3 dB/cm for 110 µW fabricated waveguide structures. The transmission was measured for the 30 mm waveguides yielding 2.38 dB/cm (at 633 nm) for the structure, which had been written at 120 µW. This value comes close to that of the bulk material, which is in fact the cladding material. Due to time constraints, it was not possible to get damping values from NIR-wavelengths (850 nm), which are common in the telecommunications industry. Preliminary optical transmission measurements of the bulk material with the inscribed waveguides (also carried out by Nicole Galler, KFU Graz) showed a significantly lower absorption at 850 nm compared to 633 nm. 850 nm is the working wavelength for the printed circuit boards provided by AT&S, so corresponding cut-back measurements would be highly interesting in the future.

Further common wavelengths for optical data transfer in the telecommunications industry are 1300 and 1550 nm. To get an idea about the suitability of the material for the aforementioned wavelengths a near-infrared absorption spectrum was taken between 600 and 1600 nm (Figure 59) from a sample based on formulation **WG 1.4/20** (see also Experimental Section).

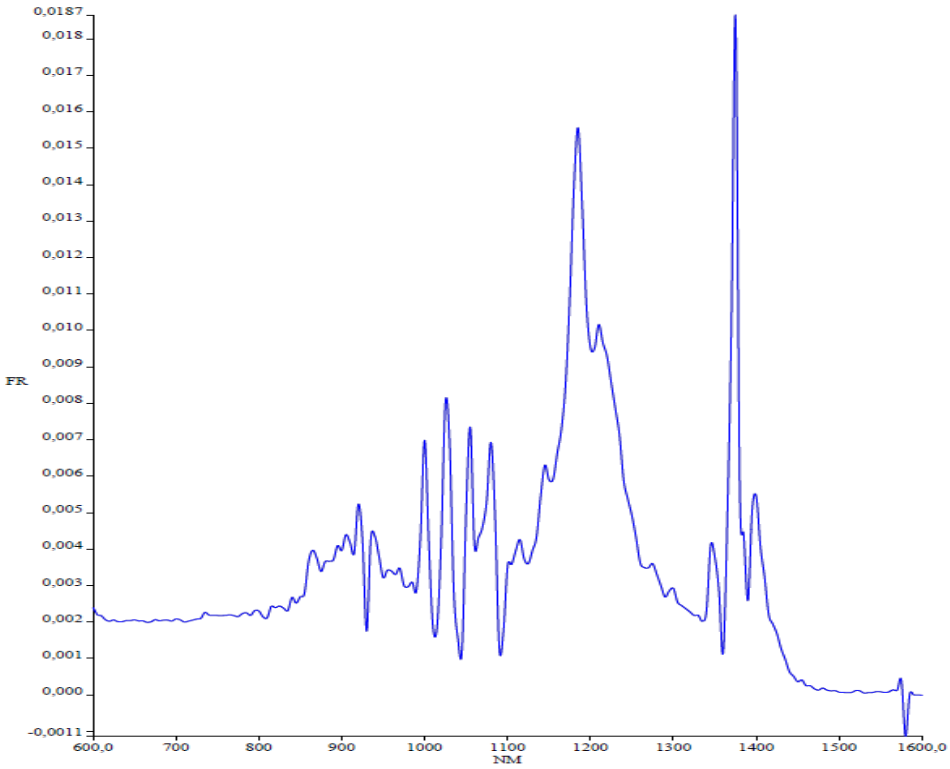

Figure 59: Absorption spectrum waveguide cladding material

While the absorptions typical to PDMS (around 1200 and 1400 nm) no major absorption peaks were detected at the aforementioned telecommunication wavelengths. Note that the bulk material used for the absorption measurement represents the cladding material. As discussed above, the waveguide core material exhibits a distribution of higher content of photopolymer.

3. 2PP waveguide fabrication inside epoxy silicone rubbers by curing thiol-ene monomer

3.1 Preliminary experiments

Preliminary attempts towards waveguide materials consisting of silicone polyether acrylate-based matrix material and thiol-ene networks had already been conducted in earlier works, where UV-cured specimens had been swollen by a thiol-ene formulation prior to 2PP structuring (see Figure 60 for the entire processing).[82] After 2PP fabrication, unreacted monomer had been removed to develop the whole refractive index change and stabilize the material. The first to use this process were Infuehr et. Al. using acrylic monomers and Si-H addition cured silicone.[79]

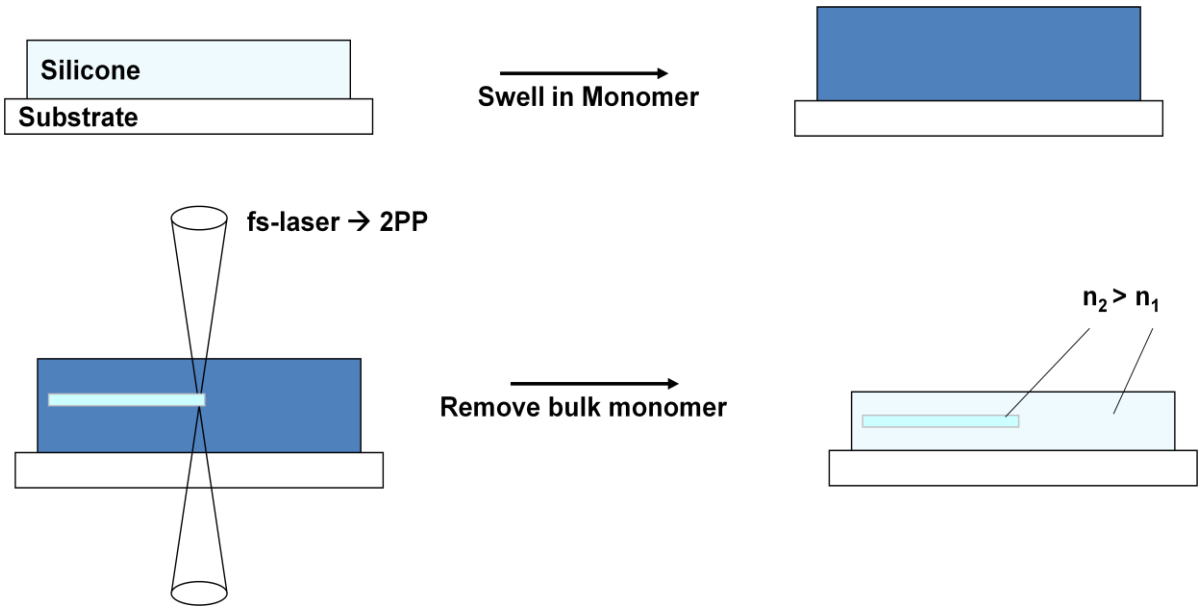

Figure 60: 2PP structuring process including a swelling and developing step

The matrix material in the latter case had been silicone polyether acrylate-based as the above mentioned TEGO RAD 2200N. Considering the large set of advantages of thiol-ene-based materials and chemistry it was worthwhile finding other matrix materials and processes to exploit these for waveguide fabrication.

For clarity, all formulations used in section 3 are given in Table 7, Table 8 and Table 9. Ratios are given in wt %.

Table 7: Formulations used in for epoxy-silicone based waveguide fabrication

	DDT	DOD	TT	TMMD	Dicumyl peroxide	Darocur 1173	Hycar 2000x162	Elastosil RT 601
PRE/2.1	15.0					2.0	83.0	
PRE/2.1a					6.0		94.0	
PRE/2.2	10.0							90.0
PRE/2.2a		10.0						90.0
PRE/2.2b			10.0					90.0
PRE/2.2c				10.0				90.0

Abbreviations: DDT:1,10-decanedithiol; DOD: 2,2′-(Ethylenedioxy)diethane thiol; TT: tetrathiol pentaerythritol tetrakis(3-mercaptopropionate); TMMD: 1,3-bis(3-mercaptomethyl)-1,1,3,3-tetramethyldisiloxane

Table 8: Formulations used in for epoxy-silicone based waveguide fabrication

	Trifluorosulfonic acid (5% in isopropanol)*	DBTDA	Citric Acid (saturated solution in THF)*	Trifluoro Acetic Acid (75% in isopropanol	APMS	ECES
PRE/2.3	0.3				49.85	49.85
PRE/2.3a		3.0			48.5	48.5
PRE/2.3b			3.0		48.5	48.5
PRE/2.3c				3.0	48.5	48.5
PRE/2.4	3.0				19.4	77.6
PRE/2.4a		3.0			19.4	77.6
PRE/2.4b			3.0		19.4	77.6
PRE/2.4c				3.0	19.4	77.6
PRE/2.5				3.0	9.7	87.3
PRE/2.6				3.0		97.0

***given ratios with respect to the acid catalyst

Abbreviations: DBTDA: Dibutyltin diacetate; APMS (4-5% Aminopropylmethylsiloxane) – dimethylsiloxane copolymer (viscosity 150-300 cSt); ECES: Epoxycyclohexylethylmethylsiloxane(8-10Mol%)-dimethylsiloxane copolymer; viscosity 300-450 cSt

Table 9: Formulations used in for epoxy-silicone based waveguide fabrication.

	DDT	TMMD*	TVMS	TFA	Darocur 1173	IMIT	ECES	P3K	Irgacure 819
PRE/2.7	46.0		53.0		1.0				
PRE/2.8		52.0	47.0		1.0				
PRE/2.9		10.0	9.0	3	1.0		77.0		
UV/2.9a		60.0	39.2		0.8				
UV/2.9b		56.4	42.7		0.9				
UV/2.9c		51.9	47.1		1.0				
UV/2.9d		46.3	52.7		1.0				
UV/2.9e		39.6	59.3		1.1				
UV/2.9a/epox		24.1	15.6	3.0	0.3		57.0		
UV/2.9b/epox		22.5	17.1	3.0	0.4		57.0		
UV/2.9c/epox		20.8	18.8	3.0	0.4		57.0		
UV/2.9c/epox		18.5	21.1	3.0	0.4		57.0		
UV/2.9d/epox		15.8	23.7	3.0	0.5		57.0		
DMTA/2.6						0.5	99.5		
2PP/2.9/20		10.0	9.0		1.0		79.8	0.2	
2PP/2.9/40		20.8	18.8	3.0	1.0		56.2	0.2	
2PP/2.9/40a		20.8	18.8	3.0	1.0		55.4		1.0
2PP/2.9/40b		20.8	18.8	3.00	1.00		56.34	0.06	
2PP/2.9/40c		20.8	18.8	3.00	1.00		56.36	0.04	

*containing 0.2% pyrogallol (inhibitor)

Abbreviations: DDT: 1,10-decandithiol; TMMD: 1,3-bis(3-mercaptopropyl)-1,1,3,3-tetramethyldisiloxane; TVMS: tris(vinyldimethylsiloxy)methylsilane; TFA: trifluoroacetic acid; IMIT: (*p*-Isopropylphenyl)(*p*-methylphenyl)-iodonium tetrakis(pentafluorophenyl) borate; ECES: Epoxycyclohexylethylmethylsiloxane(8-10Mol%)-dimethylsiloxane copolymer; viscosity 300-450 cSt; P3K: 1,5-Bis[4,*N*,*N*-diphenylaminophenyl]penta-1,4-diyn-3-*p*-one

Incompatibility of thiol-ene networks with matrix materials had turned out to be a central bottleneck, so covalent linkages between them were desirable to avoid phase separation fatal to waveguiding efficiency. For the thiol-ene situation, this would be possible by providing enes in the matrix material. A first approach into this direction was Hycar 2000x162 butadiene rubber (mixed with 15% 1,10-decanedithiol (DDT), which was compatible due its long alkyl chain, and 2% Darocur 1173 (formulation

PRE/2.1). UV-curing this formulation yielded a highly flexible, perfectly transparent material. Thus the plan was to cure the butadiene rubber first thermally and then swell it with 1,10-decanedithiol, which could undergo photoinduced thiol-ene polymerization with remaining double bonds in the matrix material (Figure 61).

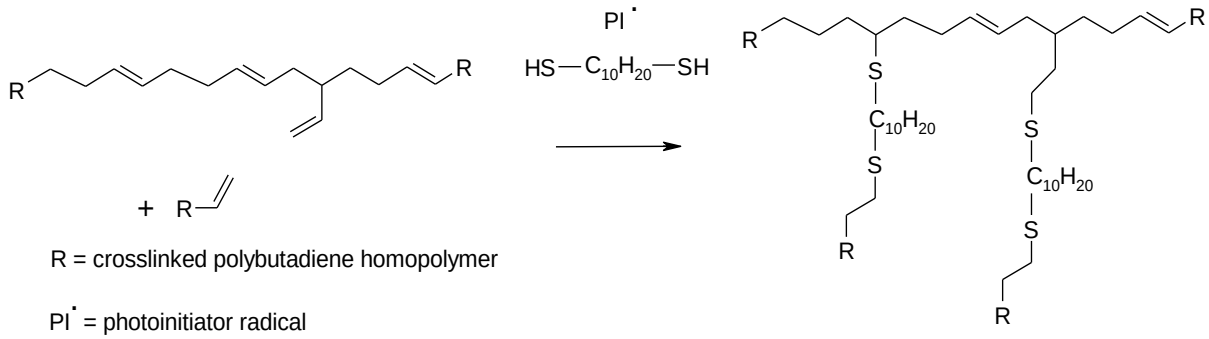

Figure 61: Dithiol crosslinking of butadiene rubber

After thermally curing the rubber at 130°C overnight by means of 6% dicumyl peroxide it turned out that this matrix material (**PRE/2.1**) exhibited an n of 1.517, which was clearly higher than that of 1,10-decane dithiol. It is possible that by means of further crosslinking the cured polybutadiene by means of DDT during the 2PP process, but the dithiol molecule itself by its lower n would lower the total n of the waveguide core. Moreover, the fact that no higher refractive compatible thiols were on hand suggested abandoning this concept. Besides searching for a new matrix material for thiol-ene-based waveguide fabrication, it was desirable to find alternative processes for sample preparation. The above mentioned swelling procedure is rather impractical, time consuming and problems arise regarding the homogeneity of swelling. It was also discovered, that during swelling the adhesion of the polysiloxane film to its substrate diminuished making it necessary to react the substrate surface with coreactive groups.[82] For this reason, a system was desired where the matrix material could be cured in the presence of thiol-ene monomer while leaving the latter untouched. Due to its suitability in the field of photonics a Si-H addition cure PDMS material (RT 601 from Wacker) was tested (Figure 62).

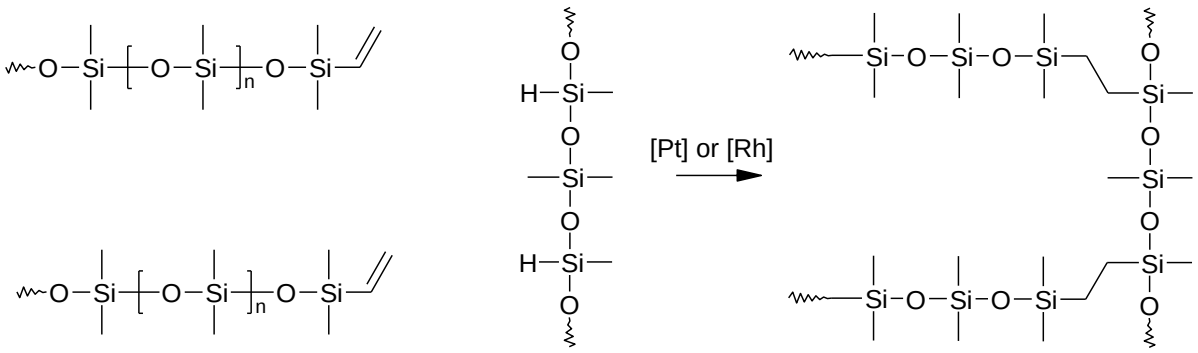

Figure 62: The principle of Si-H curing

This is a room temperature curing system consisting of a component A (platinum catalyst and vinyl-functional PDMS) and a component B (Si-H crosslinker), which are recommended by the producer to be formulated in a ratio 9:1. In a preliminary experiment three different thiols of 10% concentration (1,10-decanedithiol, TT, DOD in formulations **PRE/2.2, PRE/2.2a** and **PRE/2.2b**, respectively) were added to the recommended formulation of the latter components A and B of Elastosil RT 601 and left overnight at 80°C, but no thermal curing was observed in any case. The reason was probably poisoning of the Pt-based hydrosilylation catalyst as sulfur is known to be very capable of catalyst poisoning. A possibility to circumvent this problem might be the Si-H curing catalyst tris(dibutyl)rhodium trichloride. The latter, however, was not commercially available, so the following concept was abandoned.

The subsequent strategy was curing the matrix material mixture with the thiol-ene monomer via nucleophilic reaction using aminofunctional silicones (Figure 63) as (4-5% Aminopropylmethylsiloxane) – dimethylsiloxane copolymer (viscosity 150-300 cSt) (APMS) in combination with epoxycyclohexylethylmethylsiloxane(8-10Mol%)-dimethylsiloxane copolymer; viscosity 300-450 cSt (ECES).

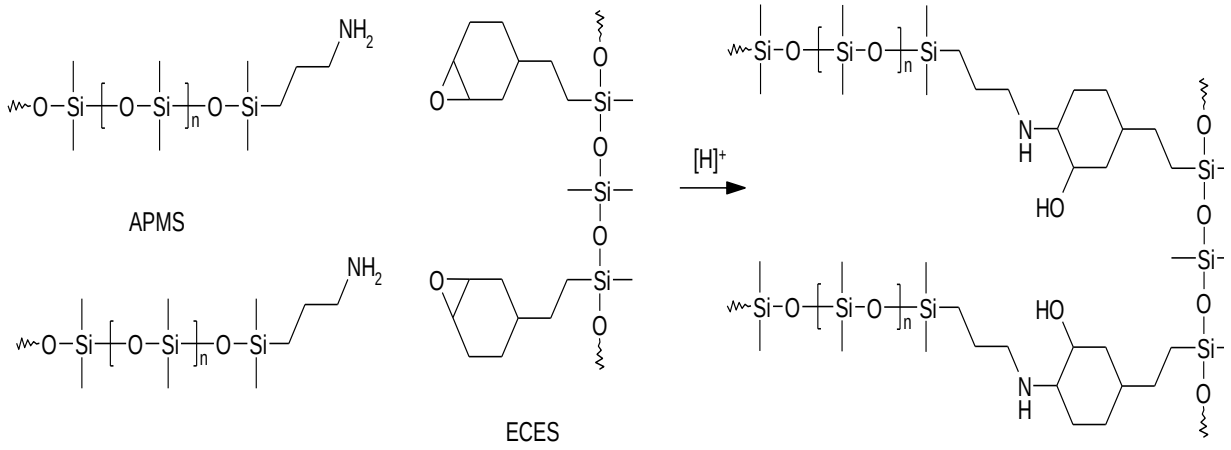

Figure 63: Amino-epoxy silicone crosslinking

Initially, the curing of APMS in combination with ECES was tested: The mass ratios 1 and 0.25 of APMS:ECES was tested using acidic catalysts such as dibutyl tin dilaurate (DBTDL) and citric acid (formulations **PRE/2.3a, PRE/2.3b, PRE/2.4a** and **PRE/2.4b**). While DBTDL caused only some increase in viscosity, a rather good performance with respect to handling and curing time was achieved by means of 3% citric acid in THF, which turned out to cure a 4:1 formulation of ECES and APMS in the course of a few hours, even in the presence of 15% 1,10-decanedithiol. 90% of the monomer could be evaporated after curing proving the vast orthogonality of the silicone curing chemistry to that of the thiol-ene system as only the unreacted monomer had a boiling point low enough for evaporation at the applied pressure. A serious problem, however remained, because it was not possible to create homogeneous and smooth films: round domains formed on the surface upon crosslinking which incompletely cured in contrast to the fully cured surroundings. The reason for this could be demixing due to the better compatibility of citric acid with the amino-functional polysiloxane compared to the epoxy component ECES. Thus, the strong acid F_3CSO_3H was applied at very diluted concentration eliminating these problems (formulations **PRE/2.3a** and **PRE/2.4**)

3.2 Matrix material

The incompatibility of citric acid with the epoxy silicone ECES, as discussed in the last section, caused unacceptable turbidity of roundly shaped spots on the surface of the curing films. For this reason, citric acid was abandoned as curing catalyst and

substituted by the more compatible trifluoromethyl sulfonic acid (formulations **PRE/2.3** and **PRE/2.4**) showing a more homogeneous film. At APMS:ECES ratios of 0.1 and below, really good curing performance was observed in the presence, so it was not surprising that APMS turned out to be absolutely dispensable. As discussed by Pham et. al. the cyclohexyl ring carrying the epoxy functionality is less electronegative as e.g. in bisphenol A-based epoxy resins and this more susceptible to cationic ring opening polymerization.[86] This indicated that an acid catalyzed cationic ring opening polymerization must have taken place in ECES when mixed with the sulfonic acid catalyst. A further improvement was achieved by using 3% trifluoro acetic acid (75% in isopropanol), which would evaporate after having fulfilled its function as a catalyst und thus not cause any incompatibility (formulations **PRE/2.3c, PRE/2.4c, PRE/2.5, PRE/2.6**). In case of **PRE/2.6** problems with homogeneous curing were encountered due to the rapid crosslinking upon addition of catalyst to ECES. Despite of this, the latter concept was followed as in the presence of monomer this inhomogeneity was thought not to be problem.

As an advantage of this curing technology the transparency and optical attenuation of the waveguide hybrid material consisting of the crosslinked polysiloxanes and the thiol-ene photonetwork was assumed. During the cationic ring opening polymerization, polyether domains were formed (Figure 64) which were thought to enhance the compatibility between photopolymer and matrix material due to the molecular mimicry of oxygen-based polyethers and by thioethers from the thiol-ene photonetwork formed upon 2PP.

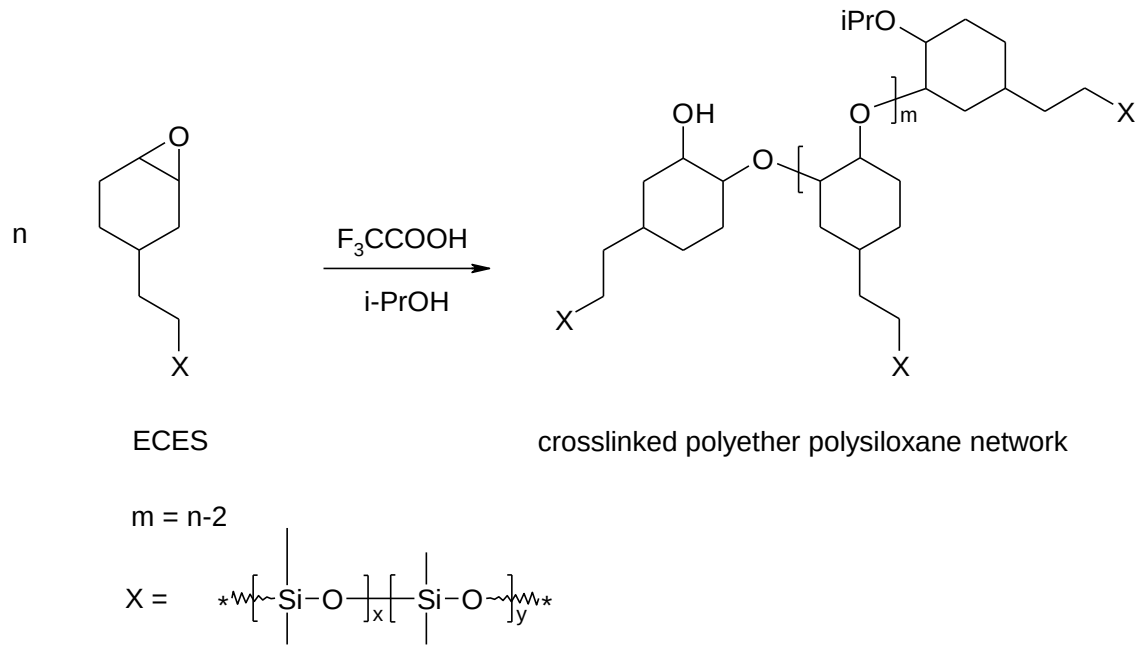

Figure 64: Curing reaction for the waveguide matrix material

3.3 Selection of monomer and synthesis

Compared to most monomer prerequisites described in section 1, compatibility caused the major problems. As discussed in the previous section the curing of the matrix material proceeded via cationic ring opening polymerization of cyclohexyl epoxides yielding a polyether domain and a hydroxyl group per cationic polymerization center, which was a good step towards compatibility with thiol-ene networks. But there was also potential for improvement of the latter on the monomer side: dithiols with long alkyl chains like 1,10-decandithiol were better compatible with the matrix material than the tetrathiol TT, which features a high concentration of mercaptanes and ester moieties and more than double the molecular weight worsening the miscibility. Furthermore dithiols advantageously tend to have a relatively lower viscosity, which was highly important to achieve as it was crucial to a diffusion-based enrichment effect of high refractive thiol-ene material into the waveguide core region. Besides integrating a high amount of sulfur atoms, another possibility to raise the value of n in the photopolymer was to have certain degree of crosslinking. Thus, the ene for the reaction with the dithiol had to exhibit a functionality of at least three. As a strategy to increase compatibility of the photopolymer with the siloxane matrix tris(vinyldimethylsiloxy)methylsilane (TVMS) a trivinyl oligosiloxane was tested in combination with 1,10-decandithiol, but mixing

these components failed. It seemed that only at the phase boundary some kind of thermal thiol-ene reaction allowed for mixing after certain time (formulation **PRE/2.7**). Owing to the molecular mimicry with respect to the siloxane-based matrix material, TVMS had turned out to have very high compatibility with the matrix system ECES so it was reasonable to test a siloxane-based thiol as a reaction partner for TVMS.

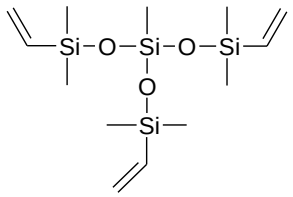

TVMS

For siloxane-based thiol-ene reaction only high molecular mercapto-functional siloxanes are commercially available making synthesis necessary: The desired molecule should feature

- a siloxane backbone causing compatibility with TVMS and the epoxy matrix material ECES
- n as high as possible
- no ester bonds lowering the thermal stability of the corresponding thiol-ene material
- low viscosity, to allow for diffusion-based enrichment of high-refractive material in the waveguide core
- the possibility to evaporate to enable optional removal of unreacted monomer after 2PP writing

The latter criteria were thought to be met by the siloxane based tetrathiol 2,2‘,2‘‘,2‘‘‘-(2,2‘,2‘‘,2‘‘‘-(2,4,6,8-tetramethyl-1,3,5,7,2,4,6,8-tetraoxatetrasilocane-2,4,6,8-tetrayl)tetrakis(ethane-2,1-diyl))tetrakis(sulfanediyl)tetraethanethiol (TTE, Figure 65) was taken into consideration. The high amount of mercaptogroups in this molecule would boost the change in refractive indexdue to the tendency of molecules with high sulfur content to exhibit extremely high RIs. The thiol-ene reaction has a step-growth character in thus crosslinking densities are rather low until high conversion compared

to acrylic systems. The tetrafunctionality of the molecule TTE would allow for extensive crosslinking, which helps to increase the local change in n.

An attempt to synthesize TTE was conducted via photoinduced radical thiol-ene reaction (Figure 65) derived from a technique to synthesize oligofunctional thiol mentioned in the review of Hoyle et. al.[10]

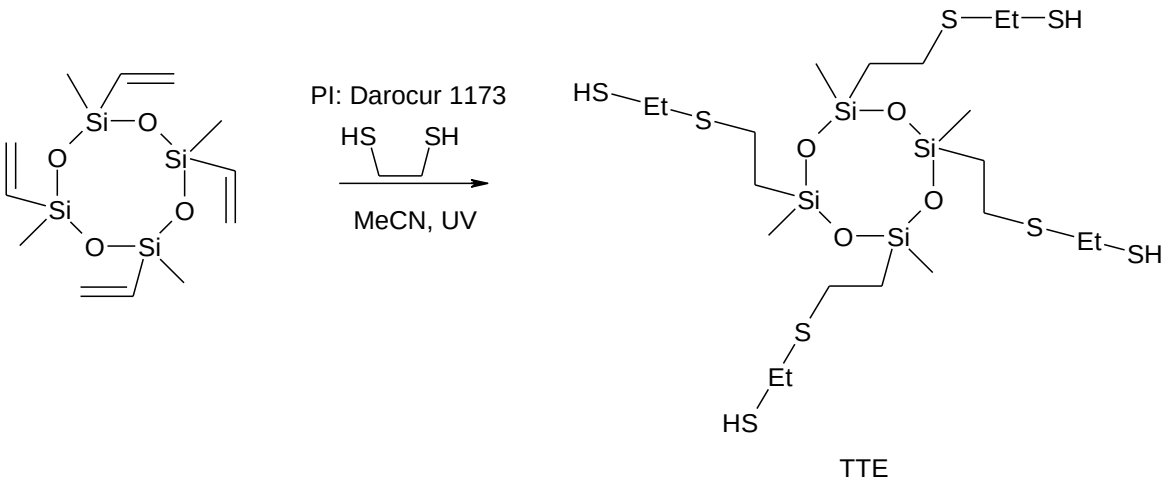

Figure 65: Thiol-Ene based synthesis of TTE

Therefore, the reaction bulb for the synthesis of TTE was equipped with a quick-fit with a quartz window allowing for the insertion of the light guide attached to an OMNICURE 2000 lamp and a septum. 0.5 g (1 equivalent) of the educt 2,4,6,8-tetramethyl-2,4,6,8-tetravinyl-cyclotetrasiloxane was dissolved in 10 g of acetonitril and 0.1 wt% (with respect to the educt) pyrogallol as well as 0.16 equivalents of Darocur 1173. Subsequently the liquid was flushed with nitrogen and 40 equivalent of ethane dithiol was added quickly under stirring in order to achieve a large excess of ethane dithiol. The reaction mixture was illuminated at 3000 mW cm^{-1} for one hour. Subsequently acetonitril was removed on a rotary vap and excess ethane dithiol at high vacuum (0.01 mbar) to give a slightly turbid liquid. Due to the very unpleasant odor of ethane dithiol, distillating the crude product DMF was carried out giving a product with n = 1.57. In Figure 66 the ^{1}H-NMR spectra of the educt 2,4,6,8-tetramethyl-2,4,6,8-tetravinyl-cyclotetrasiloxane and the non-purifyable product are given.

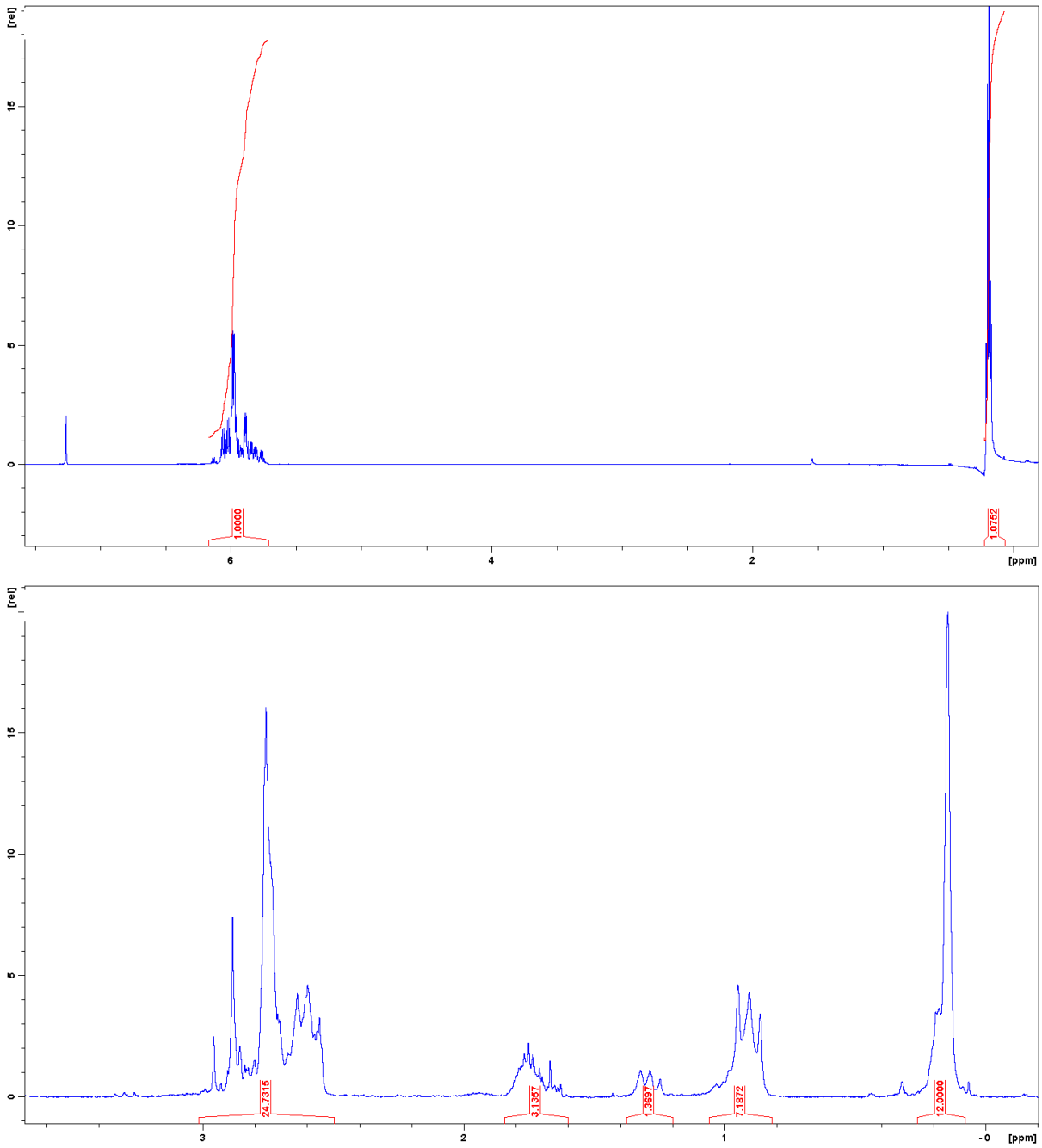

Figure 66: top: ^{1}H-NMR spectrum of the educt 2,4,6,8-tetramethyl-2,4,6,8-tetravinyl-cyclotetrasiloxane; bottom: ^{1}H-NMR non-purifyable product TTE

Comparison of the spectra in shows that the double bonds featured in the educt (multiplet signal around 6ppm) were completely reacted.

An experimental ^{1}H-NMR spectrum of TTE, to the knowledge of the author, has not yet been published. Hence, interpretation shall be attempted by means of literature spectra of ethane dithiol[87] and 2,6-dimethyl-2-(β-ethylthioethyl)-1,3-dioxa-6-aza-2-silacyclooctane (DASO)[88].

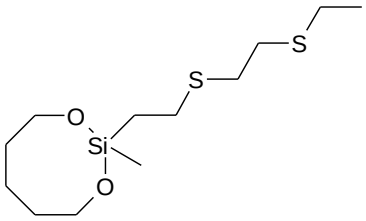

DASO

The accumulation of peaks from 3 to 2.5 ppm is thought to comprise signals for the ethylene hydrogen atoms in α and β-position to the mercapto functionality as well as in β-position to the silicon atom. The signal for the mercapto moiety in the literature spectrum of ethane dithiol is situated at 1.76 ppm, which fits rather well the multiplet from 1.6 ppm to 1.8 ppm. These signals probably result from TTE and ethane dithiol impurities. The multiplet ranging from 0.8 ppm to 1.1 ppm stems most probably from ethylene hydrogen atoms in α-position to the silicon atom. Si-CH_3 should be accounted for by the signal around 0 ppm. The ratio of peak integrals (Si-CH_3 to –SH) <3 indicates, that not each silicon atom features a methyl and a mercaptyl substituent. The information content of this ratio is limited by the unknown content of ethane dithiol, which contributes to the accumulation of signal in the range, which is attributed to –SH. Summing up, TTE is thought to have formed to a certain extent accompanied by oligomeric species of bridged siloxane ring structures and ethane dithiol impurity.

Nevertheless, the impure product was tested towards compatibility with the epoxy-based matrix material ECES. As with all other silicones compatibility could be achieved neither in mixture with the uncured silicone nor with the cured silicone rubber. Due to the fact that TTE could not be purified to a satisfying extent, it cannot be excluded that the pure TTE was actually compatible to ECES. Apart from this, the unpleasant odor, which remains until extremely low concentrations, was a criterion for exclusion.

The latter criteria are fulfilled by 1,3-*bis*(3-mercaptomethyl)-1,1,3,3-tetramethyldisiloxane (TMMD, see Figure 67), which has received very limited attention in chemical literature. Few patents mention this molecule in context with hair dyes, surface modifiers for resins and dental cements etc.[89-92] In a procedure similar to that presented in a patent of Mogi, TMMD was synthesized by the route shown in Figure 67.[93]

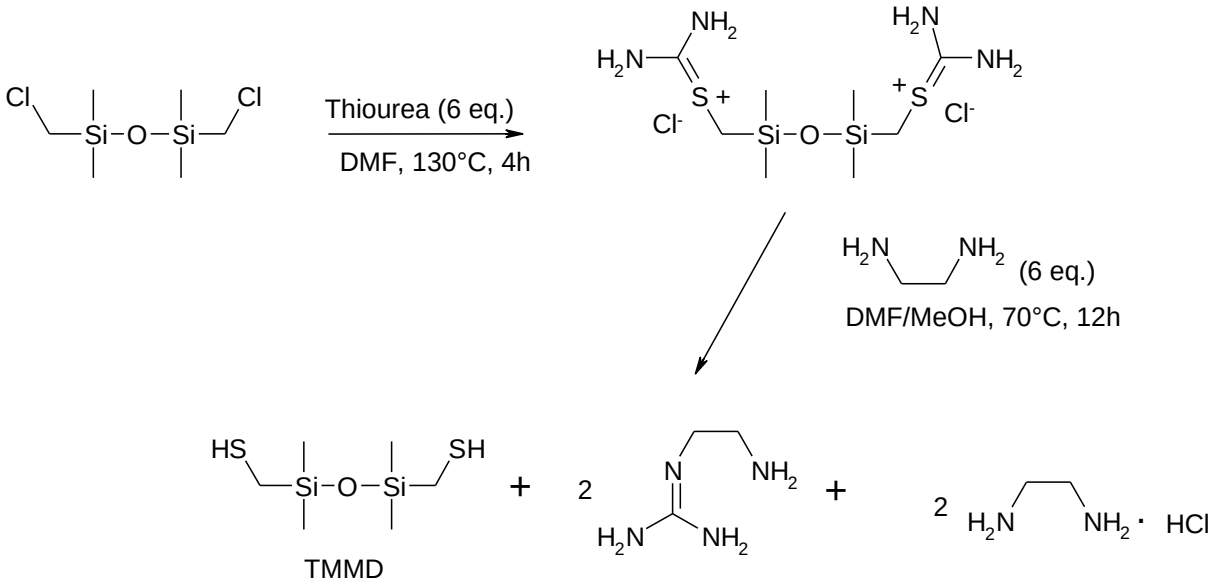

Figure 67: Synthetic route to the dithiol TMMD

At least two by-products with higher molecular weight could be separated from TMMD neither by repeated column chromatography nor by fractionated distillation. TMMD could be proved by NMR as well as by its mass spectrometry (MS) pattern. According to the NMR signals below 0 ppm the by-products are also siloxane-based (for details see Experimental part). GC-MS investigation showed that their molar mass must be higher than the one of the desired product TMMD (MW 226.51g/mol), but the MS patterns (for details see Experimental part) did not allow identification of these by-products.

The UV-detector of the MPLC used for column chromatography gave very broad, largely overlapping peaks of product and by-product. For this reason, only the purest fractions of product were isolated, giving only a yield of 20% and thus sacrificing yield for purity as the yield of crude product had been 90%. The amount of mercapto moieties was determined via titration with lead(IV)acetate in glacial acetic acid with quinalizarine as indicator according to the method of Verma et. al.[94] Assuming that mercapto groups are exclusively present in TMMD molecules, an acceptable purity of 90% was achieved.

Preliminary UV-curing experiments involving TMMD showed that it built a highly crosslinked, brittle and –judging by eye- perfectly transparent photonetwork (using Darocur 1173 as PI, formulation **PRE/2.8**) when reacted with the trivinyl siloxane TVMS in an equimolar ratio regarding thiol and ene moieties. An appropriate

stabilizer for this thiol-ene formulation was pyrogallol added at a concentration of 0.2%.

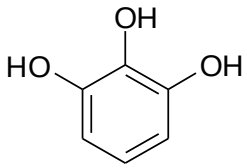

Pyrogallol

Next, the orthogonality of the monomer and the matrix-reactivity were tested. Therefore, an equimolar combination of the dithiol TMMD and the trivinylsiloxane TVMS was mixed with the matrix material ECES, trifluoroacetic acid solution and the one-photon initiator Darocur 1173. Afterwards, this formulation was poured into two separate vessels (0.5 ml each), where the curing effect kicked in within a few minutes. Subsequently one vessel was UV-flood-illuminated giving a material that was perfectly transparent judging by eye (**PRE/2.9**). The other vessel was exposed to high vacuum of approximately 0.01 mbar, where 90% of the monomer formulation could be removed within approximately 6 h, which indicates that only a negligible amount of monomer had interfered with the epoxy-based cationic ring-opening polymerization of ECES. Thus the base of a process had been established, where monomer would be cured inside a crosslinked matrix via two-photon polymerization. In contrast to former works no developing step would be required.[77-79] The procedure is schematically shown in Figure 68.

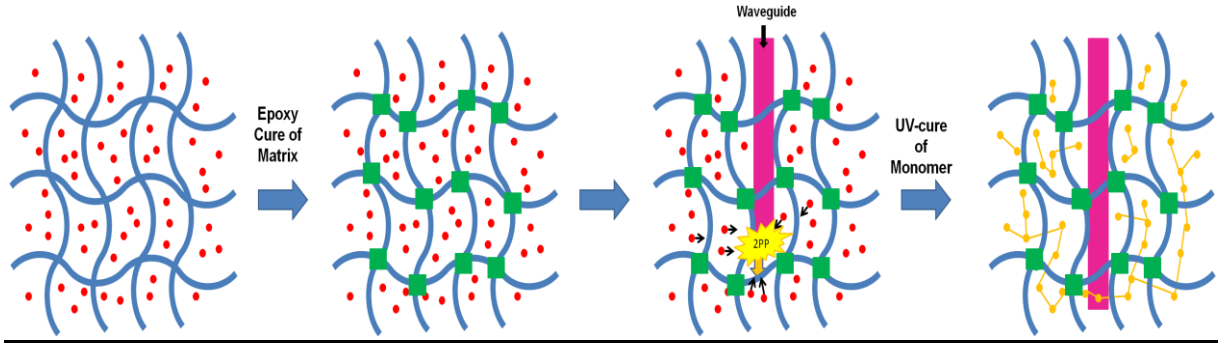

Figure 68: Manufacturing steps of polysiloxane/thiol-ene based waveguides. Snakelines represent polysiloxane-based matrix material, red dots photoreactive monomer formulation, green squares epoxy crosslinks, interconnected yellow dots: UV-cured photoreactive monomer formulation.

The siloxane-based thiol-ene reaction is shown in Figure 69. The low-viscosity thiol-ene monomer TMMD and TVMS diffuse towards the two-photon illuminated region through the epoxy silicone rubber, where they encounter initiating radicals and undergo polymerization. As the thiol-ene polymer is very well compatible with this polyether-containing silicone, very transparent interpenetrating networks are formed.

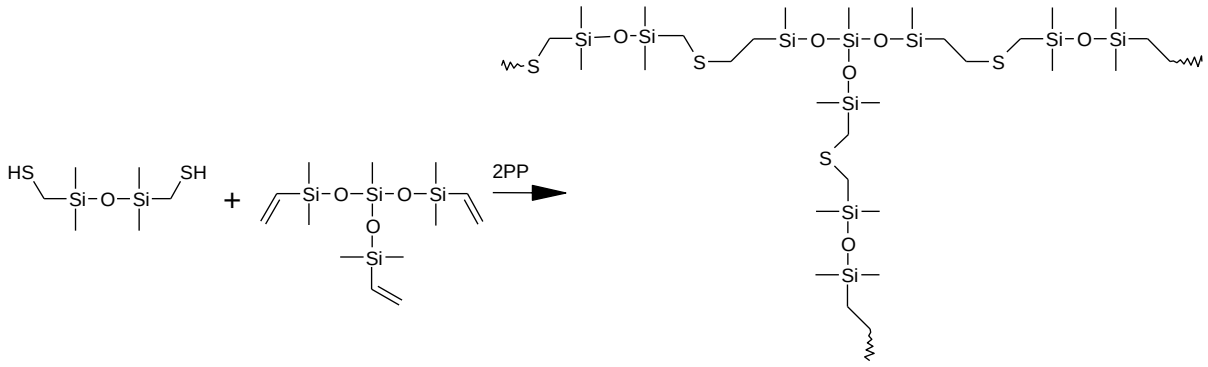

Figure 69: Two-photon induced thiol-ene polymerization yielding the waveguide core

It was thus reasonable to start investigations considering reactivity, mechanical and optical properties as well as the 2PP performance.

3.4 ATR and photo-DSC investigations

A major bottleneck in two-photon-lithography is the level of throughput. For waveguide inscription on a mass production scale, highly two-photon reactive materials are required. Beside the PI, the electron density of monomers at the reacting moieties and others, the thiol-ene photoreactivity is also influenced by the ratio of thiol:ene moieties present. This stoichiometry has also an effect on the double bond conversion (DBC), which is central to a high refractive index change in the waveguide core. These properties are not accessible for a real 2PP situation so one-photon-initiated UV-curing of formulations with a varying thiol:ene ratio were subject of analytics instead. Note that the comparability of the obtained results to the two-photon-microfabrication is limited due to the different mechanism of photoinitiation. To get a hint towards the optimum ratio of thiol and ene moieties, photo-DSC as a fast and reliable method to quantify the reactivity of one-photon-reactive compositions was used. This information was complemented by ATR-IR (attenuated reflection infrared) experiments allowing to determine the theoretical polymerization heat to a value of 70.1 kJ mol^{-1} applied to the number vinyl of moieties. This could be calculated from the DBC of the pure thiol-ene resin without matrix material (Table 10, for calculation methods see Section Materials and Methods).

Table 10: Photo-DSC measurements of thiol-ene photopolymerization of the pure thiol-ene resin without matrix material

Formulation	Thiol/Ene Ratio	DBC (%)	R_{pmax} (mol s^{-1} L^{-1})	T_{max} (s)
UV/2.9a	1.4	100	0.098	11.8
UV/2.9b	1.2	100	0.125	11.1
UV/2.9c	1.0	100	0.129	9.7
UV/2.9d	0.8	78	0.161	9.6
UV/2.9e	0.6	64	0.201	7.4

The measurement series of mixtures of the dithiol TMMD and the trivinyl siloxane TVMS with thiol:ene moiety ratios from 0.6 to 1.4 (see Table 10) gave increasing DBCs reaching 100% at equimolarity of thiol and ene functionalities. Also in the formulations **UV/2.9a** and **UV/2.9b** with thiol:ene ratios 0.8 and 0.6 all available thiol groups were reacted. The DBC value of 64% is actually higher than the stoichiometry would allow, which is attributed to inaccuracy of the ATR determination of DBC. The reaction speed, represented by the rate of polymerization R_{pmax} and by T_{max},

increases with rising ene content. The explanation for this behavior is that the rate limiting step of this thiol-ene reaction is the propagation step, where the thiyl radical adds to the double bond making the polymerization rate more dependent on the concentration of vinyl groups than the concentration of mercapto groups

With the theoretical polymerization heat in hand, it was possible to determine the DBC via photo-DSC also from the materials, where the thiol-ene system was diluted by the matrix material (Table 11).

Table 11: Photo-DSC measurements of thiol-ene photopolymerization inside the epoxy matrix

Formulation	Thiol/Ene Ratio	DBC (%)	R_{pmax} (mol s^{-1} L^{-1})	T_{max} (s)
UV/2.9a/epox	1.4	72	0.033	12.2
UV/2.9b/epox	1.2	69	0.038	11.7
UV/2.9c/epox	1.0	83	0.060	9.5
UV/2.9d/epox	0.8	61	0.065	8.4
UV/2.9e/epox	0.6	37	0.058	6.8

Figure 70 illustrates the DBC of the epoxy hybrid materials in question as a function of time.

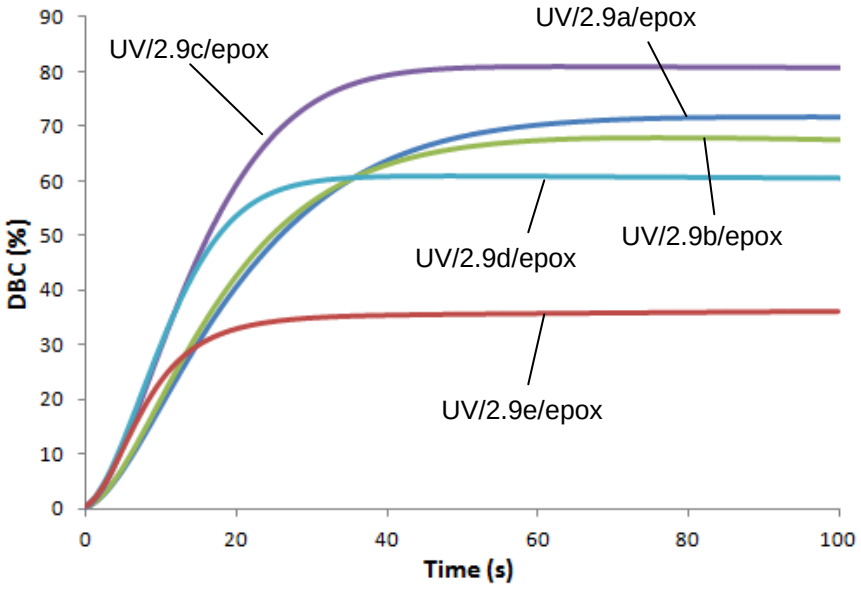

Figure 70: Photo-DSC curves of thiol-ene photopolymerization inside the epoxy matrix

When cured in the epoxy matrix at a monomer content of 40%, the highest double bond conversion was observed at ratio 1.0 (formulation **UV/2.9a/epox**). In contrast to the pure thiol-ene system shown in Table 10, the dilution of the monomer by epoxy-based silicone rubber caused the DBC to remain incomplete. It is unclear, why R_{pmax}

keeps increasing from thiol:ene ratio of 1.4 to 0.8 and subsequently drops from 0.8 to 0.6.

With the latter results in hand, two further points were considered with a view to later 2PP experiments: The tendency of thiol-ene systems to form less dense networks with increasing thiol content suggest facilitated diffusion of thiol-ene monomers into the waveguide core region and enhanced enrichment of high refractive material. Another advantage of systems rich in thiol is the higher amount of sulfur atoms incorporated into a mercapto-terminated photopolymer. The latter two points would suggest thiol:ene ratio 1.4 as the ideal case.

But as shown in Table 11, the DBC at thiol:ene ratio 1.0 (formulation **UV/2.9c/epox**) is significantly higher than for formulations **UV/2.9a/epox** and **UV/2.9b/epox** of thiol excess. Furthermore, R_{pmax} at an equimolar thiol:ene ratio is the second highest in Table 11 and outperforms **UV/2.9a/epox** and **UV/2.9b/epox**. Thus, equimolarity of thiol and ene functionalities was preferred for 2PP.

3.5 Real time-FTIR measurements

During waveguide structuring the DBC distribution in the VOXEL is not uniform and further very dependent on the writing parameters such as laser power and feed rate. Hence, the development of the DBC over time with varying thiol:ene stochiometry is relevant. It was possible to monitor the latter function already via photo-DSC. Thus UV-curing of the pure thiol-ene formulations **UV/2.9a-e** was investigated by Real time FT-IR in order to control the photo-DSC results without the need to calculate the $\Delta H_{0,P}$.

The same setup and parameters as discussed in section 2.4 were applied sandwiching the samples with PE-foils to avoid oxygen inhibition. Figure 71 shows the spectrum of the material prior to and after UV-curing by the example of formulation **UV/2.9e**. For the determination of the double bond conversion the areas of the vinyl peak (integration between 985 and 937 cm^{-1}) and the CH_3 symmetric deformation of Si-CH_3 as reference (integration between 1217 and 1321 cm^{-1}) were used.

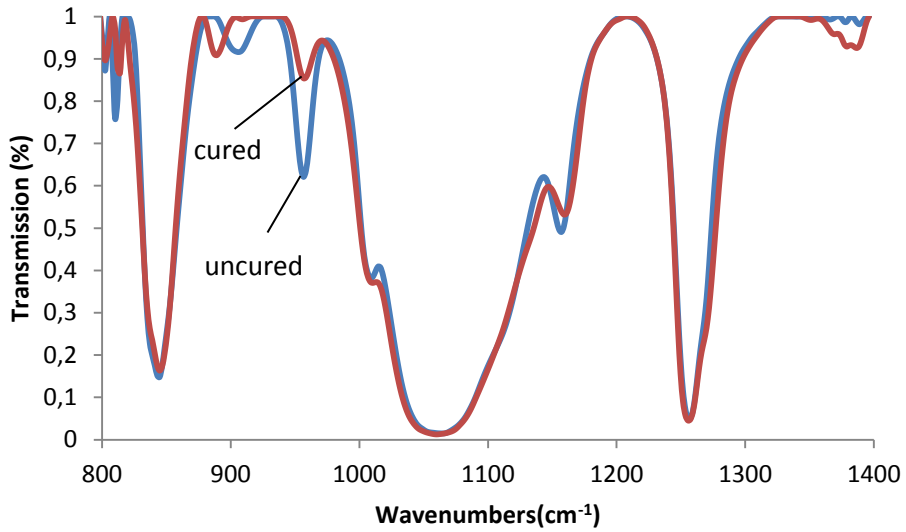

Figure 71: Real time FT-IR spectra from formulation **UV/2.9e** prior to and after curing

Figure 72 shows the results from the Real time FT-IR measurements:

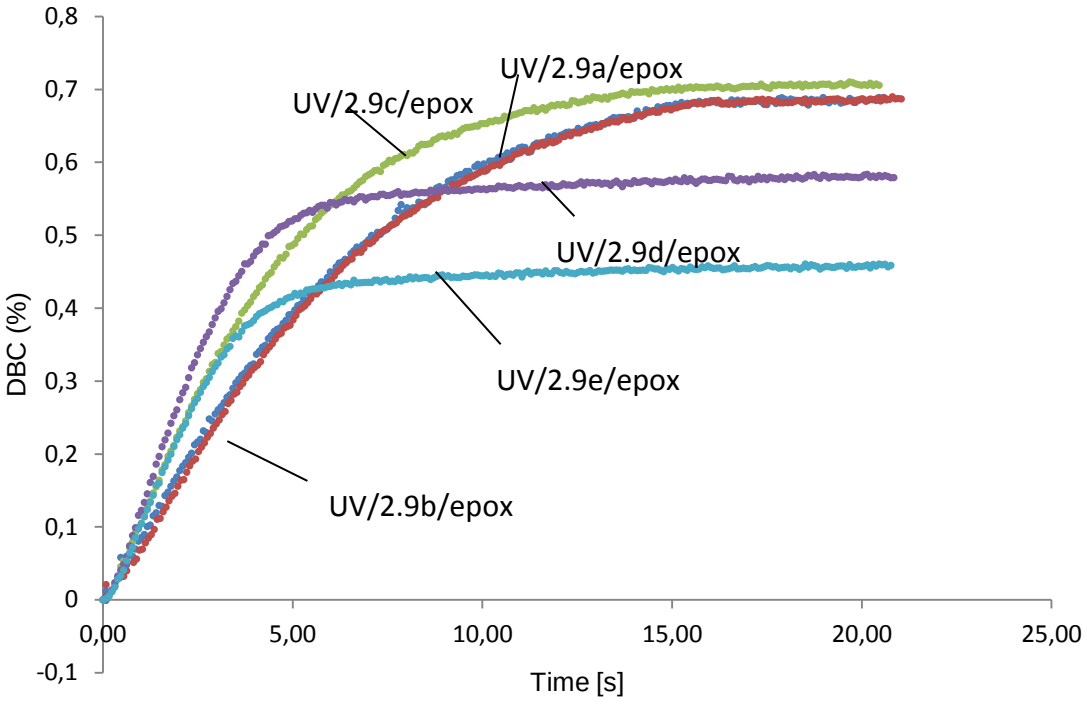

Figure 72: DBC of UV-illuminated thiol-ene systems of different thiol:ene moieties ratio VS. time. Curve A corresponds to ratio thiol:ene 1.4, curve B 1.2, curve C 1.0, curve D 0.8 and curve E 0.6.

Generally reflecting the tendencies from the previous sections for the pure thiol-ene mixtures: Thiol excess yields higher DBCs while ene excess accelerates the reaction. The lower DBC compared to the photo-DSC measurements is probably due to the

lower light intensity. The generally lower reaction times are attributed to the very low film thickness in the course of these measurements.

Real time FT-IR measurements for thiol-ene system in question in the presence of the crosslinked epoxy matrix material ECES (formulations **UV/2.9a/epox** to **UV/2.9e/epox**) were not conducted as the FT-IR signals of the vinyl moieties in the formulations were too weak.

3.6 DMTA tests

As discussed in section 2.5, the mechanical stability at temperatures around 240°C of the waveguide cladding and core materials is of interest due to a temperature ramp, which the material undergoes during the industrial lamination process of the printed circuit boards. A suitable method to investigate this aspect is DMTA: If no sudden change in the storage modulus is detected, failure of the material can be excluded.

In comparison to the thixotropic liquid–based concept discussed above, the material in question does not contain any acryate or ester bonds, which was a central consideration in the design of this epoxysilicone/thiol-ene hybrid material in terms of thermal stability. DMTA results are given in Figure 73.

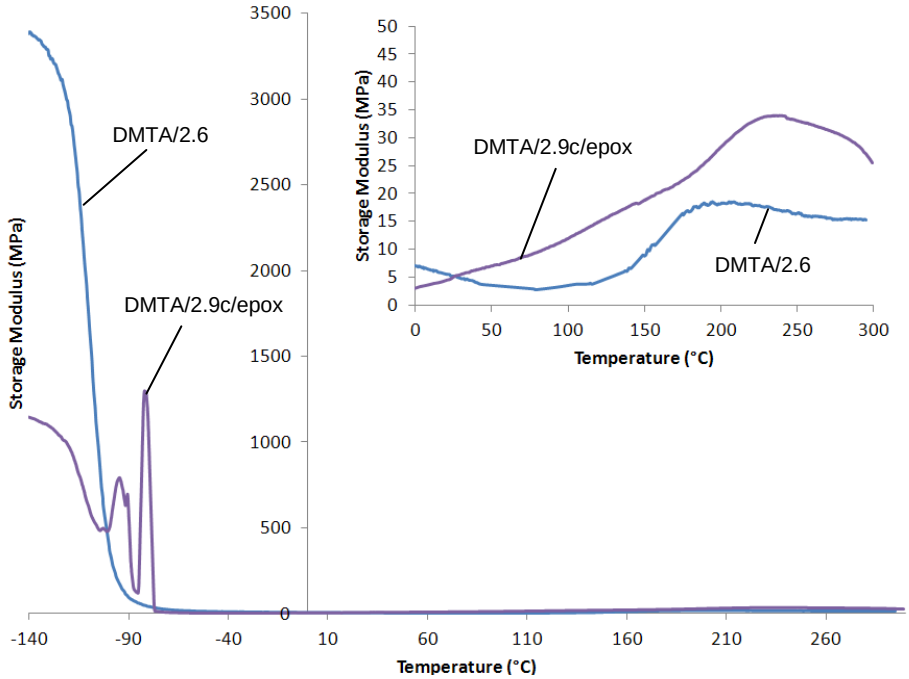

Figure 73: Testing of the epoxy-based materials towards mechanical stability via DMTA

DMTA measurement of the waveguide cladding material (formulation **UV/2.9c/epox**) showed a very low storage modulus and no failure from over the whole investigated temperature range. The material is comparatively low in storage modulus at -140°C. The up- and downturns around -90°C should be attributed to the inhomogeneity resulting from UV-curing of the test bar. After exhibiting very low storage moduli a slight increase was observed until approximately 240°C (see magnification), which is explained by thermal polymerization of unreacted monomer still present in the material. After completion of thermal polymerization of the material becomes softer until 300°C. The waveguide core material could not be investigated as its content of thiol-ene material is not known due to the above mentioned diffusion-based enrichment effect upon 2PP. The plain ECES matrix material (formulation **DMTA/2.6**) was much stiffer than the cladding material at -140°C. Note that trifluoro acetic acid could not be used as curing catalyst to produce a test bar of the plain matrix material, because ECES would rapidly undergo curing making it impossible to create a homogenous formulation. Instead, the photoacid generator (*p*-Isopropylphenyl)(*p*-methylphenyl)-iodonium tetrakis(pentafluorophenyl) borate (IMIT) was applied (for details, see Experimental Section). Above 0°C, it shows a similar behavior to the cladding material with a slightly lower curve with the maximum around 200°C.

3.7 Refractive Index

Analogously to the previous concept, the value of n in the cladding material was measured by means of an Abbé refractometer (Table 12), but there was no method available to determine the distribution of n within the 2PP-illuminated waveguide core volumes, where high refractive thiol-ene network was present in a higher concentration than in the surroundings. It lies somewhere between the TMMD/TVMS cured photopolymer (**PRE/2.8**) and the cladding materials, which is a cured hybrid material of epoxy matrix and cured TMMD/TVMS.

Table 12: Relevant n values from the 2PP formulations. Exact formulations are given in the photo-DSC experimental section.

Sample	n
TMMD	1.476
TVMS	1.417
TMMD/TVMS uncured (formulation **PRE/2.8**)	1.446
TMMD/TVMS cured (formulation **PRE/2.8**)	1.487
Epoxy cured matrix material (formulation **DMTA/2.6**)	1.423
Cured hybrid material of epoxy matrix and cured TMMD/TVMS (formulation **UV/2.9c/epox**)	1.443

The dithiol TMMD featured a value for n more than 0.05 higher than the pure cured epoxy matrix material (formulation **DMTA/2.6**), whereas the value of n in TMVS was 0.006 less. The mixture of TMMD and TVMS (**PRE/2.8**) featured quite well the RI, which was expected from calculation considering their contents (1.4465). The UV-curing of **PRE/2.8** yielded a refractive index increase by more than 0.04. The cladding material consisting of the epoxy-based ECES and the thiol-ene network was 0.04 higher than the pure cured ECES.

3.8 2PP writing

The extensive formulating and analytics presented in the previous sections had afforded highly transparent, high refractive, flexible and thermally stable waveguide materials. Furthermore the formulation had been optimized with respect to the ratio of thiol:ene moieties to obtain the maximum DBC (thiol:ene 1.0).

As a start for 2PP, firstly a screening for a suitable TPI was carried out. B3FL had performed well in case of acrylic waveguide fabrication in section 2, but faced serious solubility problems in the siloxane-based thiol-ene. B3K has been presented in literature as a very efficient TPI in acrylic resins, but in combination with thiol-ene

resins it formed a precipitate within seconds after having been completely dissolved. This was thought to be either caused by addition of mercaptanes to its triple bonds or salt formation of the catalyst trifluoro acetic acid and B3K due to its basic amine groups. Hence, P3K was tested, because the lone electron pair of its nitrogen atoms is well delocalized into the three neighbouring aromatic structures.

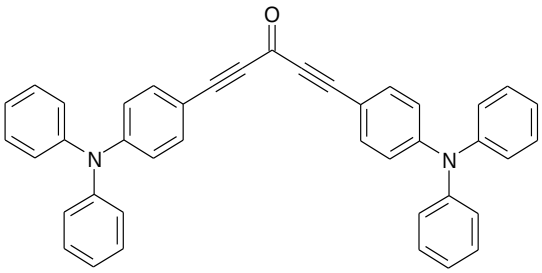

P3K

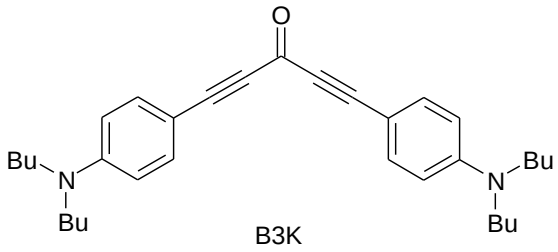

B3K

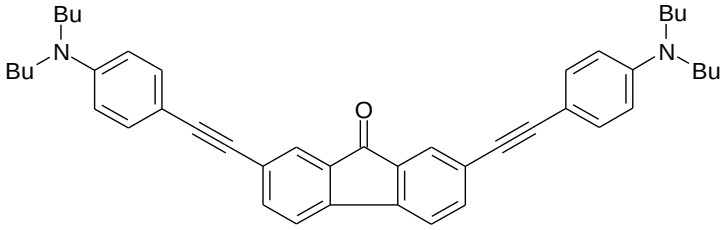

B3FL

No solubility problems were encountered for P3K but upon the addition of the acid the colour of the formulation changed from yellow to reddish/orange, which is probably attributed to oxidation of the nitrogen lone pairs of P3K. This phenomenon, however, was not thought to necessarily disturb 2PP.

As mentioned above, the thiol-ene photonetwork resulting from the dithiol TMMD and the trivinyl siloxane TVMS contributed brittleness to the hybrid material with the epoxycyclohexyl-based matrix material. Hence, a monomer content of 20% was tested using P3K as two-photo-initiator (formulation **2PP/2.9/20**, for pre- and post processing see Section Materials and Methods) The phase contrast was rather poor when structuring at a feed rate of 10 mm/min but also at 4 mm/min (Figure 74). The best results were still obtained at laser powers between 200 and 250 µW.

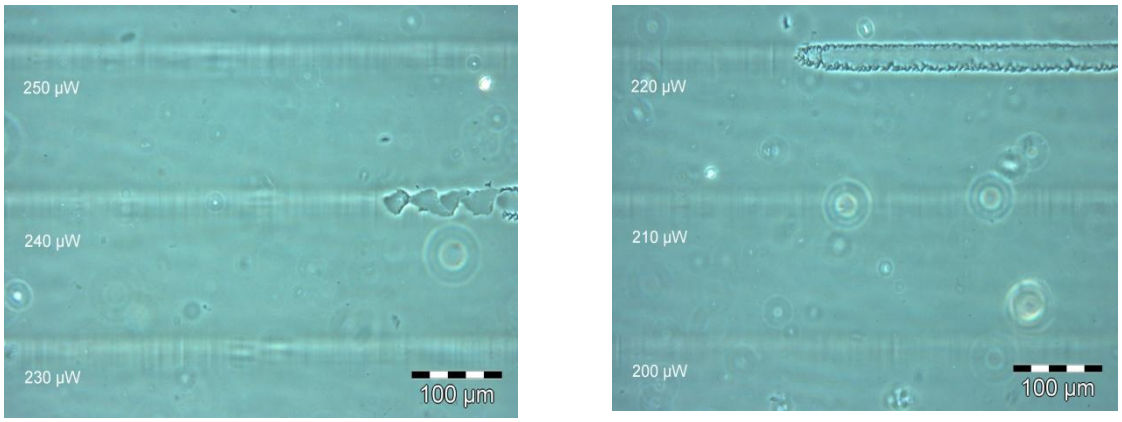

Figure 74: Phase contrast view of screening for laser power for optimum waveguide fabrication in an epoxy cure silicone rubber containing 20% thiol-ene monomers and 0.2% P3K (formulation 2PP/2.9/20) by writing over the volume once. The waveguide structures were fabricated at laser powers between 200 and 250 µW at 4 mm/min feed rate.

This could be improved by increasing the monomer content to 40% (formulation **2PP/2.9/40**) facilitating diffusion of high refractive monomer in the less crosslinked silicone rubber at a feed rate of 4 mm/min (Figure 75), which was kept for all the following experiments in this section. This doubling of monomer content, however, meant accepting lower toughness of the waveguide material

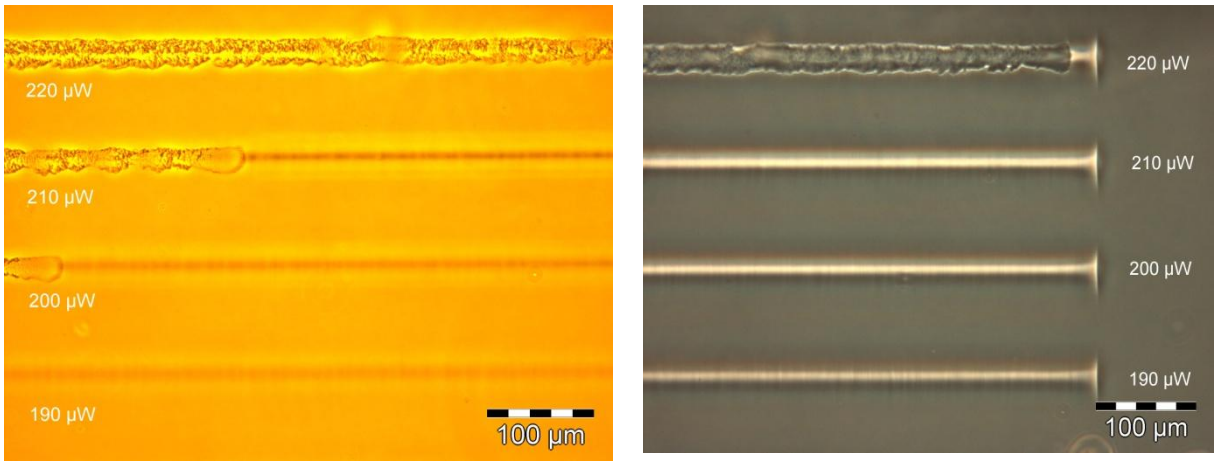

Figure 75: Phase contrast view of screening of laser power for optimum waveguide fabrication in an epoxy cure silicone rubber containing 40% thiol-ene monomers and 0.2% P3K by writing over the volume once (formulation **2PP/2.9/40**). The image on the left is from the sample prior to UV-curing and the image on the right from after UV post-processing. The waveguide structures were fabricated at laser powers of 160 to 200 µW at 4 mm/min feed rate.

The structuring was found in the range of 200 µW being with a limit at 220 µW, where the waveguides were continuously burnt. Some burnt spots also occurred already at 210 µW. Comparing the phase contrast picture prior to and after UV-flood-curing an additional refractive index increase in the core material can be observed as after 2PP the waveguide was swollen with unreacted monomer, which would be polymerized upon UV-illumination. The orange color of the phase contrast view prior to curing comes from the filter, which was used to prevent the microscope light from inducing photopolymerization.

Further improvements on the local change in refractive indexcould be achieved by moving the VOXEL firstly three times (Figure 76) and subsequently five times (Figure 77) through the waveguide core volume. Thereby monomer would diffuse into the already cured regions after each run and be polymerized there in the next yielding an additional enrichment of high refractive thiol-ene material in the illuminated regions.

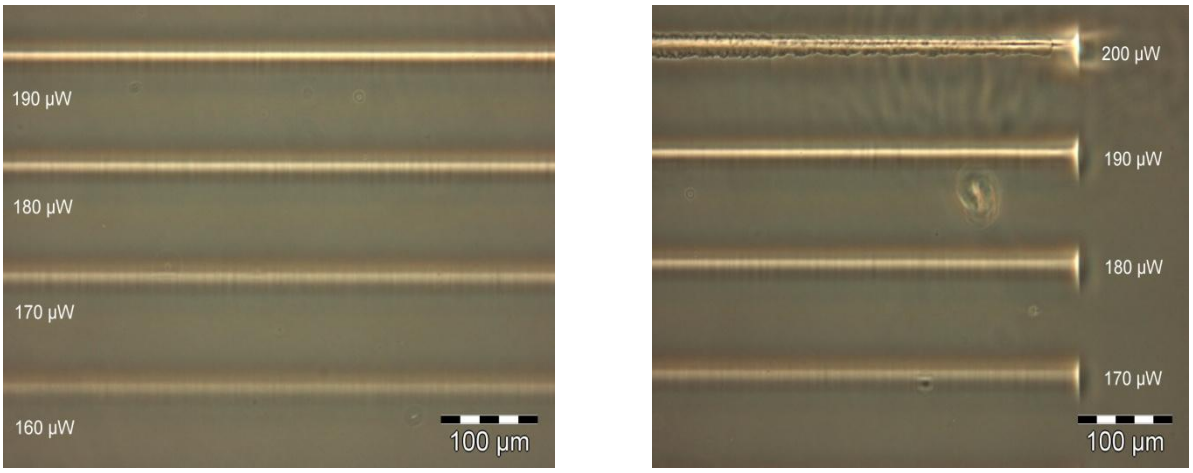

Figure 76: Phase contrast view of screening of laser power for optimum waveguide fabrication in an epoxy cure silicone rubber by writing over the volume 3 times (formulation 2PP/2.9/40). The waveguide structures were fabricated at laser powers of 160 to 200 µW at 4 mm/min feed rate.

A screening with respect to waveguide writing speed and laser power yielded a structuring window around 200 µW and 4 mm/min. The latter feed rate was applied in all following 2PP experiments in this section. As shown in Figure 76, the phase contrast increased from 170 to 190 µW. At 200 µW the waveguide structure was continuously burnt.

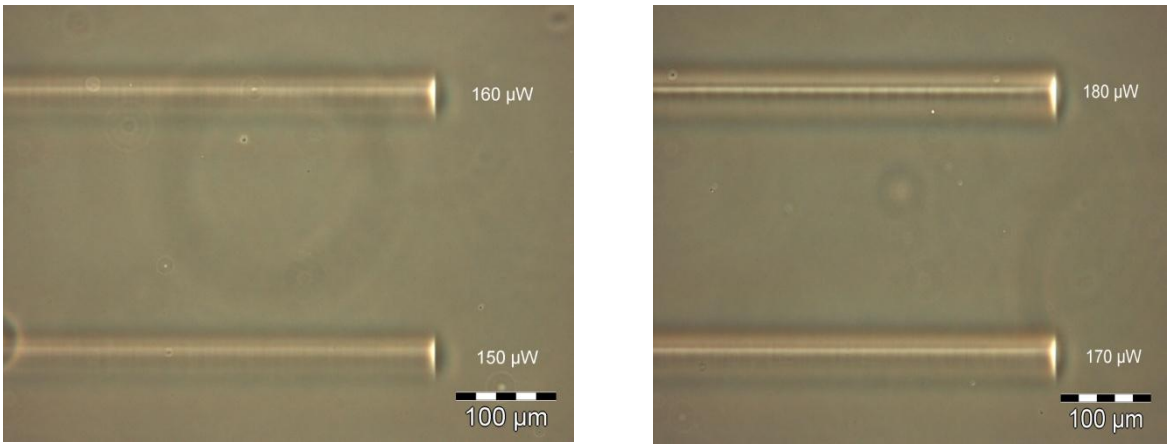

Figure 77: Phase contrast view of screening of laser power for optimum waveguide fabrication in an epoxy cure silicone rubber by writing over the volume 5 times (formulation **2PP/2.9/40**). The waveguide structures were fabricated at laser powers of 150 to 180 µW at 4 mm/min feed rate.

The samples, where the VOXEL had run through each waveguide structure five times (Figure 77) showed good structures at slightly lower laser powers around 170 and 180 µW than the cases shown in Figure 76 and Figure 77. The reason for this is that each additional run also thermally stresses the medium and thus the burning happens at lower laser powers. Comparing Figure 75, Figure 76 and Figure 77 also shows that each additional run broadens the waveguide structure. Sharp waveguide boundaries as in case of the acrylic system described above could produced in none of the latter trials.

The sharpening of the waveguide edges was thought to be possible by low amounts hindered amine stabilizers (HALS) to quench radicals in the periphery volumes around the waveguide. Preliminary attempts using 2,2,6,6-tetramethyl-piperidin-1-yl)oxyl (TEMPO) did not give any sharper waveguide boundaries, when added to formulation **2PP/2.9/40** with 0.1 and 0.5 wt%. A screening of other HALS might be worthwhile.

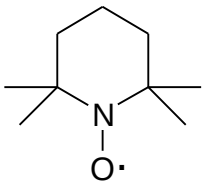

TEMPO

As mentioned in the beginning of this section, formulation **2PP/2.9/40** upon the addition of P3K gained a yellow colour. Within one hour of curing the sample turned greyish-yellow and overnight it would become intensively pink (see Figure 78). 2PP was also carried out with this “pink” P3K.

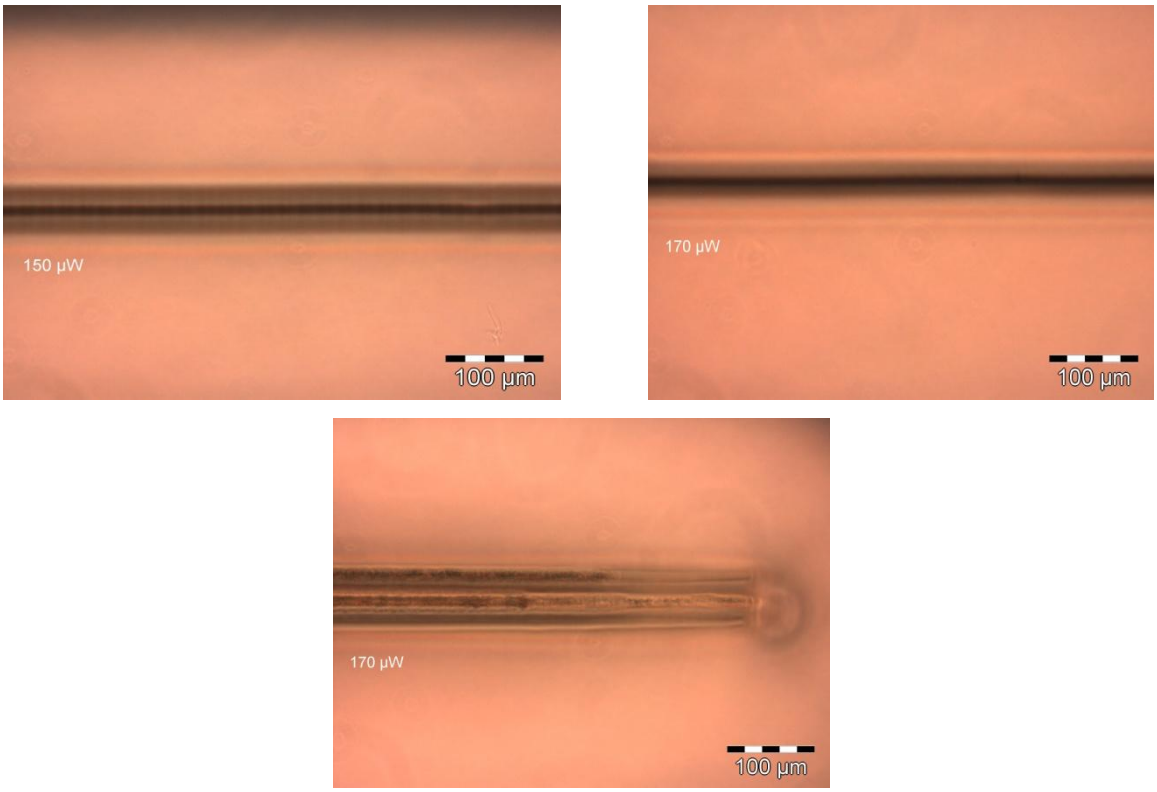

Figure 78: Phase contrast view of waveguides fabrication with 4 mm/min feed rate inside an epoxy cure silicone rubber (**2PP/2.9/40**) over the waveguide volume once (top right,170 µW) and three times (top left: 150 µW and bottom: 170 µW).

These experiments gave even better results with respect to local change in refractive index than the freshly prepared samples. Waveguides were structured at 170 µW in a single writing process and at 150 µW in a triple writing process significantly strengthening the phase contrast. The triple writing process at 170 µW (as carried out with freshly prepared samples) yielded a burnt structure.

The aforementioned coloring of the waveguide material results from photoinitator absorption and is disadvantageous for of waveguiding. For this reason the TPI P3K, which provides the system with intensive color, was substituted with the phosphine-based, one-photon initiator Irgacure 819 (**formulation 2PP/2.9/40a**). The latter becomes colorless upon UV-curing. It was applied at the elevated concentration of 1% as it is a one-photon-initiator with a much lower two-photon-cross-section (less

than 4 GM) than e. g. P3K (256 GM in THF).[95] The obtained structures are shown in Figure 79.

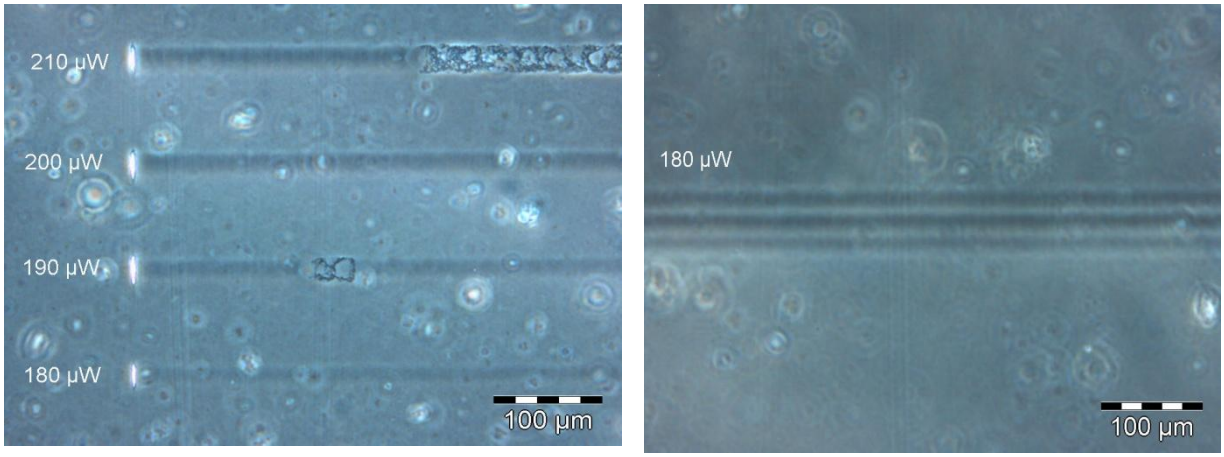

Figure 79: Phase contrast top views of waveguide structures fabricated at 4mm/min feed rate by means of 1% Irgacure 819 inside an epoxy cure silicone rubber (formulation **2PP/2.9/40a**) Left: waveguide structures after a triple writing step (from 180 to 210 µW). Bottom: 6+1 waveguide bundle written at 180 µW with a triple writing step

Irgacure 819 was designed for one-photon initiation, so its ability to absorb two photons almost simultaneously is poor compared to TPIs. Hence, problems with burned spots in the waveguide structures arose, especially in case of triple writing. A single writing step, however yielded no visible local change in n. The only waveguide structures exhibiting no burnt spots could be fabricated around 180 µW. 1% was the solubility limit for Irgacure 819, so there was no possibility to improve the fabrication performance by increasing the one-photon-initiator concentration.

An approach to lower the coloring was logically to reduce the content of P3K, which was tested for a concentration of 0.06% (formulation **2PP/2.9/40b**, Figure 80).

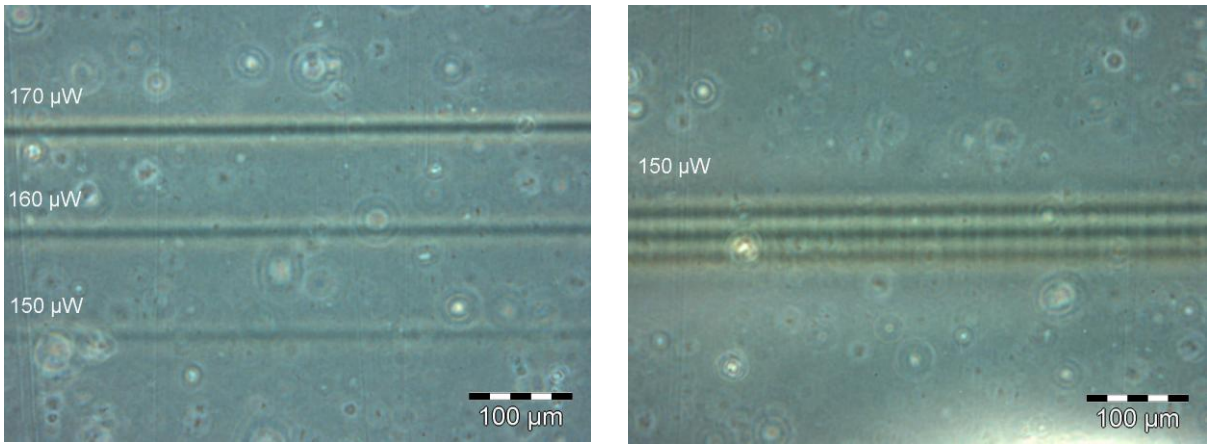

Figure 80: Phase contrast top views of waveguide structures fabricated at 4mm/min feed rate inside an epoxy cure silicone rubber (formulation **2PP/2.9/40b**) at laser powers from 150 to 170 µW (left) and a 6+1 waveguide bundle at 150 µW. A triple writing process was applied.

This measure turned out to be even beneficial regarding the local change in refractive index yielding the best results in this section. The optimum writing window was found between 150 and 170 µW laser power at 4 mm/min feed rate.
But compared to the acrylate based material discussed in section 2, these results were clearly less promising due to the lower phase contrast and the diffuse phase boundaries. A significant potential to achieve higher phase contrasts (and thus higher refractive index changes) is seen in the application of a higher functional but compatible (!) thiol instead of the difunctional TMMD.

3.9 Waveguiding

After the optimization of 2PP waveguide fabrication it was necessary to gain a proof principle for light guiding and test light guiding performance qualitatively with a view to optical damping measurements.
As described in section 2, this was carried out by making the waveguide cross-sections visible by cutting pieces out of the film containing the waveguides and bringing them into the white light of a microscope. Formulation **2PP/2.9/40b** (for waveguide top view see Figure 81), which i) had shown a better local change in refractive index than most of the other formulations in the previous section and ii) had no intensive color as the “pink” formulation (top view: Figure 78), was considered as the most promising.

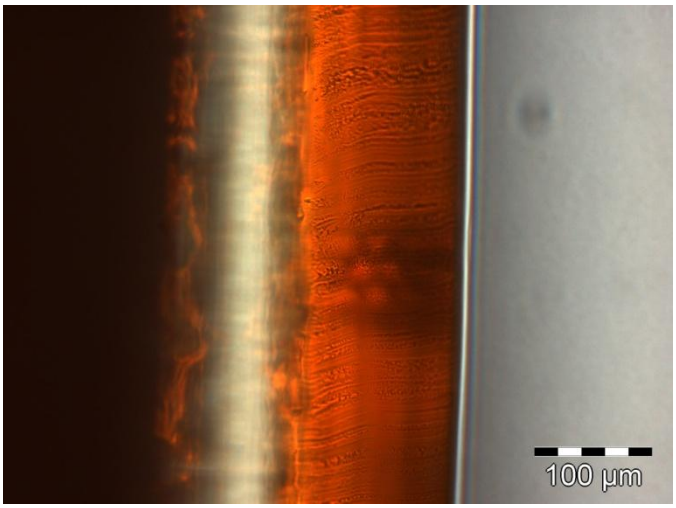

Figure 81: Illuminated cross-section (within circle) of a bundle of 6 +1 waveguides fabricated inside an epoxy cure silicone rubber containing 40% thiol-ene monomers by means of 0.06% P3K (formulation 2PP/2.9/40b) at 150 µW laser power 4 mm/min writing speed waveguide.

The coupling-in test however showed very weak waveguiding of white light making the cross-section of a 6+1 waveguide hardly visible (Figure 81). Single waveguides could not even be found on the microscope.

With the one-photon-initiator 1% Irgacure (formulation **2PP/2.9/40a**, for waveguide top view see Figure 82) the results were slightly better in case of the 6+1 waveguide bundles. Single waveguide cross-sections were weak, but could at least be located. At 200 µW the waveguide guided the highest amount of white light

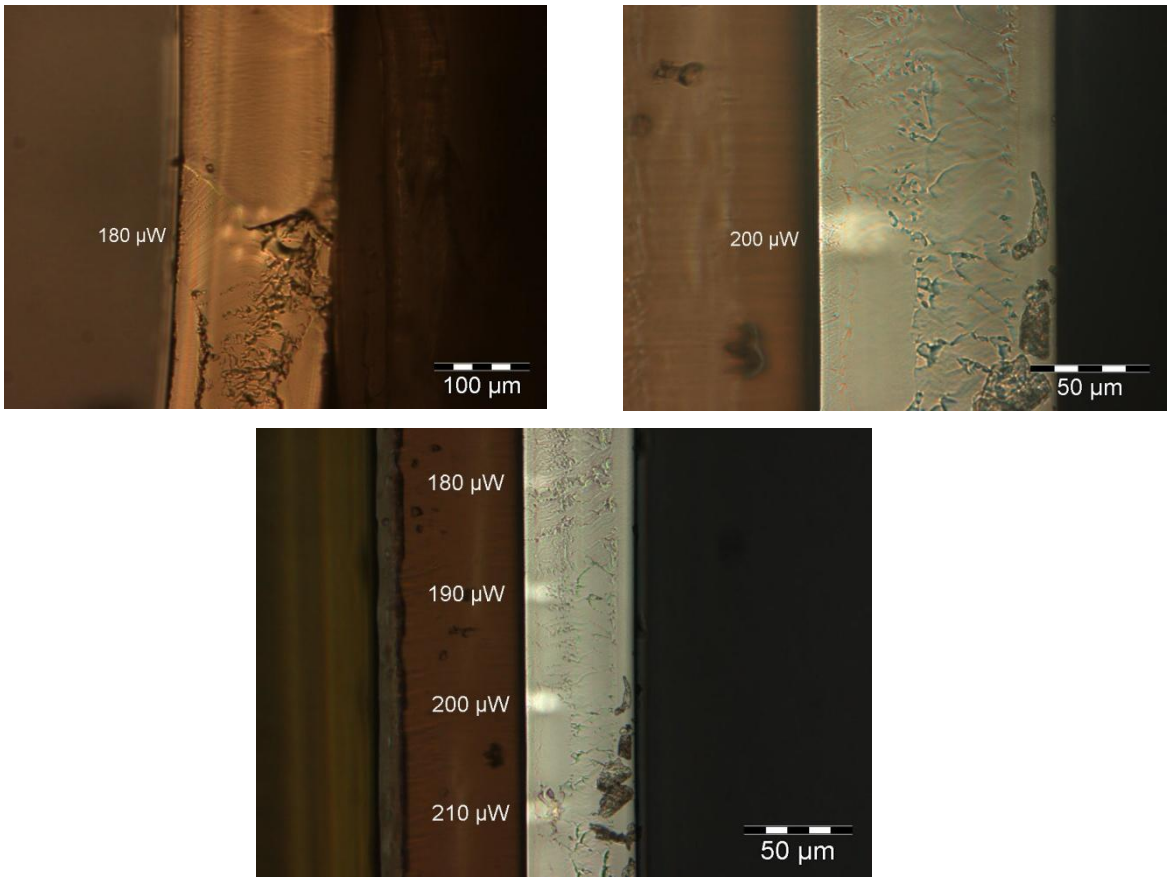

Figure 82: Illuminated cross-section of waveguides fabricated inside an epoxy cure silicone rubber containing 40% thiol-ene monomers by means of 1% Irgacure 819 at 4 mm/min (formulation **2PP/2.9/a**) feed rate. Upper left: Illuminated cross-sections of a bundle of 6 +1 waveguides at 180 µW laser power. Upper right: Zoomed view of the cross-section of a waveguide fabricated at 200 µW

As another measure to improve the waveguiding ability of the material, the P3K concentration was reduced from 0.06% to 0.04% (formulation **2PP/2.9/40c**) The quality of the phase contrast was again in the same range (Figure 83).

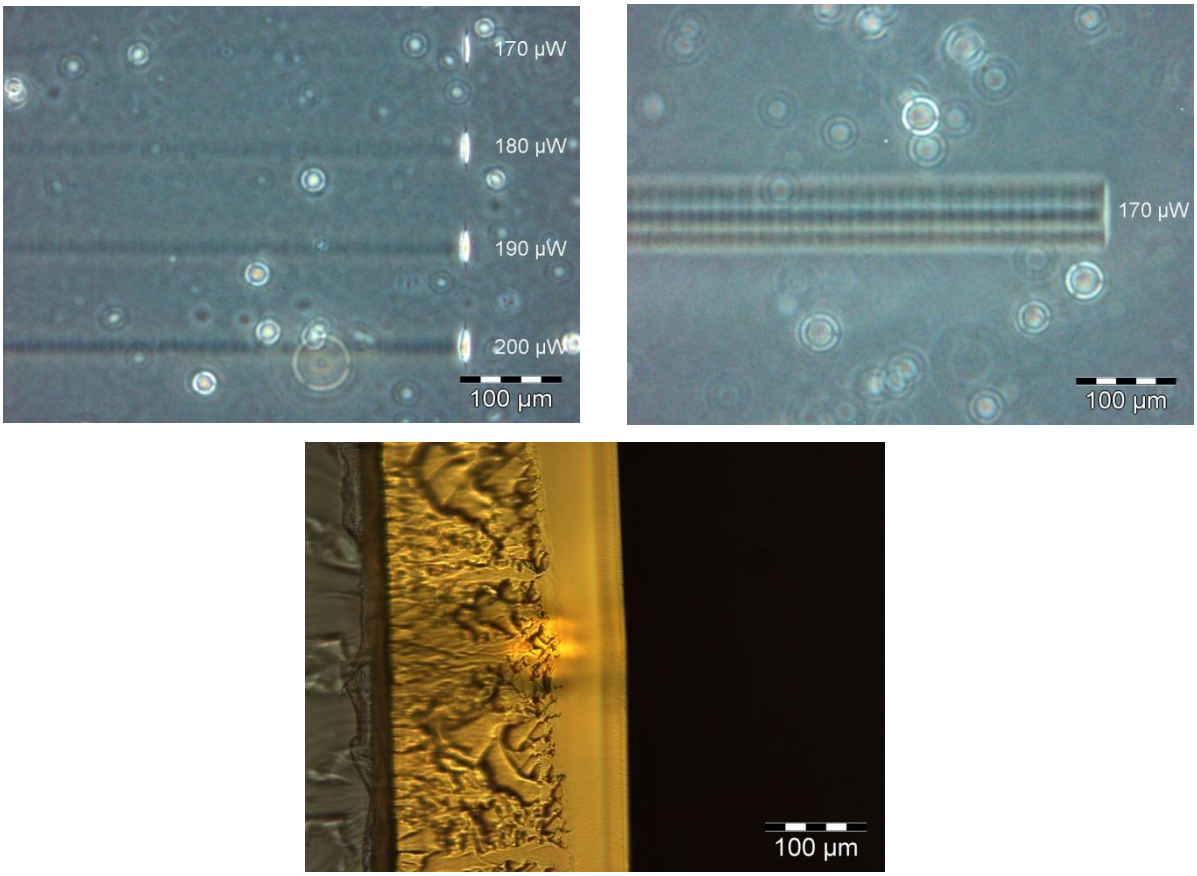

Figure 83: Phase contrast top views and cross-section of waveguide structures fabricated at 4mm/min feed rate inside an epoxy cure silicone rubber containing 40% thiol-ene monomers by means of 0.04% P3K (**2PP/2.9/40c**). Top left: Single waveguide structures written at laser powers from 170 to 200 µW. Top right: 6+1 waveguide bundles processed at 170 µW Bottom: Illuminated cross-section of the waveguide bundles shown in the middle). Triple writing steps were applied.

Compared to formulation **2PP/2.9/40a**, the waveguide cross-section was significantly stronger. But experience has shown that it is very difficult to obtain optical damping values from waveguides of this quality.

3.10 Optical damping & Absorption Behavior

Apart from the optical damping of the 2PP fabricated waveguides, which is the crucial property after all, the damping of the bulk material is also of great interest. Therefore, test bars were produced (for details see Section Materials and Methods) and brought into laser beams. Preliminary damping measurements of the bulk material containing

20% thiol-ene monomers (formulation **PRE/2.9**) gave promising values of 0.4 (850 nm) and 0.6 dB/cm (632 nm). Note that the latter is actually the cladding material as the thiol-ene content of the waveguide core is not known. Analogous measurements of the plain matrix material ECES (formulation **DMTA/2.6**) was very transparent with 0.1 dB/cm (850 nm) and 0.2 dB/cm (632 nm). Unfortunately the problems encountered during thiol-ene-based waveguide structuring inside this material in the previous section did not allow yet to fully exploit this very low bulk damping.

Further common wavelengths for optical data transfer in the telecommunications industry are 1300 and 1550 nm. To get an idea about the suitability of the bulk material for the aforementioned wavelengths an absorption spectrum was taken between 600 and 1600 nm (Figure 84) from a sample also based on the cladding formulation **UV/2.9c/epox** (for details see Section Materials and Methods).

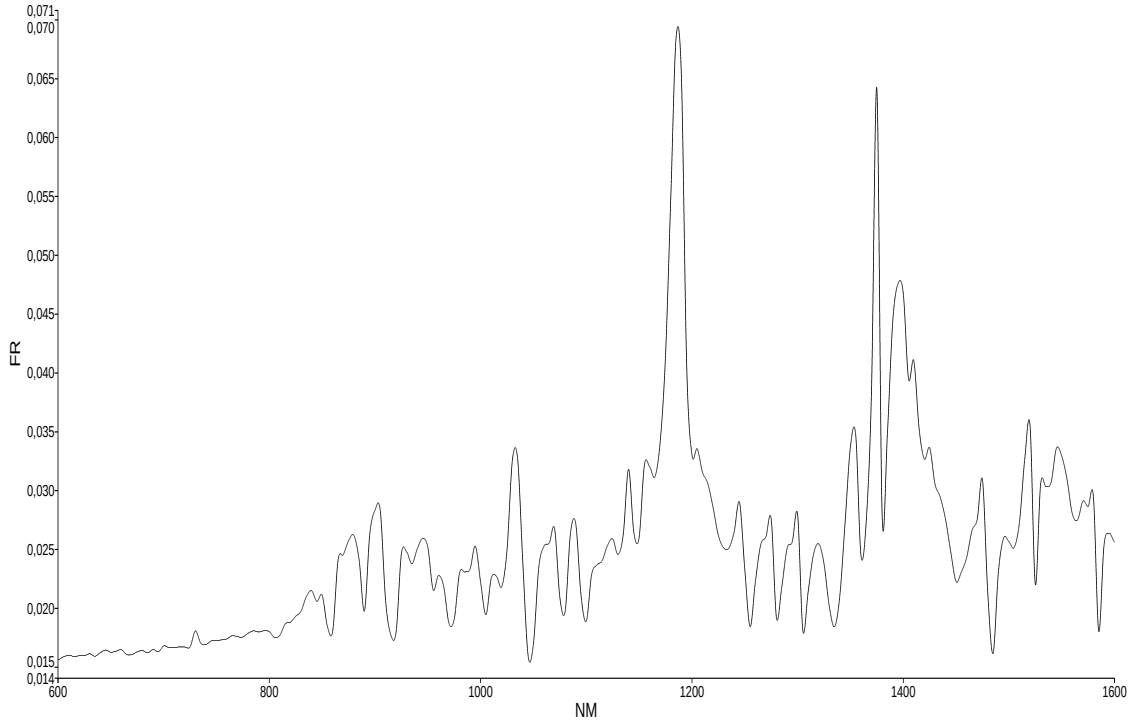

Figure 84: Absorption spectrum waveguide cladding material

As expected, signals from the PDMS domains (see section 1) of the matrix material are observed around 1200 and 1400 nm. In terms of absorption the telecommunication wavelengths 850, 1300 and 1550 nm perform equally well.

Cut-back measurements of waveguides shown in Figure 83(formulation **2PP/2.9/40c**) did not yield any damping values, as the waveguides could not be located. This has probably its reason in insufficient change in refractive indexand diffuse boundaries between waveguide core and cladding. Judging damping measurements of the bulk the difficulty with waveguiding is not attributed to insufficient transparency of the material.

4. 2PP waveguide fabrication inside condensation cured silicone rubbers by curing thiol-ene monomer

4.1 Selection of matrix material

Acetoxy and alkoxy-based condensation cured silicone systems (Figure 85) are not frequently used in photonics applications, but for the highly specialized task of 2PP-based waveguide fabrication they have been relevant because of their orthogonal curing reactivity in the presence of several monomer systems such as acrylates and methacrylates.[82, 96]

In this work, however, PDMS condensation curing was seeked to be applied leading to a new approach: Crosslinkers with several polymerizable functionalities (vinyl, acrylate, mercaptopropyl) are available allowing for the introduction of polymerizable moieties into the matrix material (Figure 85).

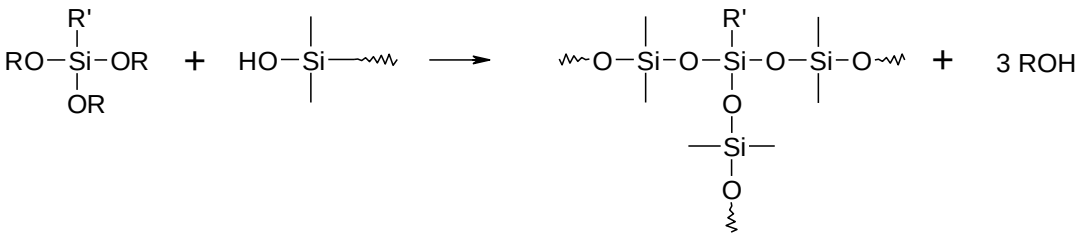

R = acetyl, methyl, ethyl

R‘ = vinyl, mercaptopropyl, acrylate

Figure 85: Using condensation curing chemistry for integration of polymerizable moieties into a PDMS rubber.

As demonstrated for the ORMOCER materials, high performance waveguides can be fabricated, when the two-photon-polymerizable moieties are covalently linked to the

matrix material.[46] Hence, an analogous thiol-ene system was aspired, which featured both mercapto and vinyl functionalities integrated into the matrix material by means of crosslinkers via a condensation mechanism. To put this concept into reality, a silanol terminated PDMS with a molecular weight of 4200 (PDMS 4200) seemed to allow for a good compromise between amount of integrated polymerizable moieties and mechanical flexibility, because for too low molecular weights the PDMS rubber would become too brittle. A corresponding attempt to have mercaptopropyl trimethoxy silane (MPTS) as coreactive crosslinker forming a thiol-ene system with TAVS as the other crosslinker via the alkoxy condensation mechanism failed due to insufficient compatibility of MPTS with the silanol terminated matrix material PDMS 4200 (formulation **PRE/3.1**, Table 13). It might be worthwhile to test an analogous concept via the acetoxy moisture cure mechanism, but a mercaptopropyl-functional acetoxy crosslinker was not commercially available.

Nevertheless, an alternative concept was feasible, where only an ene functionality would be integrated into the matrix PDMS rubber material while having liquid thiol monomer present in the material, the two of which would undergo two-photon-induced thiol-ene reaction yielding a local refractive index change. As mentioned before, PDMS 4200 was a reasonable silicone prepolymer for this purpose. Due to the good experience with acetoxy condensation curing in previous works[82] triacetoxy vinyl silane (TAVS) was tested as an acetoxy crosslinker in formulation **PRE/3.1a** giving a rather transparent PDMS rubber.

By means of a thiol it was thought to be possible to locally increase the refractive index in this vinyl functional material. With the functionality of at least two it would be possible to further crosslink the silicone rubber as discussed in the following section. Also the material concept in question involves a number of formulations, which are given for the whole section 3 in Table 13.

Table 13: Formulations used for acetoxy silicone-based waveguide fabrication given in wt %.

	MPTS	TVMS	TMMD	TAVS	DBTDA	PDMS 4200	R1	Darocur 1173	M2CHK
PRE/3.1	4	4			0.25	91.75			
PRE/3.1a				8	0.25	91.75			
PRE/3.2			10	8	0.25	81.45	0.3		
PRE/3.3		6.6	13.9	9	0.25	70.062		0.188	
UV/3.3/1.4		7.3	16.1	6.6	0.25	69.605		0.145	
UV/3.3/1.2		8.3	15.1	6.6	0.25	69.586		0.164	
UV/3.3/1.0		9.5	13.9	6.6	0.25	69.562		0.188	
UV/3.3/0.8		11.0	12.4	6.6	0.25	69.530		0.220	
UV/3.3/0.6		12.9	10.5	6.6	0.25	69.492		0.258	
DMTA/3.3/ matrix				6.6	0.25	93.15			
RI/3.3		30.63	68.37					1	
2PP/3.3.1		7.1	12.9	9	0.25	69.71	0.04	1	
2PP/3.3.2		9.6	15.4	9	0.25	64.71	0.04	1	
2PP/3.3.3		7.1	12.9	9	0.25	69.71		1	0.04
2PP/3.3.4		9.6	15.4	9	0.25	64.71		1	0.04
2PP/3.3.5		12.1	17.9	9	0.25	59.73		1	0.02
2PP/3.3.6		10	21.5	9	0.25	58.21		1	0.04

Abbreviations: MPTS: Mercaptopropyl trimethoxysilane, TMMD: 1,3-*bis*(3-mercaptopropyl)-1,1,3,3-tetramethyldisiloxane; TVMS: *tris*(vinyldimethylsiloxy)methylsilane, TAVS: Triacetyvinyl silane; DBTDA: dibutyl tin diacetate; R1: E,E-1,4-*bis*[40-(*N,N*-di-nbutylamino)styryl]-2,5-dimethoxybenzene; M2CHK: (2E,6E)-2,6-*bis*(4-(dimethylamino)benzylidene)-4-methylcyclohexanone

4.2 Selection of monomer

After the development of a vinyl functional silicone rubber (formulation **PRE/3.1a**, previous section) it was necessary to find a compatible thiol with a functionality of at least two in order to locally raise the refractive index via two-photon induced thiol-ene crosslinking. For this purpose, it appeared logical to test the siloxane-based dithiol TMMD established in section 3.2. By means of formulation **PRE/3.2** it was shown,

that PDMS 4200 could be moisture-cured in the presence of TMMD suggesting the following fabrication procedure (Figure 86): All ingredients should be initially mixed, and immediately the acetoxy moisture cure would kick in the presence of the monomer. After 2PP processing the unreacted monomer would be either evaporated under high vacuum or UV-flood-cured (taking advantage of the diffusion effect described in section 2 and 3).

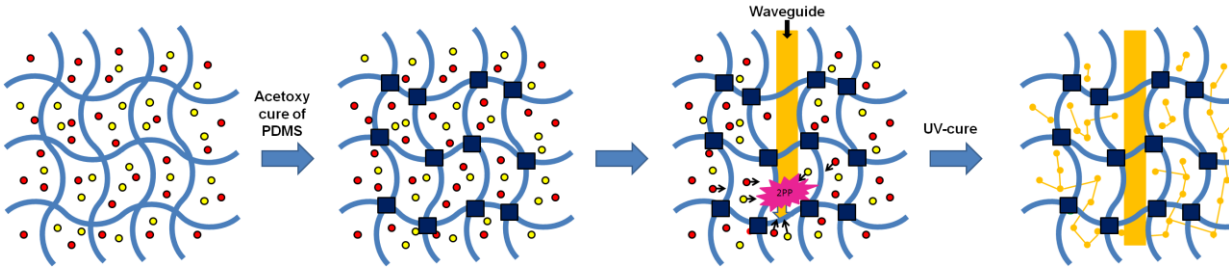

Figure 86: Manufacturing steps of polysiloxane/thiol-ene based waveguides: blue snakelines: polysiloxane-based matrix material: red and yellow dots: photoreactive monomer formulation), dark blue squares: epoxy crosslinks, interconnected orange dots: UV-cured photoreactive monomer formulation.

A preliminary 2PP test of formulation **PRE 3.2** (on the MTW device in Weiz) however, yielded no feasible increase of n despite of the excess of thiol moieties over ene functionalities in this formulation. This was thought to be attributed to an insufficient concentration of ene functionalities.

To help this, the trivinyl siloxane TVMS was implemented into the system in formulation **PRE 3.3**. as it had turned out to be very compatible in section 3. Unsurprisingly TVMS did not interfere with acetoxy moisture-curing of PDMS 4200 in the latter formulation. UV-curing gave a very transparent hybrid material.

Generally, it is unknown, how many molecules of the vinyl-functional acetoxy crosslinker TAVS had really been incorporated into the silicone rubber. The ratio of acetoxy moieties from TAVS to silanol functionalities from PDMS 4200 is approximately 3.5. This means that of the major number of functionalities on the crosslinker has no possibility to undergo condensation with PDMS 4200. The following fates are feasible for TAVS:

- incorporation into the silicone rubber by one, two or three condensation reactions with silanol groups of PDMS 4200
- homocondensation of the TAVS crosslinker

- condensation reaction with the thiol groups of TMMD
- hydrolysis to silanol moieties without subsequent condensation reaction
- evaporation (to a low extent, due to a rather high boiling point of 175°C at 10 mm Hg)
- many combinations of the latter points

Nevertheless 2PP structuring tests were successful and will be further discussed in section 4.7. Before going into detail about the optimization of waveguide fabrication a set of analytical investigations regarding the thiol:ene ratio, the thermal stability of the waveguide materials and other aspects shall be discussed in the following sections.

4.3 Photo-DSC investigations

As mentioned before, the reactivity parameter R_{pmax} and T_{max} as well the DBC are not yet accessible by any means for the real 2PP process in the acetoxy-based samples of question. Thus, again the fast and reliable photo-DSC method was applied to figure out the ideal ratio of thiol and ene moieties for photocuring inside the acetoxy-based silicone rubber.

In contrast to the epoxy-based system (section 3), where vinyl moieties were only attached to the the trivinyl siloxane monomer TVMS, vinyl moieties were provided at the crosslinks of the silicone rubber as well as by the TVMS in case of the system of question. Moreover, it must be mentioned, that probably not the whole amount of crosslinker reacted with silanol groups but underwent condensation reaction with itself or the thiol moieties. Mercapto groups were exclusively featured by the siloxane based dithiol TMMD. The overall ratios of thiol to ene were 1.4, 1.2, 1.0, 0.8 and 0.6 (formulations **UV/3.3/1.4** through **UV/3.3/0.6**). The photo-DSC data is given in Table **14** and visualized in Figure 87 (For calculation methods see Section Materials and Methods).

Table 14: Photo-DSC measurements of thiol-ene photopolymerization inside a acetoxy crosslinked matrix containing vinyl functionalities.

Thiol/Ene Ratio	DBC (%)	R_{pmax} (mol s^{-1} L^{-1})	T_{max} (s)
1.4	79	0.012	25.7
1.2	70	0.018	17.1
1.0	60	0.020	16.9
0.8	46	0.023	14.2
0.6	33	0.024	11.5

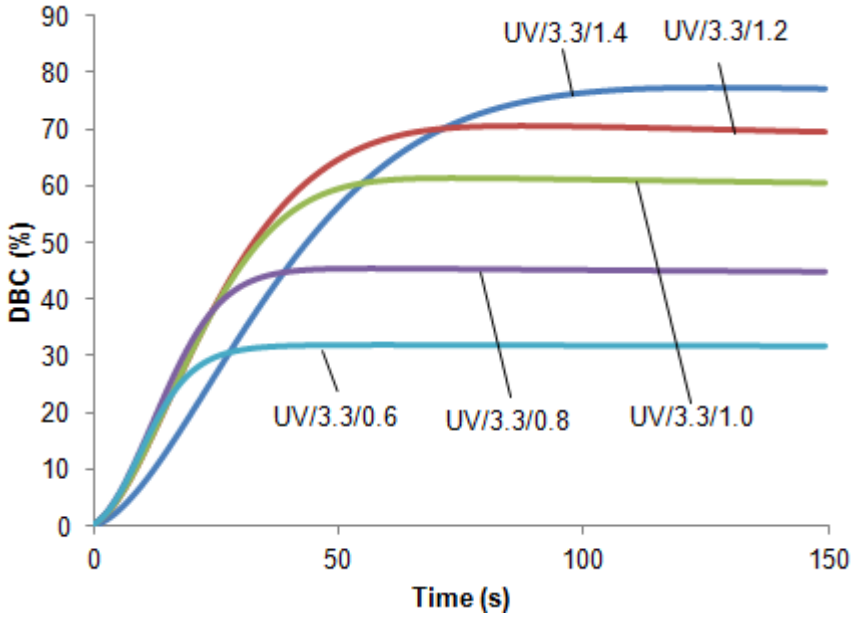

Figure 87: Photo-DSC curves of thiol-ene photopolymerization inside the acetoxy matrix

Compared to the epoxy-based system (section 3), where a monomer content of 40% still allowed for curing of the matrix in the presence of monomer, the acetoxy curing of PDMS 4200 was not possible any more at this monomer concentration, so a monomer content of 25% was applied here. So due to the higher degree of dilution of the photoreactive resin caused by the matrix material R_{pmax} and T_{max} indicate a lower reaction speed than in the epoxy concept in Table 11). The double bond conversion is more than doubled from thiol:ene ratio 0.6 to 1.4, whereas R_{pmax} is almost halved. As discussed section 3.4, this can be explained by the propagation step playing the rate limiting role in this thiol-ene reaction making the double-bond concentration crucial for the overall reaction rate. The different behavior in terms of DBC compared to the epoxy-based concept might result from the fact that in the system of question

vinyl moieties integrated in the acetoxy-cured silicone rubber participate in the thiol-ene reaction and modify the polymerization kinetics.

Due to the opposite trends of DBC and R_p, which are both important to the performance in 2PP waveguide fabrication, additional arguments had to be taken into account to decide on the thiol:ene ratio in corresponding 2PP experiments:

The tendency of thiol-ene systems to form less dense networks with increasing thiol content enables faster diffusion of thiol-ene monomers into the waveguide core region and a more pronounced enrichment of high refractive material. Another advantage of systems rich in thiol is the higher amount of sulfur atoms incorporated into a mercapto-terminated photopolymer. Thus it seemed reasonable to prefer systems with an thiol excess.

4.4 DMTA tests

Unlike the silicone polyetheracrylate–based concept discussed above and like the epoxy-based material in section 3, the elastomer in question does not contain any acrylate or ester bonds, which was a central consideration for the design of this silicone/thiol-ene hybrid material in terms of thermal stability with regard to heat exposure during the industrial printed circuit board fabrication. Analogously to the materials discussed above, DMTA measurements were carried out to verify the thermal stability. As in the previous section it had turned out, that a thiol excess with respect to vinyl moieties is favorable, formulation **UV/3.3/1.4** was of central interest regarding thermal stability. To see, how the interpenetrating thiol-ene network influenced the mechanical behavior of the acetoxy-cured matrix material, also test bars of the pure matrix material (formulation **DMTA/3.3/matrix**) were exposed to the temperature ramp from -140°C to 300°C. The corresponding curves are shown in Figure 88.

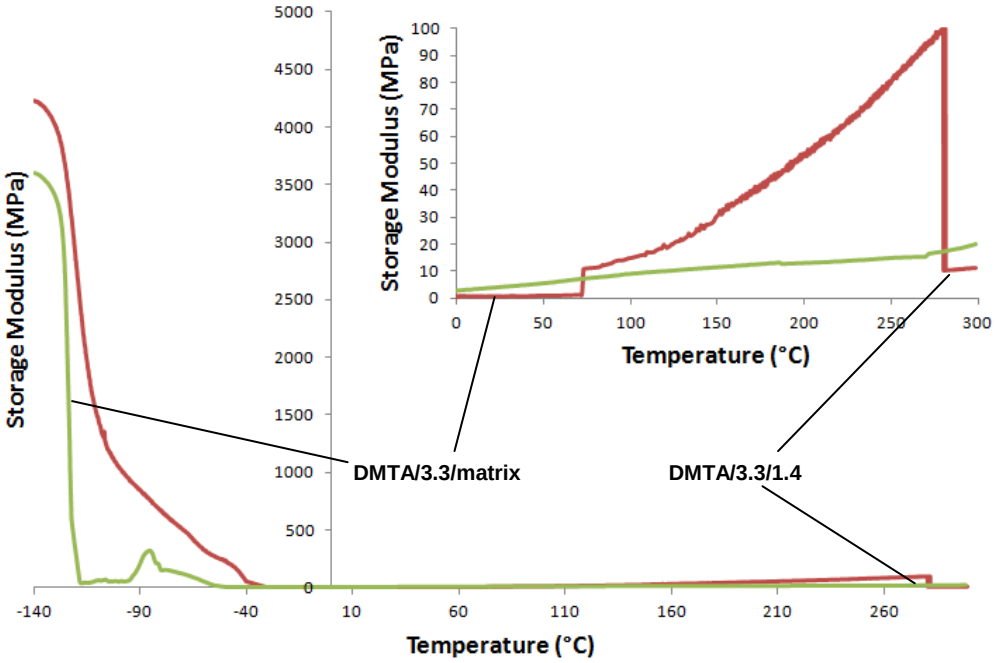

Figure 88: Testing of the mechanical stability via DMTA

The plain matrix material (formulation **DMTA/3.3/matrix**) underwent a rather sharp glass transition reaching very low storage moduli at around -120°C. Inhomogeneities coming from the moisture cure are thought to have caused an intermediate peak around -90°C. The material exhibits a very low storage modulus without any failure until 300°C.

The glass transition of the corresponding cladding material **DMTA/3.3/1.4** was very broad. The cause for the sudden increase in storage modulus at approximately 70°C is unknown. Subsequently the material undergoes a pronounced increase, which can be explained by thermal polymerization of unreacted monomer in the material. Thus the applicability for the industrial fabrication at 250°C could be proven as no sudden change in storage modulus was observed until 280°C, where a sudden drop was detected indicating failure of the test bar.

After the thermal treatment the material had a rather dark brown color which is attributed to the coloring due to the PIs. This is highly undesirable and subject to future optimization of the material.

4.5 Refractive Index

As mentioned above, there was no method on hand to determine the distribution of n within the 2PP-illuminated waveguide core volumes, where high refractive thiol-ene network was present in a higher concentration than in the surroundings. Thus, analogously to the previous concept, the n of the cladding material was measured by means of an Abbé refractometer (Table 15).

Table 15: Relevant n values from the 2PP formulations

Sample	n
TMMD	1.476
TVMS	1.417
TMMD/TVMS uncured (formulation **RI/3.3**)	1.458
TMMD/TVMS cured (formulation **RI/3.3**	1.489
Acetoxy cured matrix material (formulation **DMTA/3.3/matrix**)	1.410
Cured hybrid material of acetoxy matrix and photocured TMMD/TVMS (formulation **UV/3.3/1.4**)	1.423

The uncured formulation **RI/3.3** (with a thiol to ene ratio of 1.4) fits well the expectation deducted from the weighted RIs of TMMD and TVMS (1.4576). The crosslinking upon UV-curing boosts the refractive index by 0.031. The thiol-ene content in **UV/3.3/1.4** causes an increase in refractive indexby 0.013 compared to the pure matrix material **DMTA/3.3/matrix**. The maximum value for n in the waveguide core must have a value between 1.423 and 1.489 due to the enrichment of high refractive thiol-ene material in the VOXEL.

4.6 2PP writing

In combination with the high refractive siloxane-based dithiol TMMD and the trivinyl siloxane TVMS a highly transparent, thermally stable hybrid material could be formed. After the promising results in the analytics chapter above, 2PP writing tests were the next step towards waveguiding.

After mixing the formulations thoroughly, films of approximately 200 µm were draw-casted and cured within 30 minutes. The formulations in the following contain more acetoxy crosslinker TAVS (Si-OH : Si-O-Ac 3.5-4.2, depending on the monomer content, see Table 13), as the 2PP structuring tests were carried out in clean room in

Weiz with a lower level of air moisture. After 2PP processing, the samples were UV-cured (for more details, see Section Materials and Methods). As TPI R1 from the Marder group was chosen as it allows for performing 2PP at comparably low laser powers.

The already mentioned enrichment effect due to diffusion during 2PP into the VOXEL and/or swelling of the waveguide material can be made use of more effectively – as learned from the epoxy concept - when the waveguide is written several times back and forth as it was carried out.

The first 2PP structuring test (prior to the photo-DSC investigations) was carried out using 20% monomer content (formulation **2PP/3.3.1**, ratio thiol:ene 1:1, see Figure 89). The concentration of R1 had to be as low as 0.04% due to solubility problems.

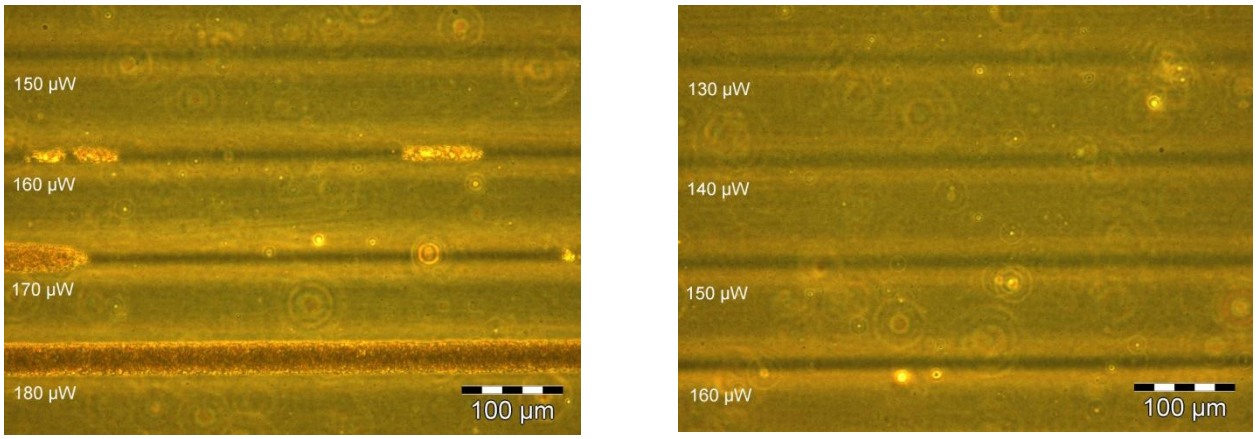

Figure 89: Thiol-ene based waveguide structures written into five times into a acetoxy cured silicone rubber containing 20% (formulation **2PP/3.3.1**, left, 150–180 µW) and 25% (formulation **2PP/3.3.2**, right, 130–160 µW) monomer.

A structuring window with rather good phase contrast was revealed around 170 µW at a feed rate of 10 mm/min (2 mm/min when considering the five-fold writing process), which is more than double the speed of the epoxy-based material, where also TMMD and TVMS were used as monomers. The feed rate was 10 mm/min for all following 2PP experiments. This acceleration with respect to the epoxy system is especially interesting, because the monomer concentration in the epoxy-based system (section 3) is higher. This acceleration could be explained by the participation of the PDMS backbone in the thiol-ene reaction, allowing for the gel point to be reached faster and thus speeding up the crosslinkage. The acetoxy-based waveguides at 20% monomer content, however, exhibited burned spots. Due to this, the monomer content was raised to 25% (formulation **2PP/3.3.2**, ratio thiol:ene 1:1)

giving the best phase contrast without any burns at 160 µW at the aforementioned feed rate. Beyond these qualitative comparisons, it would be desireable to quantify the performance by either the local change in n, the double bond conversion inside the tiny waveguide core or ideally the optical damping.

As shown in Figure 89, R1 is in fact able to initiate two-photon-induced thiol-ene polymerization. The synthesis of this TPI, however, is rather elaborate, so ((2E,6E)-2,6-)*bis*(4-(dimethylamino)benzylidene)-4-methylcyclohexanone (M2CHK), which is produced in a single-step reaction, was also tested:[97]

M2CHK suffered from a low solubility limit around 0.04%. A few M2CHK crystallites precipated in the course of the acetoxy matrix cure in formulation **2PP/3.3.4**, which has the same monomer concentration and thiol:ene ratio as formulation **2PP/3.3.2**. (see Figure 90). The performance with this easier accessible TPI was comparable with **2PP/3.3.2** in Figure 89.

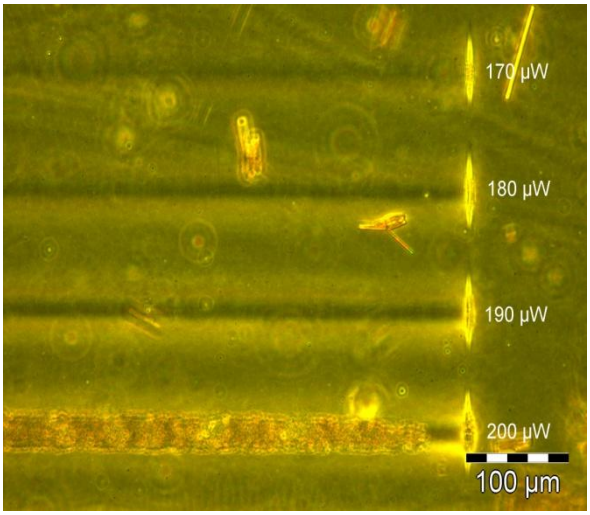

Figure 90: Thiol-ene based waveguide structures written five times in an acetoxy cured matrix material (formulation **2PP/3.3.4**) with the TPI M2CHK at 10 mm/s laser feed rate and 170 to 190 µW laser power.

Increasing the monomer content to 30% still allowed for acetoxy curing (formulation **2PP/3.3.5**). Added at a concentration of 0.02% no precipitation of M2CHK upon acetoxy curing was observed (Figure 91). Comparatively strong changes in refractive index were achieved here in the range of 150 to 170 µW.

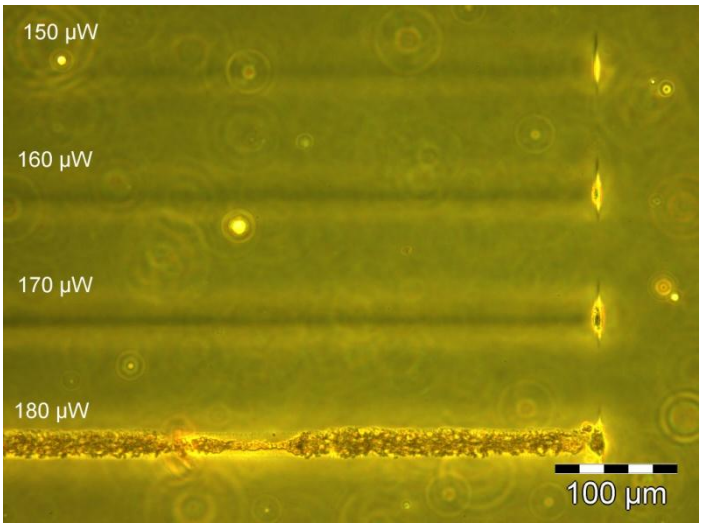

Figure 91: Thiol-ene based waveguide structures written five times in an acetoxy cured matrix material (formulation **2PP/3.3.5**, 30% monomer content) with the TPI M2CHK at 10 mm/s laser feed rate and 170 to 190 µW laser power.

Above this monomer content, problems with matrix curing arose. According to photo-DSC results a thiol ratio is beneficial for the DBC explaining the good results at a ratio of thiol:ene moieties 1.5 for in case of formulation **2PP/3.3.6** in Figure 92.

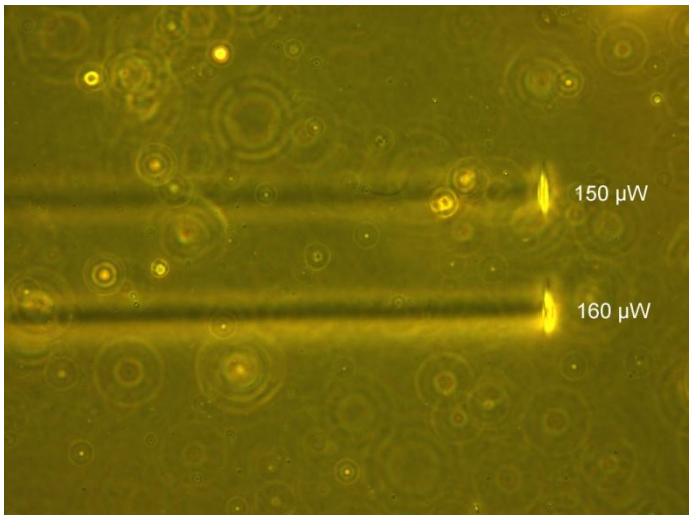

Figure 92: Thiol-ene based waveguide structures written five times in an acetoxy cured matrix material (formulation 2PP/3.3.6, 31.5% monomer content) with the TPI M2CHK at 10 mm/s laser feed rate and 170 to 190 µW laser power.

4.7 Waveguiding

As discussed previously, a useful qualitative test for the ability of waveguides to guide light is to couple in white light by means of a microscope and observe the brightness of the illuminated waveguide cross-sections. As shown in Figure 93, the proof of principle for waveguiding was achieved by coupling light into waveguides fabricated with formulation **2PP/3.3.4** (top view in **Figure 90,** section 4.7). The best phase contrast had been achieved for 170 µW, so with this laser power a 6+1 waveguide bundle was written and white light was coupled in (Figure 93, right). In this case the discrete waveguides cannot be identified as the waveguide boundaries are rather diffuse.

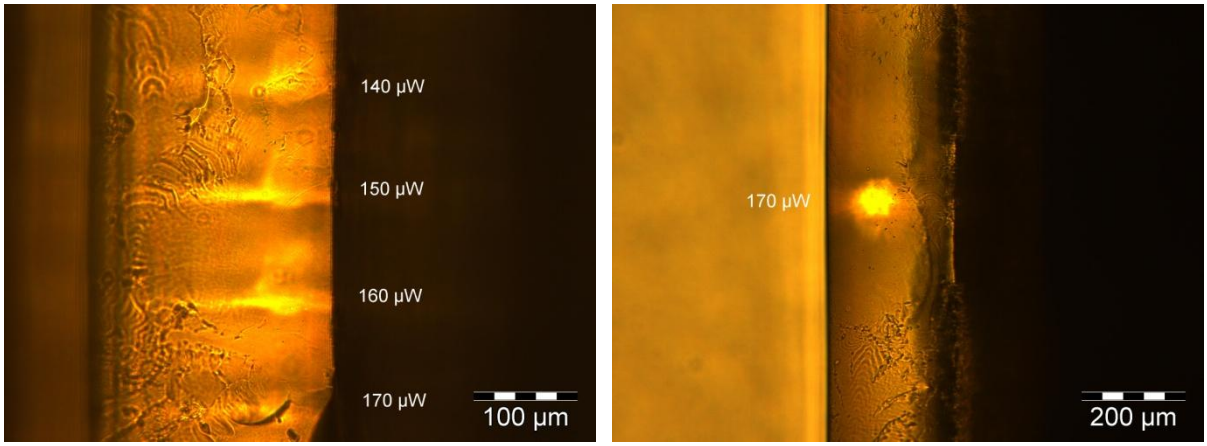

Figure 93: Illuminated cross-section of thiol-ene based optical waveguides on the basis of formulation **2PP/3.3.4**. Left: Single waveguides written at 140-170 µW laser power. Right: 6+1 waveguide bundle written at 170 µW.

When adjusting the ratio of thiol:ene moieties to 1.5 and raising the monomer content to 30% (formulation **2PP/3.3.6**) even better white-light waveguiding was observed (Figure 94, left). By adjusting the shape of the VOXEL another improvement in terms of waveguiding was observed (Figure 94, right). This was limited by the undesired lengthening of the waveguide cross-section.

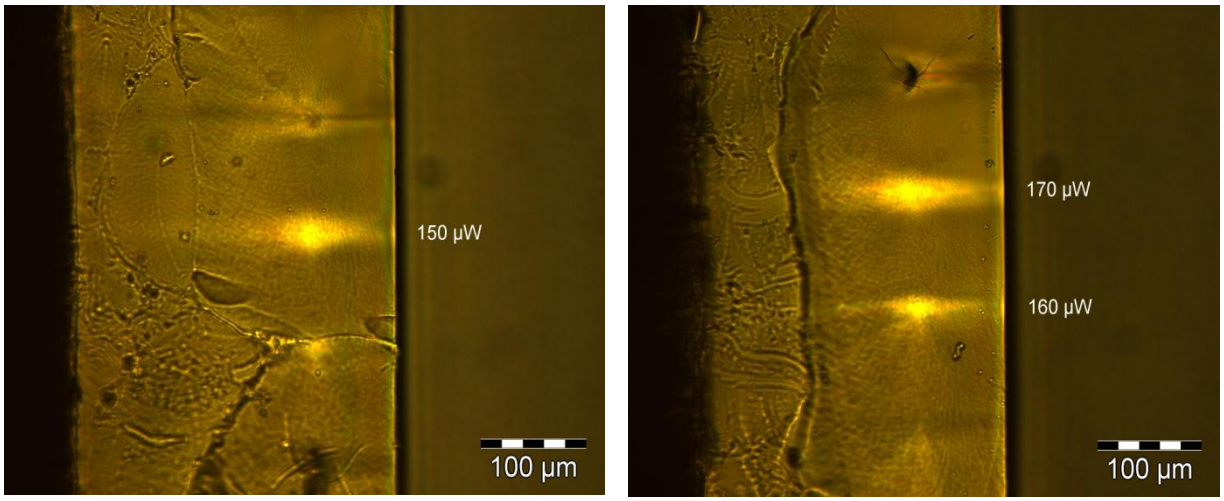

Figure 94: Illuminated cross-section of polysiloxane-based optical waveguides with 30% thiol-ene monomers written at a feed rate of 10 mm five times over the waveguide volume at 150 (left), 160 and 170 µW (right) and with 0.02% M2CHK 30% monomer content.

So far in this work, the post-processing of 2PP-processed samples with inscribed waveguides had been UV-curing. In another waveguiding attempt with formulation **2PP/3.3.6**, this UV-curing step was substituted by overnight evaporating of excess monomer (Figure 95). According to gravimetry, half of the monomer could be evaporated. The slight improvement of waveguide cross-section brightness, however, did not compensate for the time-consuming evaporation.

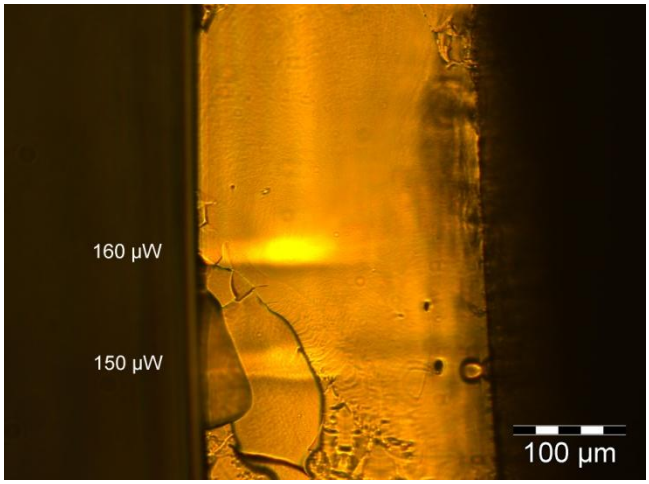

Figure 95: Illuminated cross-section of polysiloxane-based optical waveguides. Formulation was identic to Figure 94. The post-processing was evaporation in high vacuum instead of UV curing as in Figure 94

Summing up, the preliminary waveguiding results with the acetoxy-based materials of question were somewhat more promising than the epoxy concept in section 3. Also higher feed rates were possible.

4.8 Optical damping & absorption behavior

After detailed analytics and optimization of 2PP waveguide fabrication in the acetoxy formulations of question, the actual optical damping of the waveguides was of central interest.
Cut-back measurements of waveguides inscribed in formulation **2PP/3.3.6** in Figure 90 (formulation **2PP/3.3.4**) did not yield any damping values, as the waveguides-cross-section could not be located. This has probably its reason in insufficient change in refractive indexand diffuse boundaries between waveguide core and cladding. Further attempts would be worthwile with the same formulations, because the corresponding preliminary coupling-in test with white light in section 3.9 were rather promising.

An important cause for optical damping is the absorption by the material. Common infrared wavelengths for optical data transfer in the telecommunications industry are 850, 1300 and 1550 nm. The absorption behavior at these standard wavelengths is easily accessible by NIR-spectroscopy (for details, see Section Materials and Methods).To get an idea about the suitability of the material for the aforementioned wavelengths an absorption spectrum was taken between 600 and 1600 nm (Figure 96) from a sample based on formulation **UV/3.3/1.4**, as in the photo-DSC section 4.3 it had turned out, that an excess of mercapto moieties is favorable for waveguide fabrication.

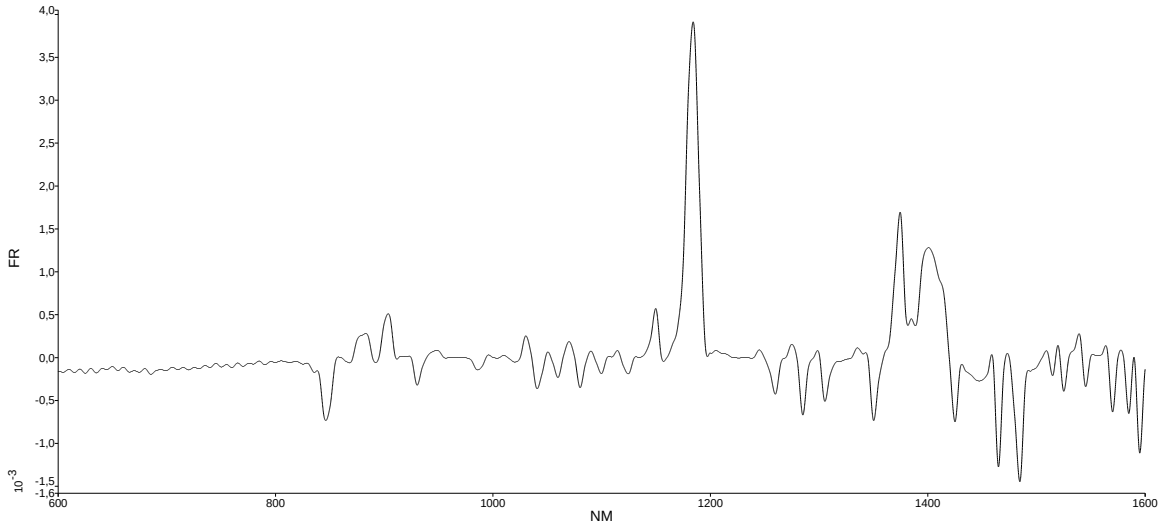

Figure 96: Absorption spectrum of acetoxy-based waveguide cladding material

As expected, signals from the PDMS domains of the matrix material are observed around 1200 and 1400 nm (Figure 41) In terms of absorption the telecommunication wavelengths 850, 1300 and 1550 nm perform equally well. The absorption is generally lower than in the materials discussed in section 2 and 3.

Experimental Part

2. 2PP Waveguide fabrication from a polysiloxane-base thixotropic liquid

2.1 General remarks on formulation

The formulation work was carried out under yellow light due to the photoreactivity of the one-photon-initiator Darocur 1173. The low one-photon-reactivity of the one-photon-initiator B3FL could be neglected. In the following the procedure and sequence to obtain a pourable formulation is described: The exact weighed in masses are given in the following chapters. The first task of formulating was the dissolution of the TPI B3FL in the triacrylic monomer TTA (if required for the formulation), which was possible either by adding the initiator in a trace of toluene or by keeping it for a few hours in an ultrasonic bath at 30°C. This solution could be stored as a stock solution for several experiments. For the waveguide formulation firstly the rheology additive was weighed in, subsequently the matrix material TEGO RAD 2200N and finally the TTA and the one-photon-initiator Darocur 1173. It was necessary to add the rheology additive with TEGO RAD 2200N first for the sake of homogeneity. Pure TTA would undergo significant interaction with BYK E 410 already during the weighing-in making it impossible to obtain a homogeneous mixture. In the final step Darocur 1173 was added. After addition of each component the formulation was vigorously mixed by tapping on the vial. After the addition of Darocur 1173 the formulation was vigorously stirred by means of a spatula causing the formation of foam. In a subsequent degassing step, the vial was placed inside an exsiccator linked to a high vacuum pump for 20 minutes. In the course of the degassing even more foam formed making it inevitable to spill a certain amount of formulation, which could be limited by using a comparatively voluminous vessel. Typically, for a 1 or 2 g batch a 5 mL beaker was applied to give the foam bubbles the possibility to decompose without having too much formulation spilt.

2.3 Photo-DSC investigations

Photo-DSC experiments were carried out and evaluated as demonstrated in section Materials and Methods. For the calculation of the rate of polymerization R_{pmax}, ρ was approximated by considering the contributions of the monomer TTA (1100 g L^{-1}), the matrix material TEGO RAD 2200N (assumed 970 g L^{-1}) and the PI Darocur 1173 (1080 g L^{-1}) according to the formulation. For this thixotropy-based system the theoretical heat of polymerization $\Delta H_{0,p}$ for one acrylate group was assumed as 78 kJ mol^{-1}. While the concentration of acrylate moieties stemming from TTA was known, the concentration of acrylate moieties belonging to the matrix material was determined via the following way. Defined amounts of toluene and TEGO RAD 2200N were weighed into an NMR tube and dissolved in $CDCl_3$. ^1H NMR gave olefine signals between 5.7 and 6.5 and the methyl signal of toluene was found at 2.3. The ratio of the peak integrals allowed for calculating the concentration of acrylic moieties in TEGO RAD 2200N (0.52 mmol g^{-1}). Thus, the amount of acrylic units in the resin c_{DB} was determined by adding the latter to the amount of TTA acrylic units.
The three properties of interest T_{max}, R_{pmax} and DBC were calculated the following way: T_{max} was straightforwardly determined by substracting the time of onset from the time until the exothermic peak maximum. Equation 4 shows the calculation method for R_{pmax}, where the height of the photo-DSC peak maximum *h*, the density of the resin ρ and the theoretical heat of polymerization $\Delta H_{0,P,}$ (J mol^{-1}) were required.

$$R_{pmax} = \frac{h\,\rho}{\Delta H_{0,P}} \qquad \textbf{Equation 4}$$

DBC was calculated by the following equation 5 additionally requiring the concentration of acrylic groups (mol g^{-1}) and the actual heat of polymerization ΔH_P (J g^{-1}).

$$DBC = \frac{\Delta H_P}{c_{DB}\,\Delta H_{0,P}} \qquad \textbf{Equation 5}$$

Masses for the formulations are given in Table 16.

Table 16: Masses of the photo-DSC acrylic-based formulation

	TTA (mg)	Darocur 1173 (mg)	TEGO RAD 2200N (mg)	c_{DB} (mmol)
UV/1.4/0		4	196	0.52
UV/1.4/10	20	4	176	1.48
UV/1.4/20	40	4	156	2.44
UV/1.4/30	60	4	136	3.40

As $\Delta H_{0,P}$ for formulations containing the tetrathiol TT (see Table 17 for masses) was not known, exclusively T_{max} could be determined (see General Part).

Table 17: Masses of the photo-DSC acrylic-based formulation containing the tetrathiol TT

	TTA (mg)	TT (mg)	Darocur 1173	TEGO RAD 2200N
UV/1.5/1:10	20	2,4	2	75,6
UV/1.5/4:6	20	14	2	64

2.5 DMTA

DMTA measurements were carried out as mentioned in the section Materials and Methods. The masses for producing the test bars are given in Table 18.

Table 18: Masses of acrylate-based formulations applied for DMTA

	TTA (mg)	TT (mg)	Darocur 1173 (mg)	TEGO RAD 2200N (mg)	BYK E 410 (mg)
DMTA/1.4/0			20	960	20
DMTA/1.4/20	200		20	760	20
DMTA/1.4/30	300		20	660	20
DMTA/1.5/4:6	200	140	20	620	20
DMTA/1.5/1:10	200	24	20	736	20

2.6 Refractive Index

Samples for measurements of n were carried out with the formulations **UV/1.4/0**, **UV/1.4/20**, **UV/1.5/1:10** and **UV/1.5/4:6** (section 2.4). The materials were removed from the Al-crucibles and n was determined as mentioned in section Materials and Methods.

2.7 Rheological Propertie

A MCR 300 device from Physica was applied to investigate the rheology of the formulations shown in Table 19.

Table 19 : Masses of acrylate-based formulations applied for Rheometry

	TTA (mg)	TEGO RAD 2200N (mg)	BYK E410 (mg)
Rheo1/1.4/10	100	890	10
Rheo1/1.4/30	300	690	10
Rheo2/1.4/20	200	780	20
Rheo3/1.4/10	100	870	30
Rheo3/1.4/30	300	670	30

For these measurements a CP25-1 cone (diameter = 24.980 mm, angle = 1.012°) was applied. All investigations were carried out with degassed formulations at 20°C. For the monitoring of the development of thixotropy over 70 h, the following procedure was carried out: The formulations were rotationally sheared at a shear rate of $d\gamma/dt$ = 200 1 s^{-1} for 20 min to destroy BYK E 410-based aggregates so as to obtain a value for shear stress at theoretically no thixotropy. Subsequently, marginal oscillations of the stamp at a gamma amplitude of 1% and an angular frequency of 10 rad/s allowed to follow the formation of the thixotropy over 70 h by measuring the shear stress assuming that the slight oscillation would not greatly influence this process. The dependence of thixotropy on the concentration of the rheology additive and the monomer content was investigated by the following procedure: After high rotational shearing at a rate of $d\gamma/dt$ = 200 1 s^{-1} for 20 min to account for unequal periods for weighing-in and unequal mixing, the sample was left for 5 hours for thixotropy to partially build up, which is a reasonable time for an industrial process. Subsequently, the shear stress of each sample was determined by the previously mentioned parameters to monitor the thixotropy.

2.8 2PP writing

The mixtures from Table 20 (for remarks regarding formulations see beginning of Experimental Part) were degassed at high vacuum, so as to remove the foam formed upon mixing. Subsequently, the formulations were draw-casted into molds made of

adhesive tape on top of a glass slide yielding a film of approximately 200 µm by means of an object slide or tip of a pasteur pipette. Air bubbles, which could not be removed in vacuum were eliminated from the film by carefully pushing them out of the basin formed by the tapes with the help of an object slide. They were stored overnight in the dark to gain thixotropy. The 2PP processing and post-processing were conducted as described in section Materials and Methods.

Table 20: Masses of acrylate-based formulations applied for 2PP writing

	DPGDA (mg)	EGDMA (mg)	DOD (mg)	TTA (mg)	TT (mg)	B3FL (mg)	Darocur 1173 (mg)	TEGO RAD 2200N (mg)	BYK E 410 (mg)
2PP/1.1	110		82			8	20	750	30
2PP/1.1/2:3	128		64			8	20	750	30
2PP/1.1/1:10	179		13			8	20	750	30
2PP/1.2		110	82			8	20	750	30
2PP/1.3			75	122		1	20	752	30
2PP/1.4/20				20		0.1	20	749	30
2PP/1.4/20a				20		0.1	20	759	20
2PP/1.4/20b				20		0.1	20	764	15
2PP/1.5/4:6				20	160	0.1	20	592	30
2PP/1.5/1:10				20	24	0.1	20	728	30
WG/1.4/20				199		0.1	20	760	25

2.9 Waveguiding

The procedure to obtain illuminated cross-sections from 2PP fabricated waveguides is shown in section Materials and Methods. Table 19 gives the formulation, which the materials are based on.

Table 21: Masses for formulating **WG/1.4/20**

	TTA (mg)	B3FL (mg)	Darocur 1173 (mg)	TEGO RAD 2200N (mg)	BYK E 410 (mg)
WG/1.4/20	199	0.1	20	760	25

Structuring parameters (laser power, feed rate) enabling high quality waveguide cross-sections were used for waveguide fabrication on printed circuit board demonstrators provided by AT&S (Figure 97). Formulation **WG/1.4/20** was draw casted carefully into the deepening of the circuit board avoiding physical contact with neither the laser diode nor the photo diode, which were embedded by the draw-casted formulation. The distance between photo and laser diode was 7cm. To enhance the probability for successful coupling in, a 6+1 waveguide bundle in hexagonal arrangement was produced.

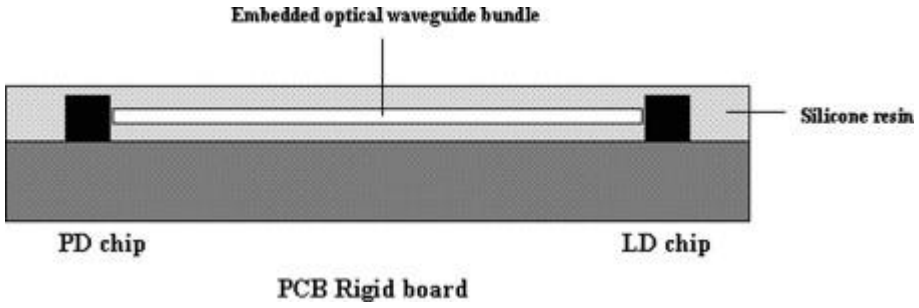

Figure 97: Printed circuit board with interconnected photo diode and laser diode[77]

2.10 Optical damping & Absorption Behavior

Optical damping of the bulk materials:

The procedures for measuring absorption measurements and the optical damping of the bulk material are described in the section Materials and Methods. Table 28 gives the formulations.

Table 22: Masses of acrylate-based formulations applied for bulk optical damping measurements

Formulation	TTA	Darocur 1173	TEGO RAD 2200N	BYK E 410
UV/1.4/0	0	20	980	
UV/1.4/20/BYK	200	20	755	25

The results of these preliminary optical damping results are summarized in the following Table 23:

Table 23: Results from preliminary bulk damping measurements

	Wavelength (nm)	Length of test bar (cm)	Refractive Index assumed for calculation	Radiation power with sample (µW)	Radiation power without sample (µW)	Optical damping (dB cm^{-1})
UV/1.4/0	632	4,1	1.5	1700	2200	0,2
	850	4,1	1.5	780	1040	0,2
UV/1.4/20/BYK	632	1	1.5	1000	2350	3,4
	850	1	1.5	600	1040	2,0
	632	5	1.5	130	2200	2,4
	850	5	1.5	170	1040	1,5

Optical damping of 2PP fabricated waveguides:

Based on formulation **WG/1.4/20** and the composition given in Table 24, waveguides of 3 cm length were inscribed by means of the MTS device (see Materials and Methods) in a depth of 125 µm with a spacing of 125 µm.

Table 24: Masses for formulations for optical damping measurements of waveguides

	TTA (mg)	B3FL (mg)	Darocur 1173 (mg)	TEGO RAD 2200N (mg)	BYK E 410 (mg)
WG/1.4/20	199	0.1	20	760	25

The applied laser powers were 0.10, 0.11, 0.12, 0.13, 0.14 and 0.15 mW. The UV-

curing of the thixotropic sample is described in section materials and methods. The waveguide at the power of 0.11 mW allowed for a cut-back measurement (carried out by Nicole Galler, KFU Graz) yielding a value of 3 dB/cm at 633 nm. In an equivalent sample the transmission of the waveguide written at 0.12 mW could be successfully measured: Assuming a coupling-in efficiency of 100%, the optical attenuation was 2.38 dB/cm at 850 nm. The real value is surely lower, as a coupling-in efficiency of 100% can never be reached.

VIS/NIR absorption measurements:

For the absorption measurements, a material based on the formulation WG/1.4/20 was used, the preparation of which is described in section 2.9.

3. 2PP waveguide fabrication inside epoxy silicone rubbers by curing thiol-ene monomer

3.1/3.2 Formulation remarks

The formulation work was carried out under yellow light due to the one-photon reactivity of the TPI R1 and also Darocur 1173. After addition of each component the formulation was vigorously mixed by tapping on the vial. Initially the inhibitor pyrogallol was mixed with the siloxane-based dithiol TMMD so as to exclude thermally induced thiol-ene reaction via the radical or the Michael mechanism. After adding the trivinyl siloxane TVMS, the acid catalyst TFA was added. Adding TFA after the matrix material ECES resulted in rapid, inhomogeneous epoxy curing of the latter. Thus TFA was diluted in the monomer formulation followed by the addition of ECES, which could then be cured homogeneously in the course of a few minutes. Degassing was carried out quickly in an exsiccator under a pressure of 10 mbar for approximately 30 seconds.

3.3 Monomer synthesis

TMMD:

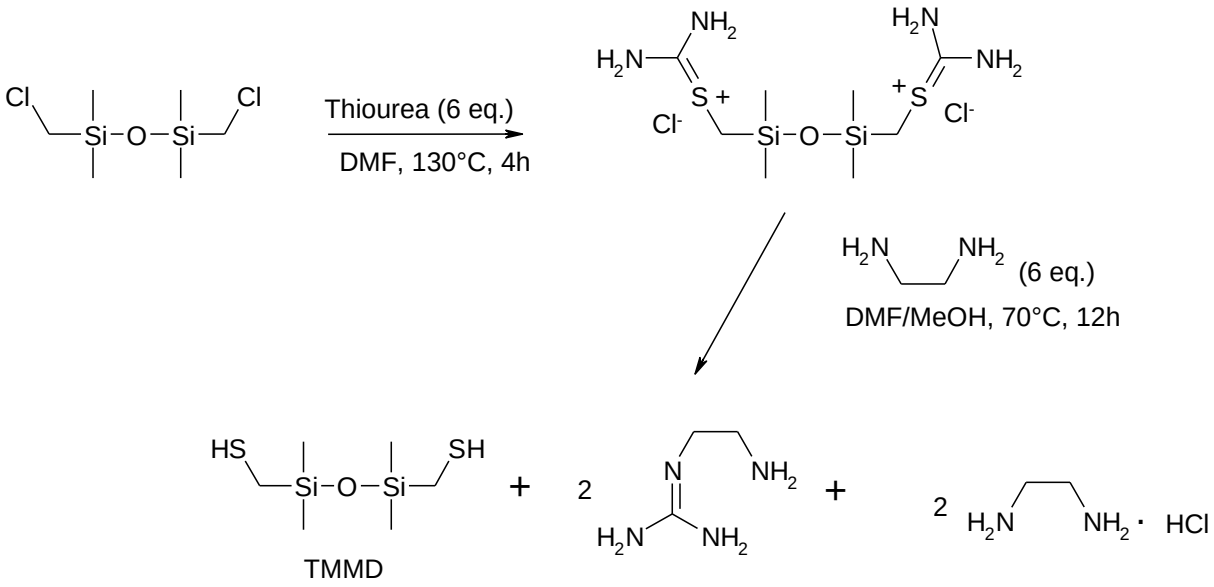

Figure 98: Synthesis of TMMD

Table 25: Chemicals applied for the synthesis of the dithiol TMMD

	Mass (g)	Amount (mmol)	Equivalents
1,3-bis(chloromethyl)-1,1,3,3-tetramethyldisiloxane	25	108	1
Thiourea	49.3	648	6
Dimethyl formamide (solvent)	214		
Ethylene diamine	39.0	648	6
Methanol (solvent)	31		
Water	225		

TMMD was synthesized by a procedure (Figure 98) derived from that proposed by Mogi.[93] The applied masses are given in

Table **25**. Therefore, 1,3-bis(chloromethyl)-1,1,3,3-tetramethyldisiloxane and thiourea were dissolved in DMF under nitrogen atmosphere and stirring. The solution was heated to 120°C and stirred at this temperature for 5 hours. Subsequently, the reation mixture was cooled to 60°C by means of an ice bath and a mixture of ethylene diamine and methanol was added dropwise over a period of 10 min. The reaction solution was stirred at 60°C overnight. After adding of water, the reaction mixture was extracted with three volumes of *n*-hexane and dried with sodium sulfate. From the combined organic phases the solvent was distilled off followed by vacuum distillation at 3 mbar in a range of 75 to 95°C. Column chromatography (Rf: 0.38, PE) yielded 4.9 g (20%) of a colorless liquid. n = 1.476. GC-MS data is given in Table 26.

Table 26: GC-MS investigation of TMMD

Retention Time	Relative abundance	m/z
7.66	90	226 (M^+), 181 (,HS-CH_2-$(CH_3)_2$Si-O-Si-$(CH_3)_2^+$) 163, 149, 135, 119, 91, 75, 59
9.97	3	298, 283, 237, 221, 207, 193, 163, 133, 115, 73
10.33	7	503, 414, 399, 380, 340, 324, 281, 221

Figure 99 shows the NMR spectrum of the purified TMMD exhibiting unknown impurities as indicated by the peaks below 0 ppm.

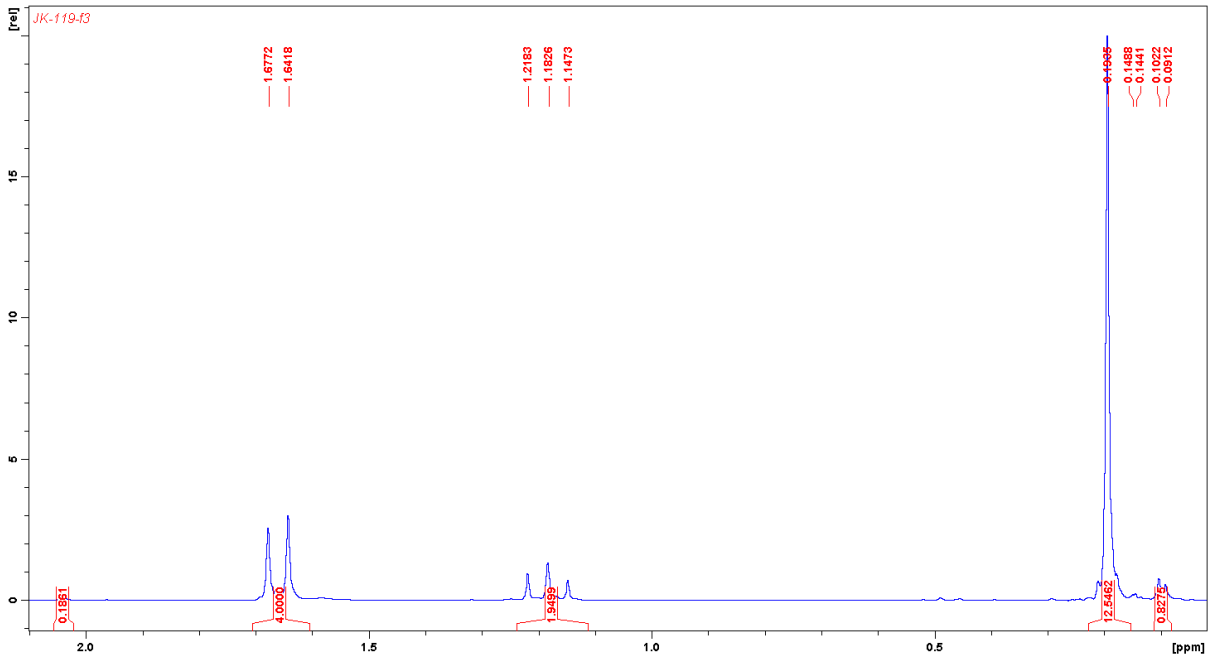

Figure 99: ^{1}H-NMR spectrum of the dithiol TMMD

The concentration of mercapto moieties was determined via a titration method from Verma et al.[94] which relies on the formation of a disulfide bond by reduction of lead(IV) to lead(II). Therefore, freshly purchased lead (IV) acetate (stabilized with 5 wt% acetic acid) was stored under high vacuum over night, where it lost 4.4% of its mass. For the following titration the "vacuum-dried" lead(IV) was assumed to be 100% pure. Subsequently 2.3360 g of lead(IV) acetate were quickly weighed into a 100mL volumetric flask, dissolved in approximately 50 mL of glacial acetic acid ([H_2O] < 0.1%) and then filled up to 100 mL. This solution was used to titrate solutions containing approximately 50 mg of TMMD in 15 mL glacial acetic acid from orange-red to blue using quinalizarine as indicator. A concentration of thiol groups ($c_{mercapto}$) was found to be 7.9 mmol g^{-1} by using the following Equation 4:

$$c_{mercapto} = \frac{c_{Pb(IV)} * (T - B) * 2}{m_{TMMD}}$$ **Equation 4**

Where $c_{Pb(IV)}$ (mol L^{-1}) is the concentration of Pb(IV), T (L) the titer, B (L) the blank value and m_{TMMD} the mass of TMMD weighed in for titration. Theoretically, TMMD with a purity of 100% would exhibit a value of 8.8 mol g^{-1} for $c_{mercapto}$

3.4 ATR and Photo-DSC

The photo-DSC setup and procedure was the same as mentioned in section Materials and Methods. Formulations were cured in the Al-pans and measured after an hour of curing. Masses are given in **Table 27**.

Table 27: Masses of thiol-ene based formulations applied for photo-DSC and ATR measurements

	TMMD (mg)	TVMS* (mg)	TFA (mg)	Darocur 1173 (mg)	ECES (mg)
UV/2.9a	60.0	39.2		0.8	
UV/2.9b	56.4	42.7		0.9	
UV/2.9c	51.9	47.1		1.0	
UV/2.9d	46.3	52.7		1.0	
UV/2.9e	39.6	59.3		1.1	
UV/2.9a/epox	24.1	15.6	3.0	0.3	57.0
UV/2.9b/epox	22.5	17.1	3.0	0.4	57.0
UV/2.9c/epox	20.8	18.8	3.0	0.4	57.0
UV/2.9c/epox	18.5	21.1	3.0	0.4	57.0
UV/2.9d/epox	15.8	23.7	3.0	0.5	57.0

*containing 0.2% pyrogallol as inhibitor

In contrast to above, the theoretical heat of polymerization with respect to vinyl moieties $\Delta H_{0,P}$ (kJ mol^{-1}) was determined by means of an Perkin Elmer Spectrum 65 FT-IR spectrometer device by comparing the integrals of the C=C stretch vibration peak at 1595 cm^{-1} before and after curing in the photo-DSC device where the Si-CH_3 peak at 1253 cm^{-1} served as a reference. This information was combined with the actual heat of polymerization ΔH_P (J g^{-1}) obtained from photo-DSC to calculate $\Delta H_{0,P}$ (kJ mol^{-1}). Furthermore, the molecular weight of the ene M_M and the functionality of the ene f, which is 3 in case of TVMS, were required (see equation 6).

$$\Delta H_{0,\mathrm{P}} = \frac{\Delta H_P M_M}{\mathrm{DBC\ f}}$$ **Equation 6**

The formulations were weighed into NETZSCH aluminum crucibles with an amount of 10 ± 1 mg, where in case of the epoxy formulations the crosslinking reaction would take place. After an hour of curing the photo-DSC measurements were started. The calculation methods for DBC and R_{pmax} are equal to the ones described above. For R_{pmax} the density of the formulations was assumed to be 0.97g mL^{-1}.

3.5 Real time FTIR

For these investigations formulations **UV/2.9a-e** (
Table 27) were applied. The procedure was equal to the one shown in section Materials and Methods.

3.6 DMTA Tests

The casted test bars were stored for curing in the molds for one hour prior to UV-curing for complete epoxy vulcanization. UV-curing was conducted as shown in the section Materials and Methods. Formulations **UV/2.9c/epox** and **DMTA/2.6** (Table 28) were applied. The measurements were carried out as described in section Materials and Methods.

Table 28: Masses for epoxy-based DMTA samples

	TMMD (mg)	TVMS (mg)	TFA (mg)	Darocur 1173 (mg)	IMIT (mg)	ECES (mg)
DMTA/2.6					0.5	99.5
UV/2.9c/epox	20.8	18.8	3.0	0.4		57.0

3.7 Refractive index

Sample preparations for the determination of n were the following: In case of **UV/2.9c** and **UV/2.9c/epox** the UV-cured materials of the photo-DSC measurements (Section 3.4) were used. For measuring **DMTA/2.6**, a test bar as mentioned in the previous chapter was prepared, where a piece of approximately 2 mm thickness was cut off by

means of a scalpel and pressed carefully between the quartz and the scattering element of the refractometer in order to have a continuous boundary with the sample. The procedure is further described in section Materials and Methods.

3.8 2PP writing

According to the procedure given in section Materials and Methods the formulations from Table 29 were quickly casted into 40x5x2 mm molds and with the help of a tip of Pasteur pipette, the excess formulation was removed. The test bars formulations were stored for epoxy-curing for an hour.

Table 29: Masses for formulations used for 2PP

	TMMD (mg)	TVMS (mg)	TFA (75% in isopropanol (mg)	Darocur 1173 (mg)	ECES (mg)	P3K (mg)	Irgacure 819 (mg)
2PP/2.9/20	40.0	36.0		4.0	319.2	0.8	
2PP/2.9/40	83.2	75.2	12.0	4.0	224.8	0.8	
2PP/2.9/40a	83.2	75.2	12.0	4.0	221.6		4.0
2PP/2.9/40b	83.2	75.2	12.0	4.0	225.36	0.24	
2PP/2.9/40c	83.2	75.2	12.0	4.0	225.44	0.16	

3.9 Waveguiding

The procedure to obtain illuminated waveguide cross-section was analogous to that discussed in section Materials and Methods. Formulations **2PP/2.9/40a-c** (masses given in the previous 2PP section) were applied.

3.10 Optical damping & Absorption behavior

The test bars for determining the optical damping of the bulk materials were produced via UV-curing as described in section Materials and Methods using the formulations **PRE/2.7** and **PRE/2.9** given in Table 30. The measuring procedure is also described in section Materials and Methods.

Table 30: Masses of formulations used for optical damping measurements and VIS/NIR measurements

	TMMD (mg)	TVMS (mg)	TFA (mg)	Darocur 1173 (mg)	IMIT (mg)	ECES (mg)
PRE/2.7					2.5	497.5
PRE/2.9	59	45	15			400
UV/2.9c/epox	20.8	18.8	3.0	0.4		57.0

4. 2PP Waveguide fabrication inside condensation cured silicone rubbers by curing thiol-ene monomer

4.1/4.2 Formulation remarks

The formulating was carried out under yellow light due to the photoreactivity of the one-photon-initiator Darcur 1173. After addition of each component the formulation was vigorously mixed by tapping the vial. Initially the inhibitor pyrogallol was mixed with the siloxane-based thiol TMMD (at 0.2% concentration) so as to exclude thermally induced thiol-ene reaction via the radical or Michael mechanism. After adding the siloxane based ene TVMS, the TPI was added in a 1.2% solution in toluene (in case of R1) or methylene chloride (in case of M2CHK). It was important to have the solvents evaporate especially in the case of methylene chloride, which would interfere with the thiol-ene reaction. Subsequently, the condensation catalyst DBTDA was added followed by the matrix material PDMS 4200. Finally, the crosslinker TAVS was added and mixed vigorously into the formulation. The degassing was conducted immediately for a few minutes at a vacuum of approximately 10 mbar until no more air bubbles were observed.

4.3 Photo-DSC investigations

The masses for weighing in the formulation used for the photo-DSC experiments regarding the acetoxy silicone-based concept are given in Table 31. Note that the concentration of double bonds c_{DB} comprises vinyl groups from TVMS and TAVS. Mercapto ($c_{mercapto}$) moieties are exclusively contributed by TMMD. The ratio acetoxy : silanol moieties was 2.6 in each case.

Table 31: Formulations used for photo-DSC investigations

	TVMS (mg)	TMMD (mg)	TAVS (mg)	DBTDA (mg)	PDMS 4200 (mg)	Darocur 1173 (mg)	$c_{mercapto}/c_{DB}$ (mmol g^{-1})
UV/3.3/1.4	29.3	64.3	26.3	3.8	275.715	0.585	1.29/0.92
UV/3.3/1.2	33.2	60.6	26.3	3.8	275.436	0.664	1.20/1.00
UV/3.3/1.0	38.1	55.7	26.3	3.8	275.338	0.762	1.11/1.11
UV/3.3/0.8	44.1	49.7	26.3	3.8	275.218	0.882	0.99/1.24
UV/3.3/0.6	51.6	42.2	26.3	3.8	275.068	1.032	0.84/1.40

For $\Delta H_{0,P}$ the value obtained in section 3.4 of the experimental part was assumed to be also valid also for the thiol-ene system in question. The photo-DSC setup, measuring procedure was the same as mentioned in section Materials and Methods and the formulations given in Table 31 were used. The calculation methods for DBC and R_{pmax} were carried out according to Equations 4 and 5. For R_{pmax} the density of the formulations was assumed to be 0.97 g mL^{-1}.

4.4 DMTA tests

The curing of the test-bars prepared from the formulations given in Table 32 were casted into molds as described in section Materials and Methods.

Table 32: Masses of acetoxy-based DMTA formulations

	TMVS (mg)	TMMD (mg)	TAVS (mg)	DBTDA (mg)	PDMS 4200 (mg)	Darocur 1173 (mg)
UV/3.3/1.4	51.1	112.7	46.2	1.75	487.235	1.015
DMTA/3.3/matrix			46.2	1.75	652.05	

Due to the slow moisture curing in depth, the bars were exposed to air moisture for one week. The UV-curing was carried out as discussed above for DMTA measurements. The measurements were carried out according to the description in section Materials and Methods.

4.5 Refractive Index

Samples for measurements of n were prepared the following way: In case of **UV/3.3/1.4** the UV-cured materials of the photo-DSC measurements (Section 4.3) were used. For determining n of RI/3.3 (Table 33) a film of approximately 200 µm was cured under nitrogen atmosphere in an INTELLI-RAY 600 UV device at an intensity of 120 mW cm^{-2} at a distance of 130 mm from the lamp. For measuring **DMTA/3.7/matrix**, a test bar as mentioned in the previous chapter was prepared, where a piece of approximately 2mm thickness was cut off by means of a scalpel and pressed carefully between the quartz and the scattering element of the refractometer in order to have a continuous boundary with the sample allowing for a precise measurement of n. The procedure is further described in section Materials and Methods.

Table 33: Masses used for formulation for measurements of n

	TMVS (mg)	TMMD (mg)	Darocur 1173 (mg)
RI/3.3	30.63	68.37	1

4.6 2PP writing

2PP pre- and postprocessing were conducted as described in section Materials and Methods. Table 23 lists the formulations.

Table 34: Formulations used for 2PP investigations

	TMVS (mg)	TMMD (mg)	TAVS (mg)	DBTDA (mg)	PDMS 4200 (mg)	R1 (mg)	Darocur 1173 (mg)	M2CHK (mg)
2PP/3.3.1	21.3	38.7	21	0.75	215.13	0.12	3	0
2PP/3.3.2	28.8	46.2	21	0.75	200.13	0.12	3	0
2PP/3.3.3	21.3	38.7	21	0.75	215.13		3	0.12
2PP/3.3.4	28.8	46.2	21	0.75	200.13		3	0.12
2PP/3.3.5	36.3	53.7	21	0.75	185.19		3	0.06
2PP/3.3.6	30.0	64.5	21	0.75	180.63		3	0.12

4.7 Waveguiding

The procedure to obtain illuminated waveguide cross-section is analogous to that discussed in section Materials and Methods. Formulations **2PP/3.3.4** and **2PP/3.3.6** (Table 34) enabled illuminated cross-sections.

4.8 Optical damping and absorption behavior

For the VIS/NIR spectroscopy the same preparation and spectrometer as mentioned in section Materials and Methods were used to investigate materials based on formulation **UV/3.3/1.4**). In case of **UV/3.3/1.4** the UV-cured materials of the photo-DSC measurements (Section 4.3) were used. For determining n of **RI/3.3** a film of approximately 200 µm was cured under nitrogen atmosphere in an INTELLI-RAY 600 UV device at an intensity of 120 mW cm^{-2} at a distance of 130 mm from the lamp. For measuring DMTA/3.7/matrix, a test bar mentioned in the previous chapter was prepared, where a piece of approximately 2 mm thickness was cut off by means of a scalpel and pressed carefully between the quartz and the scattering element of the refractometer in order to have a continuous boundary with the sample allowing for a

precise measurement of n. The procedure is further described in section Materials and Methods.

Materials & Methods

2PP instrumentation:

For 2PP processing two different facilities at the Vienna University of Technology (M3D) and Joanneum Research in Weiz (MTS) were applied. The M3D device served for preliminary experiments and establishing the formulations given in Table 20. MTS, due to its higher laser power in a roundly shaped VOXEL was used to produce waveguides to give the proof of principle for waveguiding and for optical damping measurements. If not explicitly mentioned differently, the MTS device was applied. In the following the most important technical features of the two 2PP devices in question shall be summarized. An important difference was that the samples were processed in the M3D with the laser below the sample, which thus had to be turned upside-down (possible due to the thixotropy of the samples), while the MTS device allowed for structuring from above.

M3D:[98] In the Micro-3-Dimensional Structuring System M3D a femtoTRAIN Ti:Sapphire oscillator (High Q Lasers) was applied. This compact all diode pumped solid state oscillator was a source of light with a wavelength of 793 nm and a typical pulse width of 100 fs. The pulse repetition rate was 73 MHz and the average output power was 690 mW. The laser beam firstly passed through a collimator positioned after the laser head. Then the first order of the collimated beam passed through a rotating λ/2 wave-plate. By placing a polarized beam splitter after the wave-plate the laser power coupled into the objective was controlled. The key component of the M3D was the X - Y scanner exhibiting two linear air-bearing stages. The latter carried the complete optical setup including a CCD-Camera for live monitoring and the microscope objective. The air bearing stages had very high position accuracy at high structuring speed. Structuring speeds up to 30 mm/s were possible. The use of high precision air-bearing stages allowed for the fabrication of structures with an accuracy of 50 nm over the whole building envelope.

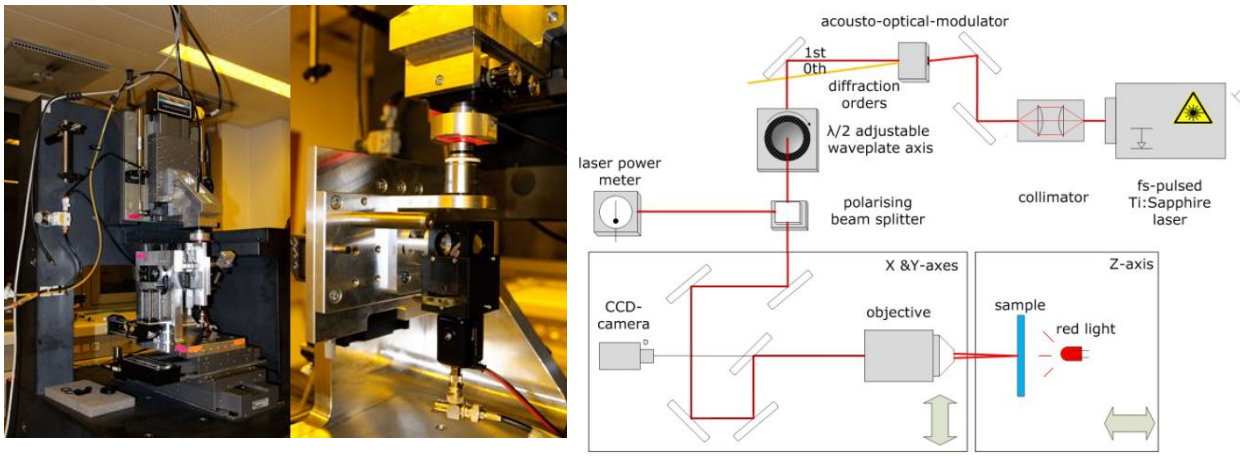

Table 35: Left: Views of the M3D 2PP device; Right: Schematical drawing of the M3D setup

After processing at the M3D device, an INTELLI-RAY 600 UV device at an intensity of 120 mW cm^{-2} at a distance of 130 mm from the lamp was used illuminating the samples for 2 minutes under nitrogen atmosphere and thus curing them.

MTS, Weiz: An amplified ultrafast Ti:Sapphire laser system from Spectra Physics (Mai Tai® - Spitfire® combination) was applied for the 2PP experiments providing pulses in the range of 800 nm wavelength and a pulse duration of a 130-150 fs. The repetition rate was 1 kHz and the maximum pulse energy 1 mJ sufficing even for laser ablation metals. By means of a single shot autocorrelator (Femtos) the pulse width of the laser was monitored. The sample was moved on a 3-axial stage (Aerotech), which exhibited an accuracy with respect to positioning of 100 nm and a travel range of several centimeters.[10] By an extra cavity electro-optical switch, which featured a remote control of the high voltage applied to the Pockels cell, the laser power was computer-controlled. A combination of a 20x microscope objective (Zeiss) with a numerical aperture of 0.5 was combined with a cylindrical telescope served as the focusing optics. A threefold reduction of the spherical beam cross-section was accomplished with the telescope, which comprised a pair of cylindrical lenses exhibiting focal lengths of f1 = 75mm and f2 = 25mm. The elliptic beam cross-section formed by this apparatus allowed for astigmatic beam focusing and shaping of the focal volume. The home-made LabView Program allowed for controlling the lithographic setup. The 2PP processed liquid samples, where examined by phase contrast microscopy using an Olympus BX 51 microscope using an orange foil as a

filter. Subsequently they were cured by means of a UV 236 A UV-lamp in a nitrogen chamber (Waldmann Medizintechnik; 5 min at 360 mJ cm^{-2} min^{-1}; lamp to sample distance 10 cm).

Photo-DSC

For the photo-DSC measurements a Netzsch DSC 204 F1 Phoenix device was used. A double light guide, which was attached to the DSC unit from top, enabled irradiation of the sample with filtered UV-light (280 – 500 nm) from an EXFO-Omnicure 2000 lamp, where the light intensity on the tip of the light guide was 3000 mW cm^{-2}. The degassed formulations were weighed into NETZSCH aluminum crucibles with an amount of 10 ± 1 mg. The samples underwent the following intervals in the photo-DSC device at 25°C: 4 min N_2 purge without illumination – 5 min with illumination – 2 min without illumination– 5 min with illumination – 2 min without illumination. The first illumination caused photopolymerization. Subsequently two small exotherms as well as an endotherm were detected, which by means of curve substraction allowed to account for the heat flow not originating from photopolymerization.

The three properties of interest were the time from the onset of the lamp until the maximum of the exothermic photopolymerization peak T_{max} the rate of polymerization R_{pmax} and the double bond conversion DBC. T_{max} was straightforwardly determined by substracting the time of onset from the time until the exothermic peak maximum. Equation 5 shows the calculation method for R_{pmax}, where the height of the photo-DSC peak maximum *h* (W g^{-1}) , the density of the resin ρ and the theoretical heat of polymerization $\Delta H_{0,P,}$ (J mol^{-1}) were required.

$$R_{pmax} = \frac{h\,\rho}{\Delta H_{0,P}} \qquad \textbf{Equation 5}$$

DBC was calculated by the following Equation 6 additionaly requiring the concentration of double bonds c_{DB} (mol g^{-1}) and the actual heat of polymerization ΔH_P (J g^{-1}).

$$DBC = \frac{\Delta H_P}{c_{DB}\,\Delta H_{0,P}}$$ **Equation 6**

Real time FTIR

For these investigations the same formulations as for photo-DSC were applied. PE foils were fixed in the sample holder. Subsequently, they were roughened with abrasive paper on both sides in order to give a better base line in case of the FT-IR spectra. From these foils pieces of approximately 1 x 2 cm were cut. On one foil a draw-down bar-rod #8 was used to give a film of the liquid formulations with a thickness of 20 µm. Subsequently a second piece of roughened PE foil was laid onto of the film sandwiching the formulation and tackling oxygen inhibition. In the spectrometer, the distance from the light guide coming from an EXFO-Omnicure 2000 lamp interface to the sample was 3 cm and the angle of incidence 30°. The monitoring involved 14 FT-IR spectra per second taken on a VERTEX 80 FT-IR spectrometer (Bruker). The base line correction of choice was the rubber band method.

DMTA

DMTA (dynamical mechanical thermal analysis) tests were carried out applying a DMA 2980 device (TA Instruments) using a single cantilever clamp over a temperature range from -140°C to 300°C for those measurements. The temperature gradient was 3 K min^{-1}, the frequency 1 Hz and the amplitude 10µm. Degassed formulations were – depending on their stiffness - cast into flexible silicone molds or plastic molds (40x5x2 mm^3) and stored at room temperature overnight to obtain thixotropy. An INTELLI-RAY 600 UV device at an intensity of 120 mW cm^{-2} at a distance of 130 mm from the lamp was used for illuminating the samples for 2 minutes. All cured samples were removed from the mold by means of a spatula and illuminated in the same manner from the opposite side. Then they were used for measurement without any further processing. The weighed-in masses are given in Table 18.

Refractive index:

Refractive indices were in all cases measured applying the photo-DSC cured samples on a Abbé Refractometer, manufactured by the Carl Zeiss Company, Germany, and equipped with a Schott Geraete CT 050 Thermostat, filled with distilled water (adjusted to 20°C). The operating wavelength was 589 nm (sodium D-line).

Waveguiding

In order to obtain illuminated cross-sections of the waveguides, samples were processed with the same procedure and 2PP parameters on a non-transparent polymer substrate and finally UV-cured as in the previous section on a breakable substrate. At the predetermined break point of the breaking substrate being 7 mm apart from each other the film with the inscribed waveguides was cut and the refrangible substrate was broken at the corresponding predetermined breakpoint. The sample on the substrate piece was brought vertically into the beam of the phase contrast microscope by means of a sample holder built with glass slides and foam rubber.

Optical damping and absorption behavior

Optical damping of the bulk material

For the preliminary optical damping measurements test bars were cured according to the procedure from the experimental DMTA section above using 50x5x5mm molds printed by means of an OBJET printer, where the bottom was plastic tape. Subsequently the test bars were cut to give long pieces without any breaks with a focus on cutting areas as smooth as possible considering coupling in losses. To achieve planar areas for the laser beam to penetrate and finally exit the test bars, thin glass object holders (n= 1.5) were stuck to these cutting areas by means of the immersion oil 518 from Zeiss. The primed test bars were adjusted within the laser beam having the latter penetrating approximately the middle of the test bars and finally reaching the detector. The setup is illustrated in Figure 100.

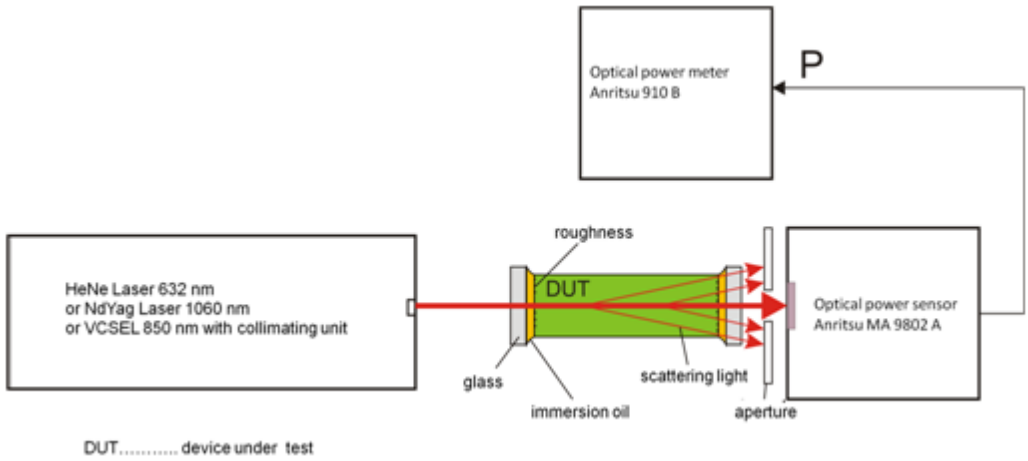

Figure 100: Experimental setup for optical damping measurements

Thus the laser power reaching the detector was measured with and without the test bar. The optical attenuation in dB/cm was calculated by means of Equation 7:

$$OA = \frac{-10 \log \frac{SL_{mp}\left(1-\left(\frac{n-1}{n+1}\right)^2\right)^2}{SL_{op}}}{l_p}$$

Equation 7

In Equation 7, OA is the optical attenuation or optical damping (dB/cm), SL_{mp} the laser power with sample (µW), SL_{op} the laser power without sample (µW) and n the refractive index of surface glass object slides (n =1.50) and lp the length of the test bar.

Absorption behavior

For VIS/NIR absorption measurements between 600 and 1600 nm materials from 2PP fabrication experiments were used: The cured films were removed from the sticky tape basin and finely ground in a porcelain mortar. Cryo-milling helped to

obtain fine powders, which could be investigated in the diffuse reflection mode on a Lambda 900 UV/VIS/NIR spectrometer.

Chemicals

Product	Supplier
(*p*-isopropylphenyl)(*p*-methylphenyl)-iodonium tetrakis(pentafluorophenyl) borate (IMIT)	ABCR
1,10-dithiol 95% (DDT)	ABCR
1,3-*bis*(chloromethyl)-1,1,3,3-tetramethylsiloxane 97%	ABCR
2,2,6,6-tetramethylpiperidin-1-oxyl 98% (TEMPO)	Aldrich
2,2'-(ethylenedioxy)diethane thiol 95% (DOD)	Aldrich
2,4,6,8-tetramethyl-2,4,6,8-tetravinyl-cyclotetrasiloxane	Aldrich
4-5% aminopropylmethylsiloxane) – dimethylsiloxane copolymer (viscosity 150-300 cSt), (APMS)	ABCR
BYK 410	BYK Chemie
BYK 420	BYK Chemie
BYK E 410	BYK Chemie
citric acid, puriss. p.A.	Aldrich
Darocur 1173	BASF
dibutyltin diacetate 95% (DBTDA)	ABCR
dibutyltin dilaurate techn (DBTDL)	Fluka
dicumyl peroxide 97%	Fluka
dipropyleneglycol diacrylate (DPGDA)	Fundermax
Elastosil RT 601	Wacker
epoxycyclohexylethylmethylsiloxan(8-10% Mol)-dimethylsiloxan copolymer (ECES)	ABCR

ethylene diamine 99%	Aldrich
ethyleneglycol diacrylate (EGDMA)	Aldrich
Hycar 2000x162 butadiene rubber	RF Goodrich
Irgacure 819	BASF
lead(IV)acetate 95%, acetate stabilized	Aldrich
mercaptopropyl trimethoxy silane 95% (MPTS)	ABCR
pentaerythrol tetrakis(3-mercaptoproprionate) 95% (TT)	Aldrich
polydimethylsiloxane, hydroxy terminated (PDMS 4200)	ABCR
pyrogallol p. a.	Merck
quinalizarine p. a.	Merck
TEGO RAD 2200N	Evonik
thiourea 98%	Loba
triacetoxyvinyl silane 98% (TAVS)	ABCR
trifluoroacetic acid 98%	Aldrich
trifluorosulfonic acid 98%	Aldrich
tris(vinyldimethylsiloxy)methylsilane 95% (TVMS, containing higher homologs)	ABCR

Summary

The goal of this thesis was to invent new materials and processes, where two-photon polymerization could be elegantly applied for waveguide fabrication. Due to its outstanding mechanical, thermal and optical properties, polysiloxanes should serve as the basic matrix material for waveguide inscription by means of local increase of the refractive index during polymerization. Problems of former concepts such as scattering of guided photons due to phase separation in the waveguide materials and time-consuming pre- and post-processing should be tackled. In a recent contribution specimens for two-photon waveguide inscription had been obtained by crosslinking of silicones and subsequently swelling of these rubbers with high refractive photoreactive monomer formulations. This approach should be replaced by two alternative methods i) postponing the curing of the matrix material to the stage of post-processing or ii) via orthogonal curing chemistries of matrix and monomer system. Additionally, time-consuming evaporation of unreacted monomer formulation in order to fully develop the change in refractive index leaves space for improvement. In the course of this work simple UV-curing should suffice for post-processing exploiting the local enrichment of high refractive material in the two-photon illuminated regions due to diffusion of monomers. The high refractive index of thiol-ene photopolymers caused by sulfur atoms should facilitate the latter.

The first material concept was based on a hydrophilic silicone polyether acrylate (TEGO RAD 2200N) as a matrix material and a low molecular weight reactive diluent following the idea to write waveguides by means of two-photon-polymerization (2PP) into a liquid and curing the waveguide cladding material only after 2PP. This should feature the advantage of obtaining a very pronounced enrichment of high refractive material in the two-photon-illuminated regions and thus generating a strong change inrefractive index between waveguide core and cladding. On the other hand the waveguides had to remain in place and should not sink after 2PP. An elegant manner to solve this problem was found by successfully screening for a rheology additive providing the liquid silicone acrylate with thixotropy. BYK E 410 turned out to yield thixotropy in mixtures including the trimethylolpropane triacrylate (TTA) together with the silicone acrylate (Figure **101**).

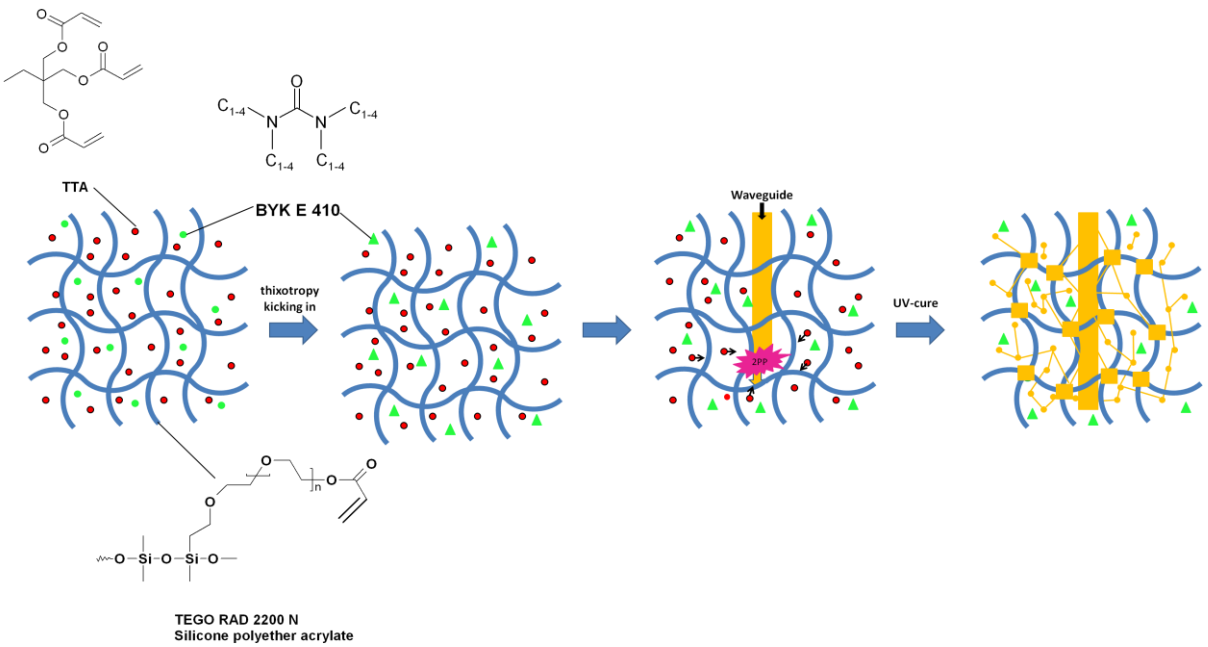

Figure 101: The “thixotropy concept” for 2PP waveguide fabrication.

This combination gave very high changes in refractive index upon 2PP using the two-photon-initiator (TPI) B3FL. After this preliminary success the reactivity of this 2PP system was tested by means of photo-DSC with varying TTA contents. As expected, the photoreactivity increased with increasing TTA content. The double bond conversion (DBC), however, was not influenced by the TTA content. An important criterion for mass production of flexible printed circuit boards is thermal stability as the process involves exposure to a temperature of 240°C. DMTA investigations showed that only in the presence of pentaerythritol tetrakis(3-mercaptopropionate (TT) the acrylate-based material in question withstood this thermal stress. This tetrafunctional thiol was also seeked to be applied as partial thiol-ene polymerization of acrylates brings along a set of further advantageous properties to the materials, such as low shrinkage, network homogeneity and a higher refractive index. These benefits of TT, however, could not be made use of as attempts to fabricate waveguides in the presence of TT were not successful as no straight waveguides could be structured. This was probably due to transfer reactions and lowered crosslink density leading to wiggly lines, which formed upon swelling of the 2PP-written structures.

The refractive index as the crucial property was measurable by means of Abbé refractometry. This could only be carried out with the cladding material while

refractive index could not be measured for the core due to the unknown concentration of TTA.

Subsequently details about the thixotropic effect, upon which the waveguide structuring was based, were elucidated: When monitoring the shear stress as a measure for thixotropy of a formulation containing BYK E 410, TEGO RAD 2200N and TTA, the thixotropy grew almost linearly for the whole 70h of measuring. The thixotropy effect of this rheology additive is based on the precipitation of needle-shaped crystals causing a certain cloudiness of the optical materials. Thus, if time did not matter, increasing the time for thixotropy to kick in would be a possibility to lower the concentration of rheology additive. The development of thixotropy furthermore turned out to be facilitated at elevated TTA concentration. An inverse tendency, however, was undesired increasing stiffness with increasing TTA content.

During the 2PP screening, the formulation containing 20% TTA and 2.5% BYK E410 content showed the best combination of local increase of refractive index and straightness of fabricated waveguides. These waveguides allowed for waveguiding demonstrations obtaining highly illuminated waveguide cross-sections on the microscope. Cut-back measurements were also carried out for these waveguides structured at 4 mm structuring speed. A waveguide written at 120 µW gave an optical damping value of 2.38 dB/cm, which is a rather modest performance. Taking into account that measurements of the bulk material also gave rather high damping it is probably not possible to achieve much lower damping values. The rheology effect of BYK E 410 relies on the fact that it precipitates into small, needle like crystals causing optical scattering and below a concentration somewhere around 2% the waveguide are not held in place any more.

A second concept was presented, where the matrix material was orthogonally cured in the presence of monomer in order to obtain the 2PP-processable sample after a single step. As a second time-saving measure, the diffusion-based enrichment effect of high refractive material in the two-photon-illuminated regions was exploited to save the evaporation of monomer to fully develop the change in refractive index, as it was done in other works.[77, 79] The greatest challenge in this aspect was the compatibility of photopolymer and matrix material. For this purpose a combination of the epoxycyclohexyl-functional polydimethyl siloxane copolymer ECES and a siloxane-

based formulation of the dithiol TMMD and the trivinyl-functional TVMS were chosen. The epoxy-functional matrix material ECES by means of its polyether backbone upon acid-catalyzed cationic ring opening polymerization gave very transparent hybrid materials together with the thiol-ene photonetwork exhibiting thioether domains Figure 102.

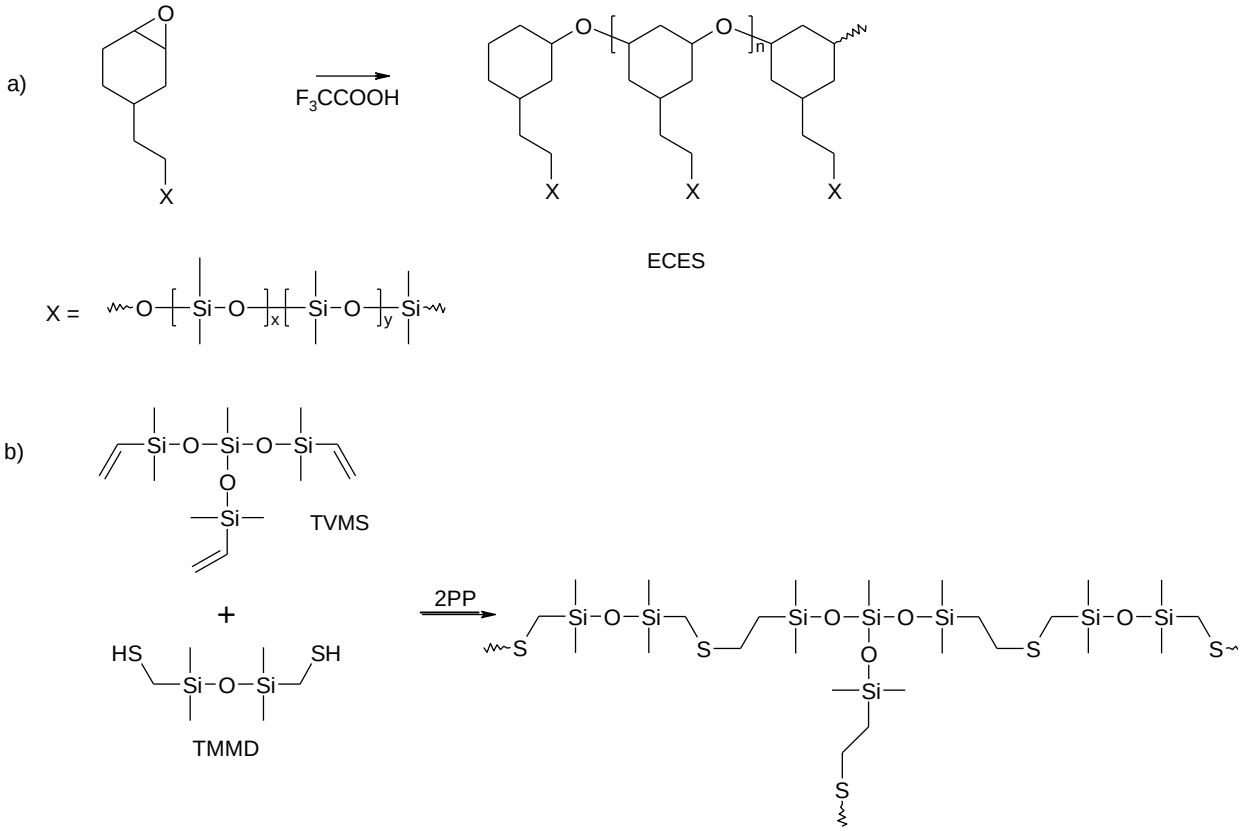

Figure 102: (a) Epoxy silicone curing chemistry; (b) Siloxane based thiol-ene monomers undergoing 2PP

For the thiol-ene system in question the ratio of thiol to ene on the photoreactivity and double bond conversion DBC arose: The highest double bond conversion was achieved at an equimolar ratio of thiol to ene groups and the rate of polymerization was the second highest among the tested ratios. Thus, it was clear that an equimolar ratio would be the best choice in case of 2PP experiments. As expected, the material could withstand the thermal stress that it would be exposed to when implemented in an industrial mass fabrication process of flexible printed circuit boards, which is an advantage over the previous concept. The latter exhibits acrylate moieties with

thermally labile ester bonds and here only more stable ether and thioether moieties are present.

The essential findings from the 2PP experiments were the following: High monomer contents until 40% and up to five writing steps (feed rate 4 mm s^{-1}) over the same volumes helped to get an acceptable local change in refractive index upon 2PP. The boundaries of the obtained waveguide structures, however, were rather diffuse in all cases. This also caused modest results with respect to illuminated cross-sections of the fabricated waveguides. Thus cut-back-measurements were not attempted. In future trials one possibility to improve on the waveguiding performance might be to sharpen the waveguide boundaries by a screening of different hindered amine light stabilizers.

A *third approach* was a thiol-ene material on the basis of an acetoxy-curing polydimethyl siloxane matrix material. After unsuccessful trials of using mercapto- and vinyl-functional methoxy-crosslinkers the attention was focused on triacetoxy vinyl silane (TAVS) as a suitable condensation crosslinker.

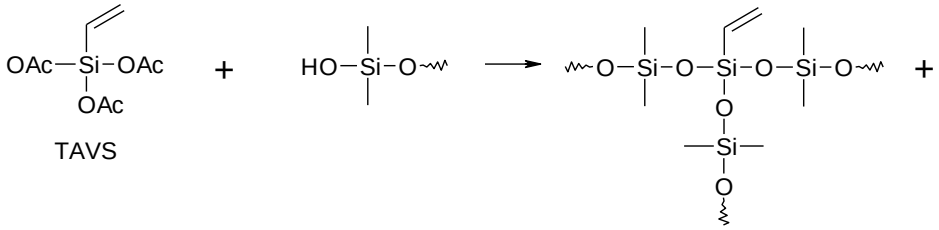

Figure 103: Introducing an ene functionality in the silicone backbone via acetoxy condensation curing

This allowed for the silicone rubber matrix material to participate in the thiol-ene reaction of the monomer formulation.

The thiol functionality was then introduced by means of the liquid monomer TMMD. The final way to obtain a significant change in refractive index upon 2PP was to add the trivinyl siloxane TVMS in addition to TAVS in order to obtain a higher ene concentration. Thus, it is very probable, that covalent linkages between photopolymer and matrix material were formed being highly beneficial for compatibility. In contrast to the epoxy-based thiol-ene concept discussed in the previous paragraph, photo-

DSC experiments gave increasing DBCs with increasing thiol content, while the rate of polymerization increased in the opposite direction. A thiol excess was, however considered as more suitable for 2PP fabrication, because looser networks and maximum thiol incorporation under thiol excess conditions would allow for an increase of the local change in refractive index.

Analogously to the previous concept, DMTA measurement proved the thermal stability of the material required for the above mentioned industrial process. The 2PP experiments showed that the TPIs R1^{99} as well as the easily synthesized novel M2CHK were suitable for waveguide fabrication. Changes in refractive index comparable to that of the previous epoxy-based thiol-ene network could be achieved at more than double of the feed rate of the latter (10 mm s^{-1}). This might be due to the vinyl moieties on the silicone rubber participating in the thiol-ene reaction making the system reach the gel point faster than in case of an inert matrix material and polymerizing functionality exclusively on the liquid monomer. The problem of rather diffuse waveguide boundaries was also encountered in this third concept. Illuminated cross-sections gave the proof of principle for waveguiding. Their brightness was better than in case of the previous material. Attempts to determine the optical damping of the waveguides failed due to incapability of coupling light into them.

Summing up, in all three cases the proof of principle for waveguiding was accomplished. The thixotropy-based (first) approach could be driven furthest by obtaining an optical damping value. Due to the fact, that the rheology additive has to precipitate in order to cause thixotropy limiting transparency, not much potential to further lower the optical damping is seen in this concept. This was well demonstrated by the optical attenuation measurements of the bulk material. As the thiol-ene based approaches exhibited very low optical damping of the bulk material their potential for future improvements towards low-damping waveguides is estimated higher. Future investigators using this work as a foundation will mainly have to find a means to sharpen the waveguide boundaries and enhance the local change in refractive index, maybe by using a thiol with a functionality higher than 2.

Abbreviations

2PP	two-photon-induced polymerization
APMS	4-5% Aminopropylmethylsiloxane) – dimethylsiloxane copolymer (viscosity 150-300 cSt)
ATR	attenuated reflection
B3FL	2,7-Bis((4-(dibutylamino)phenyl)ethynyl)-9H-fluoren-9-one
B3K	1,5-Bis(4-(N,N-dibutylamino)phenyl) penta-1,4-diyn-3-one
dB	decibel
DBC	double bond conversion
DBTDA	dibutyl tin diacetate
DBTDL	dibutyl tin dilaurate
DDT	1,10-decanedithiol
DMF	N,N'-dimethyl formamide
DMTA	dynamic mechanical thermal analysis
DOD	2,2'-(ethylenedioxy)diethane thiol
DPD	diphenylsilanediol
DPGDA	dipropylene glycol diacrylate
ECES	epoxycyclohexylethylmethylsiloxane(8-10Mol%)-dimethylsiloxane copolymer; viscosity 300-450 cSt
EGMDA	ethylene glycol dimethacrylate
ETA	ethoxylated trimethylolpropane triacrylate
FT-IR	fourier transform infrared
GM	Göppert-Mayer
h	peak height of photo-DSC plot
HALS	hindered amine stabilizers
HDDA	hexandiol diacrylate
IMIT	(p-Isopropylphenyl)(p-methylphenyl)-iodonium tetrakis(pentafluorophenyl) borate
ITX	isopropyl thioxanthone

M2CHK	((2E,6E)-2,6-)bis(4-(dimethylamino)benzylidene)-4-methylcyclohexanone
MEMO	methacryloxypropyltrimethoxysilane
MMA	methyl methacrylate
MPLC	medium pressure liquid chromatography
MPTS	mercaptopropyl trimethoxy silane
MS	mass spectrometry
n	refractive index
NEP	N-ethyl-pyrrolidone
NIR	near infrared
NMP	N-methyl-pyrrolidone
NOA	Norland optical adhesives
OA	optical attenuation/optical damping
ORMOCER	organic modified ceramics
PBG	photonic band gap
PDMS	polydimethyl siloxane
PDMS 4200	polydimethylsiloxane silanol terminated, molecular weight 4200 g mol^{-1}
PE	polyethylene
PhC	photonic crystal
PI	photoinitiator
PMMA	polymethyl methyacrylate
R1	(E,E-1,4-bis[40-(N,N-di-nbutylamino)styryl]-2,5-dimethoxybenzene)
Rms	root mean squared
R_{pmax}	maximum rate of polymerization
S_1	singulet 1
SL_{mp}	laser power with sample
SL_{op}	laser power without
T_1	triplet 1
TAVS	triacetoxy vinyl silane
TEMPO	2,2,6,6-Tetramethyl-piperidin-1-yl)oxyl
TFA	trifluoroacetic acid

THF	tetrahydrofurane
T_{max}	time from the onset of the lamp until peak maximum of photo-DSC plot
TMMD	1,3-bis(3-mercaptomethyl-1,1,3,3-tetramethyldisiloxane
TPA	two-photon-absorption
TPI	two-photon-initiator
TT	pentaerythrol tetrakis(3-mercaptoproprionate)
TTA	trimethylolpropane triacrylate
TTE	tetrathiol 2,2‘,2‘‘,2‘‘‘-(2,2‘,2‘‘,2‘‘‘-(2,4,6,8-tetramethyl-1,3,5,7,2,4,6,8-tetraoxatetrasilocane-2,4,6,8-tetrayl)tetrakis(ethane-2,1-diyl))tetrakis(sulfanediyl)tetraethanethiol
TVMS	tris(vinyldimethylsiloxy)methylsilane
UV/VIS	ultraviolet/visible
VOXEL	volume pixel
$\Delta H_{0,P}$	theoretical heat of polymerization
ΔH_P	actual heat of polymerization
Θ_{max}	angle of tolerance

References

1. Infuehr, R. Dissertation, 2008.
2. Ziemann, O., *POF-Handbuch: Optische Kurzstreckenübertragungssysteme*. Springer Verlag: Berlin, 2007.
3. Ma, H.; Jen, A. K. Y.; Dalton, L. R. *Advanced Materials (Weinheim, Germany)* **2002,** 14, (19), 1339-1365.
4. Cai, D. K.; Neyer, A.; Kuckuk, R.; Heise, H. M. *Optical Materials (Amsterdam, Netherlands)* **2008,** 30, (7), 1157-1161.
5. Henzi, P. UV-induzierte Herstellung monomodiger Wellenleiter in Polymeren. Dissertation, 2004.
6. LaFratta, C. N.; Fourkas, J. T.; Baldacchini, T.; Farrer, R. A. *Angewandte Chemie, International Edition* **2007,** 46, (33), 6238-6258.
7. Wu, S.; Serbin, J.; Gu, M. *Journal of Photochemistry and Photobiology, A: Chemistry* **2006,** 181, (1), 1-11.
8. Crivello, J. V. *Journal of Polymer Science, Part A: Polymer Chemistry* **1999,** 37, (23), 4241-4254.
9. Hoyle, C. E.; Lowe, A. B.; Bowman, C. N. *Chemical Society Reviews* **2010,** 39, (4), 1355-1387.
10. Hoyle, C. E.; Lee, T. Y.; Roper, T. *Journal of Polymer Science, Part A: Polymer Chemistry* **2004,** 42, (21), 5301-5338.
11. Hoyle, C. E.; Bowman, C. N. *Angewandte Chemie, International Edition* **2010,** 49, (9), 1540-1573.
12. Jacobine, A. F. In *Thiol-ene photopolymers*, 1993; Elsevier: 1993; pp 219-68.
13. Mueller, U.; Kunze, A.; Herzig, C.; Weis, J. *Journal of Macromolecular Science, Pure and Applied Chemistry* **1996,** A33, (4), 439-57.
14. A. F. Jacobine, S. N., In *Radiation Curing: Science and Technology*, Pappas, S. P., Ed. Plenum Press: New York, 1992.
15. Prinz, F. B.; Atwood, C. L.; Aubin, R. F.; Beaman, J. J.; Brown, R. L.; Fussell, P. S.; Lightman, A. J.; Sachs, E. J.; Weiss, L. E.; Wozny, M. J. *JTEC/WTEC Panel Report on Rapid Prototyping*; Rapid Prototyping Association of the Society of Manufacturing Engineers: 1997.
16. Guo, R.; Xiao, S.; Zhai, X.; Li, J.; Xia, A.; Huang, W. *Optics Express* **2006,** 14, (2), 810-816.
17. Duan, X.-M.; Sun, H.-B.; Kawata, S. *Journal of Photopolymer Science and Technology* **2004,** 17, (3), 393-396.
18. Duan, X.-M.; Sun, H.-B.; Kaneko, K.; Kawata, S. *Thin Solid Films* **2004,** 453-454, 518-521.
19. Takada, K.; Kaneko, K.; Li, Y.-D.; Kawata, S.; Chen, Q.-D.; Sun, H.-B. *Applied Physics Letters* **2008,** 92, (4), 041902/1-041902/3.
20. www.sartomer.com
21. Klein, S.; Barsella, A.; Taupier, G.; Stortz, V.; Fort, A.; Dorkenoo, K. D. *Applied Surface Science* **2006,** 252, (13), 4919-4922.
22. Farrer, R. A.; LaFratta, C. N.; Li, L.; Praino, J.; Naughton, M. J.; Saleh, B. E. A.; Teich, M. C.; Fourkas, J. T. *Journal of the American Chemical Society* **2006,** 128, (6), 1796-1797.
23. Li, L.; Gershgoren, E.; Kumi, G.; Chen, W.-Y.; Ho, P. T.; Herman, W. N.; Fourkas, J. T. *Advanced Materials (Weinheim, Germany)* **2008,** 20, (19), 3668-3671.

24. Haske, W.; Chen, V. W.; Hales, J. M.; Dong, W.; Barlow, S.; Marder, S. R.; Perry, J. W. *Optics Express* **2007,** 15, (6), 3426-3436.
25. Dorkenoo, K.; Klein, S.; Bombenger, J.-P.; Barsella, A.; Mager, L.; Fort, A. *Molecular Crystals and Liquid Crystals* **2006,** 446, 151-160.
26. Rinne, S. A.; Garcia-Santamaria, F.; Braun, P. V. *Nature Photonics* **2008,** 2, (1), 52-56.
27. Ramanan, V.; Nelson, E.; Brzezinski, A.; Braun, P. V.; Wiltzius, P. *Applied Physics Letters* **2008,** 92, (17), 173304/1-173304/3.
28. Pruzinsky, S. A.; Braun, P. V. *Advanced Functional Materials* **2005,** 15, (12), 1995-2004.
29. Nelson, E. C.; Garcia-Santamaria, F.; Braun, P. V. *Advanced Functional Materials* **2008,** 18, (13), 1983-1989.
30. Nelson, E. C.; Braun, P. V. *Los Alamos National Laboratory, Preprint Archive, Condensed Matter* **2007**, 1-6, arXiv:0710 0851v2 [cond-mat mtrl-sci].
31. Krivec, S.; Matsko, N.; Satzinger, V.; Pucher, N.; Galler, N.; Koch, T.; Schmidt, V.; Grogger, W.; Liska, R.; Lichtenegger, H. C. *Advanced Functional Materials* 20, (5), 811-819.
32. Pucher, N.; Rosspeintner, A.; Satzinger, V.; Schmidt, V.; Gescheidt, G.; Stampfl, J.; Liska, R. *Macromolecules (Washington, DC, United States)* **2009,** 42, (17), 6519-6528.
33. Infuehr, R.; Stampfl, J.; Krivec, S.; Liska, R.; Lichtenegger, H.; Satzinger, V.; Schmidt, V.; Matsko, N.; Grogger, W. *Materials Research Society Symposium Proceedings* **2009,** 1179E, (Material Systems and Processes for Three-Dimensional Micro- and Nanoscale Fabrication and Lithography), No pp given, Paper #: 1179-BB01-07.
34. Chandross, E. A.; Pryde, C. A.; Tomlinson, W. J.; Weber, H. P. *Applied Physics Letters* **1974,** 24, (2), 72-4.
35. Bichler, S.; Feldbacher, S.; Woods, R.; Satzinger, V.; Schmidt, V.; Jakopic, G.; Langer, G.; Kern, W. *Proceedings of SPIE* **2009,** 7413, (Linear and Nonlinear Optics of Organic Materials IX), 74130W/1-74130W/11.
36. Gong, X.; Wen, W.; Sheng, P. *Langmuir* **2009,** 25, (12), 7072-7077.
37. www.norlandproducts.com (30/06/2010),
38. Joshi, M. P.; Pudavar, H. E.; Swiatkiewicz, J.; Prasad, P. N.; Reianhardt, B. A. *Applied Physics Letters* **1999,** 74, (2), 170-172.
39. Chen, Q.-D.; Wu, D.; Niu, L.-G.; Wang, J.; Lin, X.-F.; Xia, H.; Sun, H.-B. *Applied Physics Letters* **2007,** 91, (17), 171105/1-171105/3.
40. Lange, B.; Jhaveri, S. J.; Steidl, L.; Ayothi, R.; Ober, C. K.; Zentel, R. *Macromolecular Rapid Communications* **2007,** 28, (8), 922-926.
41. Kirkpatrick, S. M.; Baur, J. W.; Clark, C. M.; Denny, L. R.; Tomlin, D. W.; Reinhardt, B. R.; Kannan, R.; Stone, M. O. *Applied Physics A: Materials Science & Processing* **1999,** 69, (4), 461-464.
42. Cojoc, G.; Liberale, C.; Candeloro, P.; Gentile, F.; Das, G.; De Angelis, F.; Di Fabrizio, E. *Microelectronic Engineering* 87, (5-8), 876-879.
43. Galajda, P.; Ormos, P. *Applied Physics Letters* **2001,** 78, (2), 249-251.
44. Asavei, T.; Nieminen, T. A.; Heckenberg, N. R.; Rubinsztein-Dunlop, H. *arXiv.org, e-Print Archive, Physics* **2008**, 1-11, arXiv:0810 5585v1 [physics optics].
45. Sanchez, C.; Julian, B.; Belleville, P.; Popall, M. *Journal of Materials Chemistry* **2005,** 15, (35-36), 3559-3592.
46. Houbertz, R.; Domann, G.; Cronauer, C.; Schmitt, A.; Martin, H.; Park, J. U.; Frohlich, L.; Buestrich, R.; Popall, M.; Streppel, U.; Dannberg, P.; Wachter, C.; Brauer, A. *Thin Solid Films* **2003,** 442, (1,2), 194-200.
47. Buestrich, R.; Kahlenberg, F.; Popall, M.; Dannberg, P.; Muller-Fiedler, R.; Rosch, O. *Journal of Sol-Gel Science and Technology* **2001,** 20, (2), 181-186.

48. Ovsianikov, A.; Passinger, S.; Houbertz, R.; Chichkov, B. N. *Springer Series in Optical Sciences* **2007,** 129, (Laser Ablation and Its Applications), 121-157.
49. Obi, S. Replicated Optical Microstructures in Hybrid Polymers: Process Technology and Applications. Dissertation, University of Neuchâtel, 2006.
50. www.ormocer.de
51. Houbertz, R.; Declerck, P.; Passinger, S.; Ovsianikov, A.; Serbin, J.; Chichkov, B. N. *Nanophotonic Materials* **2008**, 97-114.
52. Woggon, T.; Kleiner, T.; Punke, M.; Lemmer, U. *Optics Express* **2009,** 17, (4), 2500-2507.
53. Reinhardt, C.; Kiyan, R.; Passinger, S.; Stepanov, A. L.; Ostendorf, A.; Chichkov, B. N. *Applied Physics A: Materials Science & Processing* **2007,** 89, (2), 321-325.
54. Wohlleben, W.; Bartels, F. W.; Boyle, M.; Leyrer, R. J. *Langmuir* **2008,** 24, (10), 5627-5635.
55. Houbertz, R. *Applied Surface Science* **2005,** 247, (1-4), 504-512.
56. Declerck, P.; Houbertz, R.; Jakopic, G.; Passinger, S.; Chichkov, B. *Materials Research Society Symposium Proceedings* **2007,** 1007, (Organic/Inorganic Hybrid Materials), No pp given, Paper #: 1007-S01-02.
57. Li, J.; Jia, B.; Gu, M. *Optics Express* **2008,** 16, (24), 20073-20080.
58. Serbin, J.; Egbert, A.; Ostendorf, A.; Chichkov, B. N.; Houbertz, R.; Domann, G.; Schulz, J.; Cronauer, C.; Froehlich, L.; Popall, M. *Optics Letters* **2003,** 28, (5), 301-303.
59. Houbertz, R.; Declerck, P.; Passinger, S.; Ovsianikov, A.; Serbin, J.; Chichkov, B. N. *Physica Status Solidi A: Applications and Materials Science* **2007,** 204, (11), 3662-3675.
60. Bhuian, B.; Winfield, R. J.; O'Brien, S.; Crean, G. M. *Applied Surface Science* **2006,** 252, (13), 4845-4849.
61. Ovsianikov, A.; Shizhou, X.; Farsari, M.; Vamvakaki, M.; Fotakis, C.; Chichkov, B. N. *Optics Express* **2009,** 17, (4), 2143-2148.
62. Ovsianikov, A.; Gaidukeviciute, A.; Chichkov, B. N.; Oubaha, M.; MacCraith, B. D.; Sakellari, I.; Giakoumaki, A.; Gray, D.; Vamvakaki, M.; Farsari, M.; Fotakis, C. *Laser Chemistry* **2008**, 493059/1-493059/7.
63. Ovsianikov, A.; Viertl, J.; Chichkov, B.; Oubaha, M.; MacCraith, B.; Sakellari, I.; Giakoumaki, A.; Gray, D.; Vamvakaki, M.; Farsari, M.; Fotakis, C. *ACS Nano* **2008,** 2, (11), 2257-2262.
64. Lee, K. Y.; LaBianca, N.; Rishton, S. A.; Zolghamain, S.; Gelorme, J. D.; Shaw, J.; Chang, T. H. P. *Journal of Vacuum Science & Technology, B: Microelectronics and Nanometer Structures* **1995,** 13, (6), 3012-16.
65. Shaw, M.; Nawrocki, D.; Hurditch, R.; Johnson, D. *Microsystem Technologies* **2003,** 10, (1), 1-6.
66. Genolet, G. Ph. D. thesis, EPFL, Lausanne, 2001.
67. Serbin, J.; Ovsianikov, A.; Chichkov, B. *Optics Express* **2004,** 12, (21), 5221-5228.
68. Juodkazis, S.; Mizeikis, V.; Misawa, H. *Journal of Applied Physics* **2009,** 106, (5), 051101/1-051101/14.
69. Seet, K. K.; Juodkazis, S.; Jarutis, V.; Misawa, H. *Applied Physics Letters* **2006,** 89, (2), 024106/1-024106/3.
70. Kuebler, S. M.; Braun, K. L.; Zhou, W.; Cammack, J. K.; Yu, T.; Ober, C. K.; Marder, S. R.; Perry, J. W. *Journal of Photochemistry and Photobiology, A: Chemistry* **2003,** 158, (2-3), 163-170.
71. Deubel, M.; von Freymann, G.; Wegener, M.; Pereira, S.; Busch, K.; Soukoulis, C. M. *Nature Materials* **2004,** 3, (7), 444-447.
72. Seet, K. K.; Mizeikis, V.; Kannari, K.; Juodkazis, S.; Misawa, H.; Tetreault, N.; John, S. *IEEE Journal of Selected Topics in Quantum Electronics* **2008,** 14, (4), 1064-1073.

73. Wu, D.; Chen, Q.-D.; Niu, L.-G.; Jiao, J.; Xia, H.; Song, J.-F.; Sun, H.-B. *IEEE Photonics Technology Letters* **2009,** 21, (20), 1535-1537.
74. Chanda, D.; Abolghasemi Ladan, E.; Haque, M.; Ng Mi, L.; Herman Peter, R. *Opt Express* **2008,** 16, (20), 15402-14.
75. Scrimgeour, J.; Sharp, D. N.; Blanford, C. F.; Roche, O. M.; Denning, R. G.; Turberfield, A. J. *Advanced Materials (Weinheim, Germany)* **2006,** 18, (12), 1557-1560.
76. Lee, T.-w.; Mitrofanov, O.; White, C. A.; Hsu, J. W. P. *Materials Research Society Symposium Proceedings* **2003,** 776, (Unconventional Approaches to Nanostructures with Applications in Electronics, Photonics, Information Storage and Sensing), 143-148.
77. Bichler, S.; Feldbacher, S.; Woods, R.; Satzinger, V.; Schmidt, V.; Jakopic, G.; Langer, G.; Kern, W. *Optical Materials (Amsterdam, Netherlands)* 34, (5), 772-780.
78. Woods, R.; Feldbacher, S.; Langer, G.; Satzinger, V.; Schmidt, V.; Kern, W. *Polymer* 52, (14), 3031-3037.
79. Infuehr, R.; Pucher, N.; Heller, C.; Lichtenegger, H.; Liska, R.; Schmidt, V.; Kuna, L.; Haase, A.; Stampfl, J. *Applied Surface Science* **2007,** 254, (4), 836-840.
80. www.colour-europe.de http://www.colour-europe.de/pf_812_additive.htm (28.11.2012),
81. www.evonik.tego.de. **2012**.
82. Kumpfmueller, J. Strukturierung von polysiloxan-basierenden Lichtwellenleitern mittels 2-Photonen induzierter Photopolymerisation. Diploma Thesis, Vienna University of Technology, 2009.
83. J. Kumpfmüller, N. P., K. Stadlmann, J. Stampfl, R. Liska In *Photo-induced Waveguide formation in Polysiloxanes*, RadTech Europe 2009, 10-14-2009 - 10-15-2009, Nizza, FR, 2009; Nizza, FR, 2009.
84. K. Cicha, Z. L., K. Stadlmann, A. Ovsianikov, R. Markut-Kohl, R. Liska, J. Stampfl. *Journal of Applied Physics*, **2011,** 110, 1-5.
85. www.byk.de www.byk.de
86. H. Q. Pham, M. J. M., Epoxy Resins. In *Ullmann's Encyclopedia of Industrial Chemistry*, Wiley-VCH Verlag GmbH & Co. KGaA: 2005.
87. Berkovich-Berger, D.; Lemcoff, N. G.; Abramson, S.; Grabarnik, M.; Weinman, S.; Fuchs, B. *Chem.--Eur. J.* 16, (21), 6365-6373.
88. Voronkov, M. G.; Kuznetsov, A. L.; Mirskov, R. G.; Shterenberg, B. Z.; Rakhlin, V. I. *Zh. Obshch. Khim.* **1985,** 55, (5), 1038-41.
89. Bazant, V.; Cermak, J.; Dvorak, M.; Hetflejs, J.; Chvalovsky, V. Three dimensionally crosslinked silicone polymers. CS153654B1, 1974.
90. Lagrange, A. Hair dye preparations containing direct dyes with disulfide/thiol protective group and silicon compounds with thiol group. WO2009109457A2, 2009.
91. Schmidt, M.; Wieber, M. *Inorg. Chem.* **1962,** 1, 909-12.
92. Yuta, S.; Watanabe, K.; Kurata, S.; Umemoto, K.; Yamanaka, A. Dental cement primer containing mercapto compounds. JP02152915A, 1990.
93. Mogi, H. Preparation of bis(mercaptoalkyl)tetraorganodisiloxanes as surface modifiers for resins. 90-184262
04074191, 19900713., 1992.
94. Verma, K. K.; Bose, S. *Analytica Chimica Acta* **1973,** 65, (1), 236-9.
95. Pucher, N. U. Synthesis and Evaluation of Novel Initiators for the Two-Photon Induced Photopolymerization Process - A Precise Tool for Real 3D Sub-Micrometer Laser Structuring. Dissertation, TU Vienna, 2010.
96. Kumpfmueller, J.; Stadlmann, K.; Satzinger, V.; Li, Z.; Stampfl, J.; Liska, R. *Journal of Laser Micro/Nanoengineering* 6, (3), 195-198.

97. Li, Z.; Pucher, N.; Cicha, K.; Torgersen, J.; Ligon, S. C.; Ajami, A.; Husinsky, W.; Rosspeintner, A.; Vauthey, E.; Naumov, S.; Scherzer, T.; Stampfl, J.; Liska, R. *Macromolecules (Washington, DC, United States)*, Ahead of Print.
98. K. Stadlmann, K. C., J. Kumpfmüller, V. Schmidt, V. Satzinger, R. Liska, J. Stampfl In *Fabrication of Optical Interconnects with Two Photon Polymerization*, 11th International Symposium on Laser Precision Microfabrication, LPM 2010, Stuttgart, 2010-06-07 - 2010-06-10, 2010; Sugioka, K., Ed. Stuttgart, 2010.
99. Albota, M.; Beljonne, D.; Bredas, J. L.; Ehrlich, J. E.; Fu, J. Y.; Heikal, A. A.; Hess, S. E.; Kogej, T.; Levin, M. D.; Marder, S. R.; McCord-Maughon, D.; Perry, J. W.; Rockel, H.; Rumi, M.; Subramaniam, G.; Webb, W. W.; Wu, X. L.; Xu, C. *Science (New York, N.Y.)* **1998,** 281, (5383), 1653-6.